

Colourful Loops: Introduction to Quantum Chromodynamics and Loop Calculations

Gudrun Heinrich

Max Planck Institute for Physics, Munich

TUM, Sommersemester 2018



Contents

1	Quantum Chromodynamics as a non-Abelian gauge theory	4
1.1	Quarks and the QCD Lagrangian	5
1.2	Feynman rules for QCD	8
1.3	Colour Algebra	12
1.4	The running coupling and the QCD beta function	15
2	Tree level amplitudes	19
2.1	Polarisation sums	21
3	Higher orders in perturbation theory	23
3.1	Dimensional regularisation	23
3.2	Regularisation schemes	25
3.3	One-loop integrals	26
3.4	Renormalisation	36

3.5	NLO calculations and infrared singularities	38
3.5.1	Structure of NLO calculations	38
3.5.2	Soft gluon emission	41
3.5.3	Collinear singularities	44
3.5.4	Phase space integrals in D dimensions	46
3.5.5	Jet cross sections	48
3.6	Parton distribution functions	55
3.6.1	Deeply inelastic scattering	55
3.6.2	Proton structure in the parton model	58
3.6.3	Proton structure in perturbative QCD	61
3.6.4	Parton evolution and the DGLAP equations	63
3.6.5	Hadron-hadron collisions	66
3.7	Beyond one loop	67
3.7.1	Integral families, reduction to master integrals	67
3.7.2	Multi-loop integrals in Feynman parameter space	70
3.7.3	Calculation of master integrals	71
3.7.4	Sector decomposition	72
A	Appendix	74
A.1	Evidence for colour	74
A.2	The strong CP problem	76
A.3	Form factors for tensor two-point functions	77
A.4	Construction of the functions \mathcal{F} and \mathcal{U} from topological rules	79

Literature

Some recommended literature:

- G. Dissertori, I. Knowles, M. Schmelling,
Quantum Chromodynamics: High energy experiments and theory
International Series of Monographs on Physics No. 115,
Oxford University Press, Feb. 2003. Reprinted in 2005.
- T. Muta, *Foundations of QCD*, World Scientific (1997).
- R.K. Ellis, W.J. Stirling and B.R. Webber, *QCD and collider physics*, Cambridge University Press, Camb. Monogr. Part. Phys. Nucl. Phys. Cosmol. **8** (1996) 1.
- J. Wells and G. Altarelli, *Collider Physics within the Standard Model : A Primer*, Lect. Notes Phys. **937** (2017) 1. doi:10.1007/978-3-319-51920-3.
- M.E. Peskin, D.V. Schroeder,
Introduction to Quantum Field Theory, Addison-Wesley 1995.
- J. Campbell, J. Huston and F. Krauss,
The Black Book of Quantum Chromodynamics: A Primer for the LHC Era Oxford University Press, December 2017.
- V. A. Smirnov, *Analytic tools for Feynman integrals*, Springer Tracts Mod. Phys. **250** (2012) 1. doi:10.1007/978-3-642-34886-0.
- L. J. Dixon, “*Calculating scattering amplitudes efficiently*”,
Invited lectures presented at the Theoretical Advanced Study Institute in Elementary Particle Physics (TASI '95): QCD and Beyond, Boulder, CO, June 1995.
<https://arxiv.org/abs/hep-ph/9601359>.
- E. Laenen, “*QCD*”, CERN Yellow Report CERN 2016-003, pp. 1-58,
doi:10.5170/CERN-2016-003.1 [arXiv:1708.00770 [hep-ph]].
- Z. Trocsanyi, “*QCD for collider experiments*”, doi:10.5170/CERN-2015-004.65
arXiv:1608.02381 [hep-ph].
- M. L. Mangano, “*Introduction to QCD*”, <http://cds.cern.ch/record/454171>.

1 Quantum Chromodynamics as a non-Abelian gauge theory

Quantum Chromodynamics (QCD) is the theory of the strong interactions between quarks and gluons (also called *partons*).

The interactions are called “strong” since they are the strongest of the four fundamental forces at a length scale a bit larger than the proton radius. At a distance of 1 fm ($1 \text{ fm} = 10^{-15} \text{ m}$), its strength is about 10^{38} times larger than the gravitational force. However, we will see later that the strong coupling varies with energy. The higher the energy (i.e. the smaller the distance between the partons¹), the weaker it will be. This phenomenon is called *asymptotic freedom*. At large distances, however, the interaction (coupling) becomes very strong. Therefore quarks and gluons cannot be observed as isolated particles. They are *confined* in hadrons, which are bound states of several partons. Quarks come in different *flavours*, u, d, c, s, t, b are known to exist (see Fig. 2). Baryons are hadrons regarded as bound states of 3 quarks, for example the proton (uud), mesons are quark-antiquark bound states. The 9 mesons constructed from *up*, *down* and *strange* quarks are shown in Fig. 1.

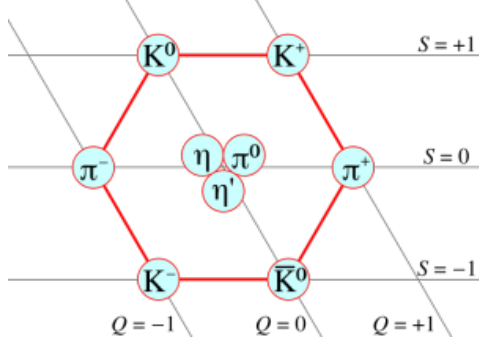


Figure 1: The Meson nonet. *Source: Wikimedia Commons.*

Why “Chromodynamics”? In addition to the well-known quantum numbers like electromagnetic charge, spin, parity, quarks carry an additional quantum number called *colour*. Bound states are colour singlets. Note that without the colour quantum number, a bound state consisting e.g. of 3 *u*-quarks (called Δ^{++}) would violate Pauli’s exclusion principle if there was no additional quantum number (which implies that this state must be totally antisymmetric in the colour indices).

The emergence of QCD from the quark model [1–3] started more than 50 years ago, for a review see e.g. Ref. [4]. QCD as the theory of strong interactions is nowadays well established, however it still gives us many puzzles to solve and many tasks to accomplish in order to model particle interactions in collider physics.

¹We will work in units where $\hbar = c = 1$.

There are various approaches to make predictions and simulations based on QCD. They can be put into two broad categories: (i) perturbative QCD, (ii) non-perturbative QCD (e.g. “Lattice QCD”). Our subject will be perturbative QCD.

1.1 Quarks and the QCD Lagrangian

The quark model and experimental evidence suggested that

- Hadrons are composed of quarks, which are spin 1/2 fermions.
- Quarks have electromagnetic charges $\pm 2/3$ (up-type) and $\mp 1/3$ (down-type) and come in 3 different colours (“colour charge”).
- There is evidence that the colour charge results from an underlying local $SU(3)$ gauge symmetry.
- The mediators of the strong force are called gluons, which interact with both the quarks and themselves. The latter is a consequence of the non-Abelian structure of $SU(3)$.
- Quarks are in the fundamental representation of $SU(3)$, gluons in the adjoint representation.
- Quarks are believed to come in 6 flavours, forming 3 generations of up-type and down-type quarks: $(\begin{smallmatrix} u \\ d \end{smallmatrix})$, $(\begin{smallmatrix} c \\ s \end{smallmatrix})$, $(\begin{smallmatrix} t \\ b \end{smallmatrix})$. They transform as doublets under the electroweak interactions. The answer to the question why quarks and leptons come in 3 generations is still unknown.

QCD as a $SU(N_c)$ gauge theory

The strong interactions can be described as an $SU(3)$ local gauge theory, where the “charges” are denoted as *colour*. They are embedded in the Standard Model (SM) of elementary particle physics, with underlying gauge group $SU(3) \times SU(2)_L \times U(1)_Y$. The particle content of the SM as we know it right now is shown in Fig. 2.

The underlying structure of gauge theories can be described by *Lie groups*. QED is an Abelian gauge theory because the underlying group is the Abelian group $U(1)$. For QCD, the underlying group is the non-Abelian group $SU(N_c)$, where N_c is the number of colours (we believe that in Nature $N_c = 3$, but the concept is more general). The non-Abelian group structure implies that gluons interact with themselves (while photons do not), as we will see shortly. Non-Abelian gauge theories are also called *Yang-Mills* theories.

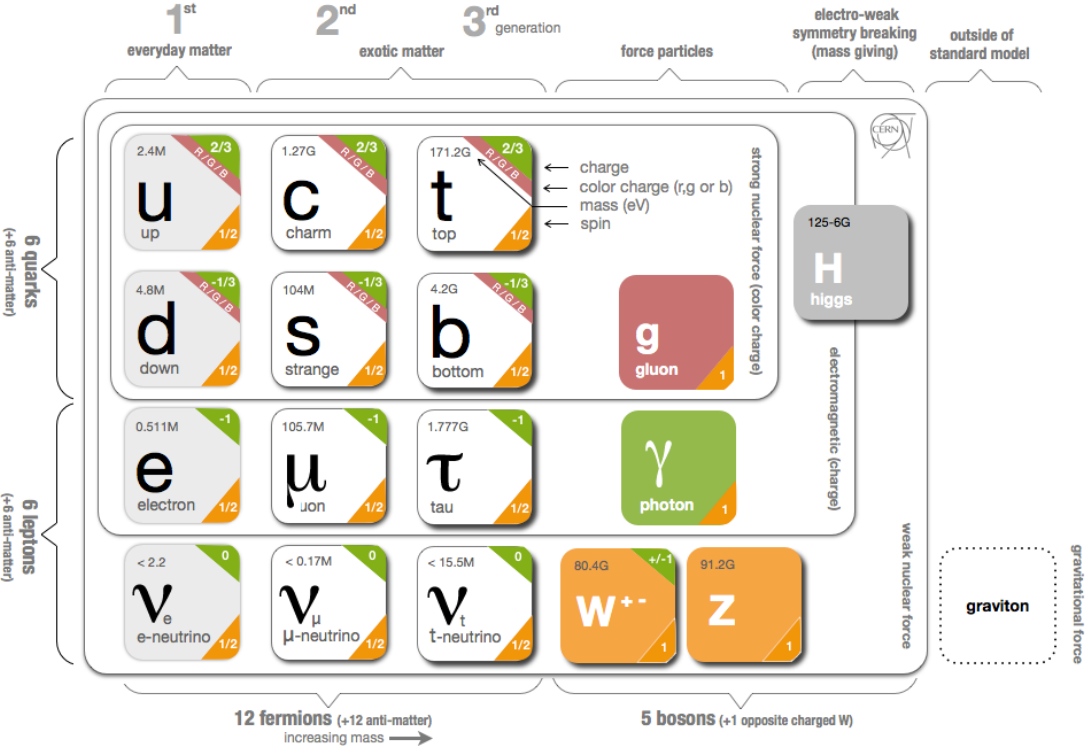


Figure 2: The particles of the Standard Model. *Source: CERN*

An important concept in QCD (and in the Standard Model in general) is the formulation as a *local* gauge theory. This means that the gauge transformation parameter depends itself on x , the position in space time.

Consider the quark fields $q_f^j(x)$ for just one quark flavour f . The index j labels the colour, $j = 1, \dots, N_c$. Treating the quarks as free Dirac fields, we have

$$\mathcal{L}_q^{(0)}(q_f, m_f) = \sum_{j,k=1}^{N_c} \bar{q}_f^j(x) (i \gamma_\mu \partial^\mu - m_f)_{jk} q_f^k(x) , \quad (1.1)$$

where the γ_μ matrices in 4 space-time dimensions satisfy the Clifford algebra,

$$\{\gamma^\mu, \gamma^\nu\} = 2 g^{\mu\nu}, \quad \{\gamma^\mu, \gamma^5\} = 0. \quad (1.2)$$

Now let us apply a transformation $q_k \rightarrow q'_k = U_{kl} q^l$, $\bar{q}_k \rightarrow \bar{q}'_k = \bar{q}^l U_{lk}^{-1}$, with

$$U_{kl} = \exp \left\{ i \sum_{a=1}^{N_c^2-1} t^a \theta^a \right\}_{kl} \equiv \exp \{i \mathbf{t} \cdot \boldsymbol{\theta}\}_{kl}, \quad (1.3)$$

where θ^a are the symmetry group transformation parameters. The Lagrangian of free Dirac fields remains invariant under this transformation as long as it is a *global* transformation, i.e. as long as the θ^a do not depend on x : $\mathcal{L}_q^{(0)}(q) = \mathcal{L}_q^{(0)}(q')$. The matrices $(t^a)_{kl}$ are $N_c \times N_c$ matrices representing the $N_c^2 - 1$ generators of $SU(N_c)$ in the so-called fundamental representation (see also Section 1.3).

However, we aim at *local* gauge transformations, i.e. the gauge transformation parameter θ in Eq. (1.3) depends on x . In QED, where the underlying gauge group is $U(1)$, a global transformation would just be a phase change. The requirement of a free electron field to be invariant under *local* transformations $\theta = \theta(x)$ inevitably leads to the introduction of a *gauge field* A_μ , the photon. The analogous is true for QCD: requiring local gauge invariance under $SU(N_c)$ leads to the introduction of gluon fields A_μ^a .

As the local gauge transformation

$$U(x) = \exp \{i \mathbf{t} \cdot \boldsymbol{\theta}(x)\} \quad (1.4)$$

depends on x , the derivative of the transformed quark field $q'(x)$ reads

$$\partial_\mu q'(x) = \partial_\mu (U(x)q(x)) = U(x)\partial_\mu q(x) + (\partial_\mu U(x)) q(x). \quad (1.5)$$

To keep \mathcal{L}_q gauge invariant, we can remedy the situation caused by the second term above if we define a *covariant derivative* D^μ by

$$(D^\mu[A])_{ij} = \delta_{ij} \partial^\mu + i g_s t_{ij}^a A_a^\mu, \quad (1.6)$$

or, without index notation

$$\mathbf{D}^\mu[\mathbf{A}] = \partial^\mu + i g_s \mathbf{A}_\mu, \quad (1.7)$$

where $\mathbf{A}^\mu = t^a A_a^\mu$ (sum over $a = 1 \dots N_c^2 - 1$ understood). The fields A_a^μ are called *gluons*, they are coloured vector fields which transform under general $SU(N_c)$ transformations as follows:

$$\mathbf{A}_\mu \rightarrow \mathbf{A}'_\mu = U(x) \mathbf{A}_\mu U^{-1}(x) + \frac{i}{g_s} (\partial_\mu U(x)) U^{-1}(x). \quad (1.8)$$

Therefore the Lagrangian for the quark fields which is invariant under local gauge transformations reads

$$\mathcal{L}_q(q_f, m_f) = \sum_{j,k=1}^{N_c} \bar{q}_f^j(x) (i \gamma_\mu \mathbf{D}^\mu[\mathbf{A}] - m_f)_{jk} q_f^k(x). \quad (1.9)$$

What is the dynamics of the gauge fields? The purely gluonic part of the QCD Lagrangian can be described by the so-called Yang-Mills Lagrangian

$$\mathcal{L}_{YM} = -\frac{1}{4} F_{\mu\nu}^a F^{a,\mu\nu}, \quad (1.10)$$

where the non-Abelian field strength tensor $F_{\mu\nu}^a$ is given by

$$F_{\mu\nu}^a = \partial_\mu A_\nu^a - \partial_\nu A_\mu^a - g_s f^{abc} A_\mu^b A_\nu^c. \quad (1.11)$$

The constants f^{abc} are the structure constants of the $SU(N_c)$ Lie algebra. They are completely antisymmetric and are related to the generators $(F^a)_{bc}$ of $SU(N_c)$ in the adjoint representation by $F_{bc}^a = -i f^{abc}$.

For $N_c = 3$, the matrices t^a are the 8 Hermitian and traceless generators of $SU(3)$ in the fundamental representation, $t^a = \lambda^a/2$, where the λ^a are called Gell-Mann matrices. They satisfy the commutator relation

$$[t^a, t^b] = i f^{abc} t^c, \quad (1.12)$$

with normalisation $\text{Trace}(t^a t^b) = T_R \delta^{ab}$. Usually the convention is $T_R = 1/2$ for the fundamental representation. More details will be given in Section 1.3.

So finally we obtain for the “classical” QCD Lagrangian

$$\begin{aligned} \mathcal{L}_c &= \mathcal{L}_{YM} + \mathcal{L}_q \\ &= -\frac{1}{4} F_{\mu\nu}^a F^{a,\mu\nu} + \sum_{j,k=1}^{N_c} \bar{q}_f^j(x) (i \gamma_\mu \mathbf{D}^\mu[\mathbf{A}] - m_f)_{jk} q_f^k(x). \end{aligned} \quad (1.13)$$

1.2 Feynman rules for QCD

We are not quite there yet with the complete QCD Lagrangian. The “classical” QCD Lagrangian \mathcal{L}_c contains degenerate field configurations (i.e. they are equivalent up to gauge transformations). This leads to the fact that the bilinear operator in the gluon fields is not invertible, such that it is not possible to construct a propagator for the gluon fields. This will be outlined in the following.

The Feynman rules can be derived from the action,

$$S = i \int d^4x \mathcal{L}_c \equiv S_0 + S_I, \quad \text{where} \quad S_0 = i \int d^4x \mathcal{L}_0, \quad \text{and} \quad S_I = i \int d^4x \mathcal{L}_I.$$

In this decomposition \mathcal{L}_0 contains the free fields, i.e. terms bilinear in the fields (kinetic terms) and \mathcal{L}_I contains all other terms (interactions). The gluon propagator $\Delta_{\mu\nu}^{ab}(p)$

is constructed from the inverse of the bilinear term in $A_\mu^a A_\nu^b$. In momentum space we have the condition (we suppress colour indices as these terms are diagonal in colour space, i.e. we leave out overall factors of the form δ^{ab})

$$i \Delta_{\mu\rho}(p) [p^2 g^{\rho\nu} - p^\rho p^\nu] = g_\mu^\nu. \quad (1.14)$$

However, we find

$$[p^2 g^{\rho\nu} - p^\rho p^\nu] p_\nu = 0, \quad (1.15)$$

which means that the matrix $[p^2 g^{\rho\nu} - p^\rho p^\nu]$ is not invertible because it has at least one eigenvalue equal to zero. We have to remove the physically equivalent configurations from the classical Lagrangian. This is called *gauge fixing*. We can achieve this by imposing a constraint on the fields A_μ^a , adding a term to the Lagrangian with a Lagrange multiplier. For example, *covariant gauges* are defined by the requirement $\partial_\mu A^\mu(x) = 0$ for any x . Adding

$$\mathcal{L}_{\text{GF}} = -\frac{1}{2\lambda} (\partial_\mu A^\mu)^2, \quad \lambda \in \mathbb{R},$$

to \mathcal{L} , the action S remains the same. The bilinear term then has the form

$$i \left(p^2 g^{\mu\nu} - \left(1 - \frac{1}{\lambda}\right) p^\mu p^\nu \right),$$

with inverse

$$\Delta_{\mu\nu}(p) = \frac{-i}{p^2 + i\varepsilon} \left[g_{\mu\nu} - (1 - \lambda) \frac{p_\mu p_\nu}{p^2} \right]. \quad (1.16)$$

The so-called $i\varepsilon$ prescription ($\varepsilon > 0$) shifts the poles of the propagator slightly off the real p^0 -axis (where p^0 is the energy component) and will become important later when we consider loop integrals. It ensures the correct causal behaviour of the propagators. Of course, physical results must be independent of λ . Choosing $\lambda = 1$ is called *Feynman gauge*, $\lambda = 0$ is called *Landau gauge*.

In covariant gauges unphysical degrees of freedom (longitudinal and time-like polarisations) also propagate. The effect of these unwanted degrees of freedom is cancelled by the ghost fields, which are coloured complex scalars obeying Fermi statistics. Unphysical degrees of freedom and the ghost fields can be avoided by choosing *axial (physical) gauges*. The axial gauge is defined by introducing an arbitrary vector n^μ with $p \cdot n \neq 0$, to impose the constraint

$$\mathcal{L}_{\text{GF}} = -\frac{1}{2\alpha} (n^\mu A_\mu)^2 \quad (\alpha \rightarrow 0),$$

which leads to

$$\Delta_{\mu\nu}(p, n) = \frac{-i}{p^2 + i\varepsilon} \left(g_{\mu\nu} - \frac{p_\mu n_\nu + n_\mu p_\nu}{p \cdot n} + \frac{n^2 p_\mu p_\nu}{(p \cdot n)^2} \right).$$

A convenient choice is $n^2 = 0$, called *light-cone gauge*. Note that we have

$$\Delta_{\mu\nu}(p, n) p^\mu = 0, \quad \Delta_{\mu\nu}(p, n) n^\mu = 0.$$

Thus, only 2 degrees of freedom propagate (transverse ones in the $n^\mu + p^\mu$ rest frame). The price to pay by choosing this gauge instead of a covariant one is that the propagator looks more complicated and that it diverges when p^μ becomes parallel to n^μ . In the light-cone gauge we have

$$\begin{aligned} \Delta_{\mu\nu}(p, n) &= \frac{i}{p^2 + i\varepsilon} d_{\mu\nu}(p, n) \\ d_{\mu\nu}(p, n) &= -g_{\mu\nu} + \frac{p_\mu n_\nu + n_\mu p_\nu}{p \cdot n} = \sum_{\lambda=1,2} \epsilon_\mu^\lambda(p) (\epsilon_\nu^\lambda(p))^*, \end{aligned} \quad (1.17)$$

where $\epsilon_\mu^\lambda(p)$ is the polarisation vector of the gluon field with momentum p and polarisation λ . This means that only the two physical polarisations ($\lambda = 1, 2$) propagate. In Feynman gauge, we have

$$\sum_{pol} \epsilon_\mu^\lambda(p) (\epsilon_\nu^\lambda(p))^* = -g_{\mu\nu}, \quad (1.18)$$

where the polarisation sum also runs over non-transverse gluon polarisations, which can occur in loops and will be cancelled by the corresponding loops involving ghost fields (*see later, exercises*).

The part of the Lagrangian describing the Faddeev-Popov ghost fields can be derived using the path integral formalism, and we refer to the literature for the derivation. The result reads

$$\mathcal{L}_{FP} = \eta_a^\dagger M^{ab} \eta_b, \quad (1.19)$$

where the η_a are $N_c^2 - 1$ complex scalar fields which obey Fermi statistics and do not occur as external states. In Feynman gauge, the operator M^{ab} (also called Faddeev-Popov matrix) is given by

$$M_{Feyn}^{ab} = \delta^{ab} \partial_\mu \partial^\mu + g_s f^{abc} A_\mu^c \partial^\mu. \quad (1.20)$$

Note that in QED (or another Abelian gauge theory) the second term is absent, such that the Faddeev-Popov determinant $\det M$ does not depend on any field and therefore can be absorbed into the normalisation of the path integral, such that no ghost fields are needed in Abelian gauge theories.

In the light-cone gauge, the Faddeev-Popov matrix becomes

$$M_{LC}^{ab} = \delta^{ab} n_\mu \partial^\mu + g_s f^{abc} n_\mu A_c^\mu, \quad (1.21)$$

such that, due to the gauge fixing condition $n \cdot A = 0$, the matrix is again independent of the gauge field and therefore can be absorbed into the normalisation, such that no ghost fields propagate.

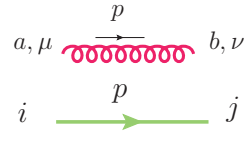
So finally we have derived the full QCD Lagrangian

$$\mathcal{L}_{QCD} = \mathcal{L}_{YM} + \mathcal{L}_q + \mathcal{L}_{GF} + \mathcal{L}_{FP} . \quad (1.22)$$

We will not derive the QCD Feynman rules from the action, but just state them below. (The pictures are partly taken from *Z. Trocsanyi, arXiv:1608.02381*).

Propagators: ($i\varepsilon$ prescription understood)

gluon propagator: $\Delta_{\mu\nu}^{ab}(p) = \delta^{ab} \Delta_{\mu\nu}(p)$



quark propagator: $\Delta_q^{ij}(p) = \delta^{ij} i \frac{p+m}{p^2-m^2}$

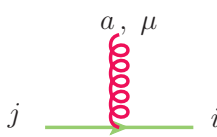


ghost propagator: $\Delta^{ab}(p) = \delta^{ab} \frac{i}{p^2}$

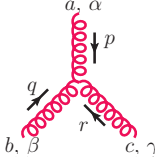


Vertices:

quark-gluon: $\Gamma_{gq\bar{q}}^{\mu, a} = -i g_s (t^a)_{ij} \gamma^\mu$

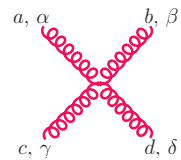


three-gluon: $\Gamma_{\alpha\beta\gamma}^{abc}(p, q, r) = -i g_s (F^a)_{bc} V_{\alpha\beta\gamma}(p, q, r)$

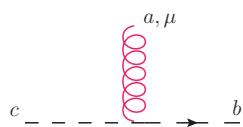


$$V_{\alpha\beta\gamma}(p, q, r) = (p-q)_\gamma g_{\alpha\beta} + (q-r)_\alpha g_{\beta\gamma} + (r-p)_\beta g_{\alpha\gamma}, \quad p^\alpha + q^\alpha + r^\alpha = 0$$

four-gluon: $\Gamma_{\alpha\beta\gamma\delta}^{abcd} = -i g_s^2 \left[\begin{array}{l} +f^{xac} f^{xbd} (g_{\alpha\beta} g_{\gamma\delta} - g_{\alpha\delta} g_{\beta\gamma}) \\ +f^{xad} f^{xcb} (g_{\alpha\gamma} g_{\beta\delta} - g_{\alpha\beta} g_{\gamma\delta}) \\ +f^{xab} f^{xdc} (g_{\alpha\delta} g_{\beta\gamma} - g_{\alpha\gamma} g_{\beta\delta}) \end{array} \right]$



ghost-gluon: $\Gamma_{g\eta\bar{\eta}}^{\mu, a} = -i g_s (F^a)_{bc} p^\mu$



The four-gluon vertex differs from the rest of the Feynman rules in the sense that it is not in a factorised form of a colour factor and a kinematic part carrying the Lorentz indices. This is an inconvenient feature because it prevents the separate summation over

colour and Lorentz indices and complicates automation. We can however circumvent this problem by introducing an auxiliary field with propagator

$a \stackrel{\gamma}{=} \stackrel{\delta}{=} b$, that couples only to the gluon with vertex

$$\text{Diagram: } a, \alpha \text{ (red wavy line)} = i \sqrt{2} g_s f^{xac} g^{\alpha\xi} g^{\gamma\zeta}.$$

We can check that a single four-gluon vertex can be written as a sum of three graphs. This way the summations over colour and Lorentz indices factorize completely.

Finally, we have to supply the following factors for incoming and outgoing particles:

- outgoing fermion: $\bar{u}(p)$
- incoming fermion: $u(p)$
- outgoing photon, or gluon: $\epsilon_\mu^\lambda(p)^*$
- outgoing antifermion: $v(p)$
- incoming antifermion: $\bar{v}(p)$
- incoming photon, or gluon: $\epsilon_\mu^\lambda(p)$.

1.3 Colour Algebra

For the generators of the group T^a , the commutation relation

$$[T^a, T^b] = i f^{abc} T^c \quad (1.23)$$

holds, independent of the representation.

The generators of $SU(3)$ in the fundamental representation are usually defined as $t_{ij}^a = \lambda_{ij}^a / 2$, where the λ_{ij}^a are also called Gell-Mann matrices. They are traceless and hermitian and can be considered as the $SU(3)$ analogues of the Pauli-matrices for $SU(2)$.

$$\lambda^1 = \begin{pmatrix} 0 & 1 & 0 \\ 1 & 0 & 0 \\ 0 & 0 & 0 \end{pmatrix}, \quad \lambda^2 = \begin{pmatrix} 0 & -i & 0 \\ i & 0 & 0 \\ 0 & 0 & 0 \end{pmatrix}, \quad \lambda^3 = \begin{pmatrix} 1 & 0 & 0 \\ 0 & -1 & 0 \\ 0 & 0 & 0 \end{pmatrix}, \quad \lambda^4 = \begin{pmatrix} 0 & 0 & 1 \\ 0 & 0 & 0 \\ 1 & 0 & 0 \end{pmatrix},$$

$$\lambda^5 = \begin{pmatrix} 0 & 0 & -i \\ 0 & 0 & 0 \\ i & 0 & 0 \end{pmatrix}, \quad \lambda^6 = \begin{pmatrix} 0 & 0 & 0 \\ 0 & 0 & 1 \\ 0 & 1 & 0 \end{pmatrix}, \quad \lambda^7 = \begin{pmatrix} 0 & 0 & 0 \\ 0 & 0 & -i \\ 0 & i & 0 \end{pmatrix}, \quad \lambda^8 = \frac{1}{\sqrt{3}} \begin{pmatrix} 1 & 0 & 0 \\ 0 & 1 & 0 \\ 0 & 0 & -2 \end{pmatrix}.$$

Quarks are in the fundamental representation of $SU(3)$. Therefore the Feynman rules for the quark-gluon vertex involve t_{ij}^a where $i, j = 1 \dots N_c$ run over the colours of

the quarks (the *degree* of the group), while $a = 1 \dots N_c^2 - 1$ runs over the number of generators (the *dimension*) of the group. Gluons are in the adjoint representation of $SU(3)$, which we denote by the matrices $(F^a)_{bc}$, related to the structure constants by $(F^a)_{bc} = -i f^{abc}$. The adjoint representation is characterised by the fact that the dimension of the vector space on which it acts is equal to the dimension of the group itself, $a, b, c = 1 \dots N_c^2 - 1$. The gluons can be regarded as a combination of two coloured lines, as depicted in Fig. 3. Contracting colour indices is graphically equivalent

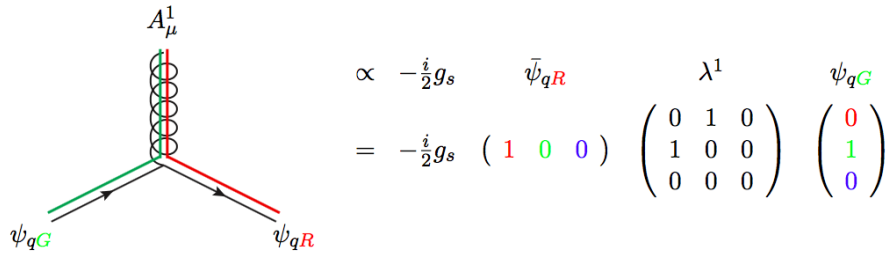


Figure 3: Representation of the gluon as a double colour line. *Picture: Peter Skands, arXiv:1207.2389.*

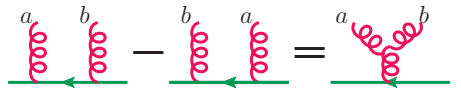
to connecting the respective colour (or anticolour) lines. The above representation of the quark-gluon vertex embodies the idea of colour conservation, whereby the colour-anticolour quantum numbers carried by the $q\bar{q}$ pair are transferred to the gluon.

The sums $\sum_{a,j} t_{ij}^a t_{jk}^a$ and $\sum_{a,d} F_{bd}^a F_{dc}^a$ have two free indices in the fundamental and adjoint representation, respectively. One can show that these sums are invariant under $SU(N)$ transformations, and therefore must be proportional to the unit matrix:

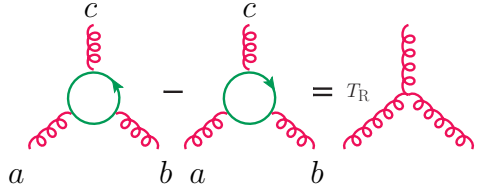
$$\sum_{j,a} t_{ij}^a t_{jk}^a = C_F \delta_{ik}, \quad \sum_{a,d} F_{bd}^a F_{dc}^a = C_A \delta_{bc}. \quad (1.24)$$

The constants C_F and C_A are the eigenvalues of the quadratic Casimir operator in the fundamental and adjoint representation, respectively.

The commutation relation (1.23) in the fundamental representation can be represented graphically by



Multiplying this commutator first with another colour charge operator, summing over the fermion index and then taking the trace over the fermion line (i.e. multiplying with δ_{ik}) we obtain the representation of the three-gluon vertex as traces of products of colour charges:



$$\text{Trace}(t^a t^b t^c) - \text{Trace}(t^c t^b t^a) = i T_R f^{abc}.$$

In the exercises we will see some examples of how to compute the colour algebra structure of a QCD diagram, independent of the kinematics. For example, taking the trace of the identity in the fundamental and in the adjoint representation we obtain

$$\text{Diagram with one gluon loop} = N_c, \quad \text{Diagram with two gluon loops} = N_c^2 - 1,$$

respectively. Then, using the expressions for the fermion and gluon propagator insertions, we find

$$\text{Diagram with one gluon loop and fermion insertion} = C_F N_c, \quad \text{Diagram with two gluon loops and fermion insertion} = C_A (N_c^2 - 1).$$

There is also something like a Fierz identity, following from representing the gluon as a double quark line:

$$\text{Diagram with two parallel gluon lines} = T_R \left(\text{Diagram with two gluon lines and a quark loop} - \frac{1}{N_c} \text{Diagram with two gluon lines and a quark loop} \right)$$

$$t_{ij}^a t_{kl}^a = T_R \left(\delta_{il} \delta_{kj} - \frac{1}{N_c} \delta_{ij} \delta_{kl} \right). \quad (1.25)$$

The Casimirs can be expressed in terms of the number of colours N_c as (*Exercise 1*)

$$C_F = T_R \frac{N_c^2 - 1}{N_c}, \quad C_A = 2 T_R N_c. \quad (1.26)$$

The colour factors C_F and C_A can indirectly be measured at colliders. As they depend on N_c , these measurements again confirmed that the number of colours is three.

1.4 The running coupling and the QCD beta function

We mentioned already that the strong coupling constant, defined as $\alpha_s = g_s^2/(4\pi)$, is not really a constant. To leading order in the perturbative expansion, it obeys the relation

$$\alpha_s(Q^2) = \frac{1}{b_0 \log(Q^2/\Lambda_{QCD}^2)} , \quad (1.27)$$

where Λ_{QCD} is an energy scale below which non-perturbative effects start to dominate, the mass scale of hadronic physics, and Q^2 is a larger energy scale, for example the centre-of-mass energy s of a scattering process. $\Lambda_{QCD} \simeq 250$ MeV, the inverse of a typical hadron size R_0 . The coefficient b_0 is given by

$$b_0 = \frac{1}{4\pi} \left(\frac{11}{3} C_A - \frac{4}{3} T_R N_f \right) , \quad (1.28)$$

we will encounter it again later. Note that $b_0 > 0$ for $N_f < 11/2 C_A$.

Where does the running of the coupling come from? It is closely linked to *renormalisation*, which introduces another scale into the game, the *renormalisation scale* μ .

Before we enter into the technicalities of renormalisation, let us look at a physical observable, for example the R -ratio (see also Appendix A.1)

$$R(s) = \frac{\sigma(e^+e^- \rightarrow \text{hadrons})}{\sigma(e^+e^- \rightarrow \mu^+\mu^-)} . \quad (1.29)$$

We assume that the energy s exchanged in the scattering process is much larger than Λ_{QCD} .

At leading order in perturbation theory, we have to calculate diagrams like the one in Fig. 4 (we restrict ourselves to photon exchange) to obtain

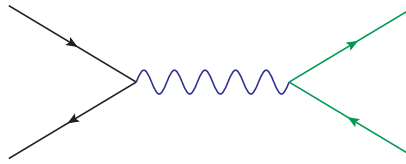


Figure 4: Leading order diagram for $e^+e^- \rightarrow f\bar{f}$.

$$R = N_c \sum_f Q_f^2 , \quad (1.30)$$

where Q_f is the electromagnetic charge of fermion f . However, we have quantum corrections where virtual gluons are exchanged, example diagrams are shown in Figs. 5a

and Fig. 5b, where Fig. 5a shows corrections of order α_s and Fig. 5b shows example diagrams for $\mathcal{O}(\alpha_s^2)$ corrections. The perturbative expansion for R can be written as

$$R(s) = K_{QCD}(s) R_0, \quad R_0 = N_c \sum_f Q_f^2,$$

$$K_{QCD}(s) = 1 + \frac{\alpha_s(\mu^2)}{\pi} + \sum_{n \geq 2} C_n \left(\frac{s}{\mu^2} \right) \left(\frac{\alpha_s(\mu^2)}{\pi} \right)^n. \quad (1.31)$$

The higher the order in α_s the harder is the calculation. Meanwhile we know the C_n up to order α_s^4 [5, 6].



(a) 1-loop diagram contributing to $e^+e^- \rightarrow f\bar{f}$. (b) 2-loop diagram example contributing to $e^+e^- \rightarrow f\bar{f}$.

However, if we try to calculate the loop in Fig. 5a, we will realize that some of the individual integrals, when integrated over the loop momentum k , are ill-defined. They diverge for $k \rightarrow \infty$. This is called an *ultraviolet divergence*. How to deal with them will be explained in Section 3.1. For the moment we just introduce an arbitrary cutoff scale Λ_{UV} for the upper integration boundary. If we carried through the calculation, we would see that the dependence on the cutoff cancels, which is a consequence of the Ward Identities in QED. However, if we go one order higher in α_s , calculating diagrams like the one in Fig. 5b, the cutoff-dependence does not cancel anymore. We obtain

$$K_{QCD}(s) = 1 + \frac{\alpha_s}{\pi} + \left(\frac{\alpha_s}{\pi} \right)^2 \left[c + b_0 \pi \log \frac{\Lambda_{UV}^2}{s} \right] + \mathcal{O}(\alpha_s^3). \quad (1.32)$$

It looks like our result is infinite, as we should take the limit $\Lambda_{UV} \rightarrow \infty$. However, we did not claim that α_s is the coupling we measure. In fact, it is the “bare” coupling, also denoted as α_s^0 , which appears in Eq. (1.32), and we can absorb the infinity in the bare coupling to arrive at the renormalised coupling, which is the one we measure.

In our case, this looks as follows. Define

$$\alpha_s(\mu) = \alpha_s^0 + b_0 \log \frac{\Lambda_{UV}^2}{\mu^2} \alpha_s^2, \quad (1.33)$$

then replace α_s^0 by $\alpha_s(\mu)$ and drop consistently all terms of order α_s^3 . This leads to

$$K_{QCD}^{\text{ren}}(\alpha_s(\mu), \mu^2/s) = 1 + \frac{\alpha_s(\mu)}{\pi} + \left(\frac{\alpha_s(\mu)}{\pi} \right)^2 \left[c + b_0 \pi \log \frac{\mu^2}{s} \right] + \mathcal{O}(\alpha_s^3). \quad (1.34)$$

K_{QCD}^{ren} is finite, but now it depends on the scale μ , both explicitly and through $\alpha_s(\mu)$. However, the hadronic R -ratio is a physical quantity and therefore cannot depend on the arbitrary scale μ . The dependence of K_{QCD} on μ is an artefact of the truncation of the perturbative series after the order α_s^2 .

Renormalisation group and asymptotic freedom

Since the hadronic R -ratio $R^{\text{ren}} = R_0 K_{QCD}^{\text{ren}}$ cannot depend μ , we know

$$\mu^2 \frac{d}{d\mu^2} R^{\text{ren}}(\alpha_s(\mu), \mu^2/Q^2) = 0 = \left(\mu^2 \frac{\partial}{\partial \mu^2} + \mu^2 \frac{\partial \alpha_s}{\partial \mu^2} \frac{\partial}{\partial \alpha_s} \right) R^{\text{ren}}(\alpha_s(\mu), \mu^2/Q^2). \quad (1.35)$$

Equation (1.35) is called *renormalisation group equation (RGE)*. Introducing the abbreviations

$$t = \ln \frac{Q^2}{\mu^2}, \quad \beta(\alpha_s) = \mu^2 \frac{\partial \alpha_s}{\partial \mu^2}, \quad (1.36)$$

the RGE becomes

$$\left(-\frac{\partial}{\partial t} + \beta(\alpha_s) \frac{\partial}{\partial \alpha_s} \right) R = 0. \quad (1.37)$$

This first order partial differential equation can be solved by implicitly defining a function $\alpha_s(Q^2)$, the *running coupling*, by

$$t = \int_{\alpha_s}^{\alpha_s(Q^2)} \frac{dx}{\beta(x)}, \quad \text{with } \alpha_s \equiv \alpha_s(\mu^2). \quad (1.38)$$

Differentiating Eq. (1.38) with respect to the variable t leads to

$$1 = \frac{1}{\beta(\alpha_s(Q^2))} \frac{\partial \alpha_s(Q^2)}{\partial t}, \quad \text{which implies } \beta(\alpha_s(Q^2)) = \frac{\partial \alpha_s(Q^2)}{\partial t}.$$

The derivative of Eq. (1.38) with respect to α_s gives

$$0 = \frac{1}{\beta(\alpha_s(Q^2))} \frac{\partial \alpha_s(Q^2)}{\partial \alpha_s} - \frac{1}{\beta(\alpha_s)} \frac{\partial \alpha_s}{\partial \alpha_s} \Rightarrow \frac{\partial \alpha_s(Q^2)}{\partial \alpha_s} = \frac{\beta(\alpha_s(Q^2))}{\beta(\alpha_s)}. \quad (1.39)$$

It is now easy to prove that the value of R for $\mu^2 = Q^2$, $R(1, \alpha_s(Q^2))$, solves Eq. (1.37):

$$-\frac{\partial}{\partial t} R(1, \alpha_s(Q^2)) = -\frac{\partial R}{\partial \alpha_s(Q^2)} \frac{\partial \alpha_s(Q^2)}{\partial t} = -\beta(\alpha_s(Q^2)) \frac{\partial R}{\partial \alpha_s(Q^2)} \quad (1.40)$$

and

$$\beta(\alpha_s) \frac{\partial}{\partial \alpha_s} R(1, \alpha_s(Q^2)) = \beta(\alpha_s) \frac{\partial \alpha_s(Q^2)}{\partial \alpha_s} \frac{\partial R}{\partial \alpha_s(Q^2)} = \beta(\alpha_s(Q^2)) \frac{\partial R}{\partial \alpha_s(Q^2)}. \quad (1.41)$$

This means that the scale dependence in R enters only through $\alpha_s(Q^2)$, and that we can predict the scale dependence of R by solving Eq. (1.38), or equivalently,

$$\frac{\partial \alpha_s(Q^2)}{\partial t} = \beta(\alpha_s(Q^2)) . \quad (1.42)$$

We can try to solve Eq. (1.42) perturbatively using an expansion of the β -function

$$\beta(\alpha_s) = -b_0 \alpha_s^2 \left[1 + \sum_{n=1}^{\infty} b_n \alpha_s^n \right] , \quad (1.43)$$

As mentioned above, the first five coefficients are known [7], where the fifth one has been calculated only very recently [8–11].

If $\alpha_s(Q^2)$ is small we can truncate the series. The solution at leading-order (LO) accuracy is

$$\begin{aligned} Q^2 \frac{\partial \alpha_s}{\partial Q^2} &= \frac{\partial \alpha_s}{\partial t} = -b_0 \alpha_s^2 \Rightarrow -\frac{1}{\alpha_s(Q^2)} + \frac{1}{\alpha_s(\mu^2)} = -b_0 t \\ \Rightarrow \alpha_s(Q^2) &= \frac{\alpha_s(\mu^2)}{1 + b_0 t \alpha_s(\mu^2)} . \end{aligned} \quad (1.44)$$

Eq. (1.44) implies that

$$\alpha_s(Q^2) \xrightarrow{Q^2 \rightarrow \infty} \frac{1}{b_0 t} \xrightarrow{Q^2 \rightarrow \infty} 0 . \quad (1.45)$$

This behaviour is called *asymptotic freedom*: the larger Q^2 , the smaller the coupling, so at very high energies (small distances), the quarks and gluons can be treated as if they were free particles. The behaviour of α_s as a function of Q^2 is illustrated in Fig. 6 including recent measurements. Note that the sign of b_0 is positive for QCD, while it is negative for QED. It can be proven that, in 4 space-time dimensions, only non-Abelian gauge theories can be asymptotically free. For the discovery of asymptotic freedom in QCD [12, 13], Gross, Politzer and Wilczek got the Nobel Prize in 2004.

Note that in the derivation of the RGE above, we have assumed that the observable R does not depend on other mass scales like quark masses. However, the renormalisation group equations can be easily extended to include mass renormalisation, which will lead to running quark masses:

$$\left(\mu^2 \frac{\partial}{\partial \mu^2} + \beta(\alpha_s) \frac{\partial}{\partial \alpha_s} - \gamma_m(\alpha_s) m \frac{\partial}{\partial m} \right) R \left(\frac{Q^2}{\mu^2}, \alpha_s, \frac{m}{Q} \right) = 0 , \quad (1.46)$$

where γ_m is called the mass anomalous dimension and the minus sign before γ_m is a convention. In a perturbative expansion we can write the mass anomalous dimension as $\gamma_m(\alpha_s) = c_0 \alpha_s (1 + \sum_n c_n \alpha_s^n)$. The coefficients are known up to c_4 [14, 15].

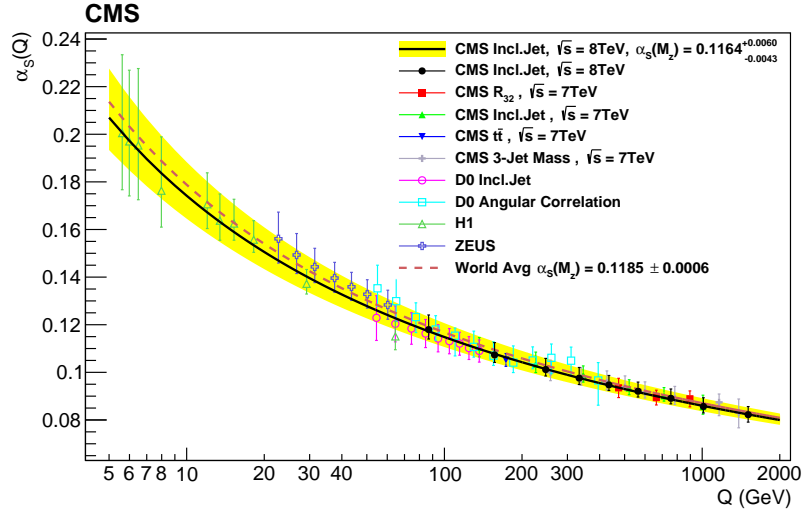


Figure 6: The running coupling $\alpha_s(Q^2)$. *Figure from arXiv:1609.05331.*

Scale uncertainties

From the perturbative solution of the RGE we can derive how a physical quantity $O^{(N)}(\mu)$, expanded in α_s as $O^{(N)}(\mu) = \sum_n c_n(\mu) \alpha_s(\mu^2)^n$ and truncated at order N in perturbation theory, changes with the renormalisation scale μ :

$$\frac{d}{d \log(\mu^2)} O^{(N)}(\mu) \sim \mathcal{O}(\alpha_s(\mu^2)^{N+1}). \quad (1.47)$$

Therefore it is clear that, the more higher order coefficients c_n we can calculate, the less our result will depend on the unphysical scale μ^2 . An example is shown in Fig. 7.

In hadronic collisions there is another scale, the factorisation scale μ_F , which needs to be taken into account when assessing the uncertainty of the theoretical prediction.

2 Tree level amplitudes

In this section we will not only see how to calculate tree level matrix elements (squared), but also how unphysical polarisations in the QCD case arise and cancel when including ghost fields.

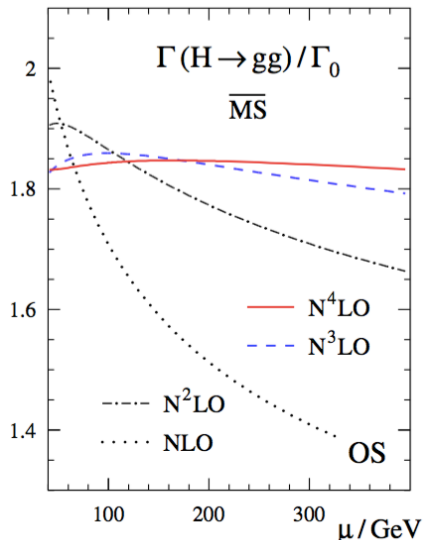


Figure 7: Example $H \rightarrow gg$ for the reduction of the scale dependence at higher orders. *Figure from Ref. [6].*

Let us first consider a simple process in QED, $e^+e^- \rightarrow \gamma\gamma$, where the contributing diagrams are shown in Fig. 8.

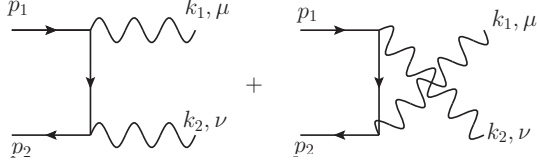


Figure 8: The process $e^+e^- \rightarrow \gamma\gamma$ at leading order.

If p_1 and p_2 are the two incoming momenta and k_1 and k_2 the two photon momenta, where $p_1 + p_2 = k_1 + k_2$, and neglecting the electron mass, we can write the amplitude as

$$\mathcal{M} = -i e^2 \epsilon_1^\mu(k_1) \epsilon_2^\nu(k_2) M_{\mu\nu}, \quad M_{\mu\nu} = M_{\mu\nu}^{(1)} + M_{\mu\nu}^{(2)}, \quad (2.1)$$

$$M_{\mu\nu}^{(1)} = \bar{v}(p_2) \gamma_\nu \frac{\not{p}_1 - \not{k}_1}{(p_1 - k_1)^2} \gamma_\mu u(p_1),$$

$$M_{\mu\nu}^{(2)} = \bar{v}(p_2) \gamma_\mu \frac{\not{p}_1 - \not{k}_2}{(p_1 - k_2)^2} \gamma_\nu u(p_1).$$

Gauge invariance requires that $\epsilon_2^\nu \partial^\mu M_{\mu\nu} = 0$, $\epsilon_1^\mu \partial^\nu M_{\mu\nu} = 0$. In fact, $J_\mu \equiv \epsilon_2^\nu M_{\mu\nu}$ is a conserved current (charge conservation) coupling to the photon k_1 . In momentum space, this means $k_1^\mu J_\mu = 0$.

Exercise: Verify explicitly that $M_{\mu\nu}$ is gauge invariant, and that this is the case independently of $k_i \cdot \epsilon(k_i) = 0$ being fulfilled or not.

Now let us look at the QCD analogue, the process $q\bar{q} \rightarrow gg$. Due to the non-Abelian structure of QCD, we have a third diagram containing gluon

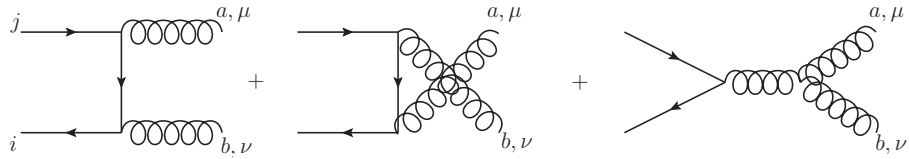


Figure 9: The process $q\bar{q} \rightarrow gg$ at leading order.

self-interactions. The leading order amplitude (in an expansion in α_s) is given by

$$\begin{aligned}\mathcal{M} &= -i g_s^2 \epsilon_1^\mu(k_1) \epsilon_2^\nu(k_2) M_{\mu\nu}^{\text{QCD}} \\ M_{\mu\nu}^{\text{QCD}} &= (t^b t^a)_{ij} M_{\mu\nu}^{(1)} + (t^a t^b)_{ij} M_{\mu\nu}^{(2)} + M_{\mu\nu}^{(3)},\end{aligned}\quad (2.2)$$

where $M_{\mu\nu}^{(1)}$ and $M_{\mu\nu}^{(2)}$ are exactly the same as in the QED case. Now we can use $(t^b t^a)_{ij} = (t^a t^b)_{ij} - i f^{abc} t_{ij}^c$ to write Eq. (2.2) as

$$M_{\mu\nu}^{\text{QCD}} = (t^a t^b)_{ij} [M_{\mu\nu}^{(1)} + M_{\mu\nu}^{(2)}] - i f^{abc} t_{ij}^c M_{\mu\nu}^{(1)} + M_{\mu\nu}^{(3)}, \quad (2.3)$$

The term in square brackets in Eq. (2.3) is the QED amplitude, for which we know that $k_i^\mu M_{\mu\nu} = 0$. Therefore, the full $M_{\mu\nu}^{\text{QCD}}$ in Eq. (2.3) can only be gauge invariant if $M_{\mu\nu}^{(3)}$ cancels the extra term $\sim f^{abc} t_{ij}^c M_{\mu\nu}^{(1)}$ when contracted with k_i^μ .

In fact, we find that

$$k_1^\mu M_{\mu\nu}^{(1)} = -\bar{v}(p_2) \gamma_\nu u(p_1) \quad (2.4)$$

$$k_1^\mu M_{\mu\nu}^{(3)} = i f^{abc} t_{ij}^c \bar{v}(p_2) \gamma_\nu u(p_1) - i f^{abc} t_{ij}^c \bar{v}(p_2) k_1 u(p_1) \frac{k_{2,\nu}}{2k_1 \cdot k_2}. \quad (2.5)$$

The first term in Eq. (2.5) cancels the one proportional to $M_{\mu\nu}^{(1)}$ in Eq. (2.3). The second term in Eq. (2.5) is left over! However, it is zero upon contraction with the polarisation vector $\epsilon^\nu(k_2)$ if k_2 is the momentum of a *physical* gluon, i.e. if $\epsilon^\nu(k_2) \cdot k_2 = 0$.

2.1 Polarisation sums

In order to obtain cross sections, we need to calculate the modulus of the scattering amplitude, $|\mathcal{M}|^2$. For unpolarised cross sections, we sum over the polarisations/spins of the final states, so we need to evaluate

$$\sum_{\text{phys. pol}} \epsilon_{\mu_1}(k_1) \epsilon_{\nu_1}(k_2) \mathcal{M}^{\mu_1 \nu_1} \epsilon_{\mu_2}^*(k_1) \epsilon_{\nu_2}^*(k_2) (\mathcal{M}^{\mu_2 \nu_2})^*. \quad (2.6)$$

In QED, we can replace the polarisation sum by $-g_{\mu\nu}$, i.e.

$$\sum_{\text{phys. pol}} \epsilon_{\mu_1}(k_1) \epsilon_{\mu_2}^*(k_1) \rightarrow -g_{\mu_1 \mu_2}. \quad (2.7)$$

Note that Eq. (2.7) is *not* an equality, but holds because the amplitude \mathcal{M} must fulfill the QED Ward Identity. This can be seen as follows:

Let us pick a reference frame where the momentum of the photon 1 (simply denoted by k instead of k_1) is $k = (k^0, 0, 0, k^0)$ and the polarisation vectors are given by

$\epsilon_{L,R} = (0, 1, \pm i, 0)/\sqrt{2}$, satisfying the usual normalisation properties $\epsilon_L \epsilon_L^* = \epsilon_R \epsilon_R^* = -1$, $\epsilon_L \epsilon_R^* = 0$. Introducing a light-like vector n which is dual to k , $n = (k^0, 0, 0, -k^0)$, we can write the physical polarisation sum as

$$\sum_{i=L,R} \epsilon_i^\mu(k) \epsilon_i^{\nu,*}(k) = \begin{pmatrix} 0 & 0 & 0 & 0 \\ 0 & 1 & 0 & 0 \\ 0 & 0 & 1 & 0 \\ 0 & 0 & 0 & 0 \end{pmatrix} = -g^{\mu\nu} + \frac{k^\mu n^\nu + k^\nu n^\mu}{k \cdot n}. \quad (2.8)$$

However, in QED the second term can be dropped. This is because $k^\mu \epsilon^\nu(k_2) M_{\mu\nu} = 0$, $\epsilon^\mu(k) k_2^\nu M_{\mu\nu} = 0$. If we define $\mathcal{M}_\mu = \epsilon^\nu(k_2) M_{\mu\nu}$ we have $k^\mu \mathcal{M}_\mu = 0 \Rightarrow \mathcal{M}_0 = \mathcal{M}_3$ and therefore

$$\sum_{i=L,R} \epsilon_i^\mu(k) \epsilon_i^{\nu,*}(k) \mathcal{M}_\mu \mathcal{M}_\nu^* = |\mathcal{M}_1|^2 + |\mathcal{M}_2|^2 = |\mathcal{M}_1|^2 + |\mathcal{M}_2|^2 + |\mathcal{M}_3|^2 - |\mathcal{M}_0|^2 = -g^{\mu\nu} \mathcal{M}_\mu \mathcal{M}_\nu^*. \quad (2.9)$$

The longitudinal (\mathcal{M}_3) and time-like (\mathcal{M}_0) components cancel each other. Therefore we have always (for n photons) $k_1^{\mu_1} \dots k_n^{\mu_n} \mathcal{M}_{\mu_1 \dots \mu_n} = 0$, regardless whether $\epsilon(k_j) \cdot k_j = 0$ or not.

This is not the case in QCD. In QCD we just showed that $k_1^\mu \mathcal{M}_\mu \sim \epsilon(k_2) \cdot k_2$, which vanishes only for physical polarisations. If $\epsilon(k_2) \cdot k_2 \neq 0$, then $\mathcal{M}_0 \neq \mathcal{M}_3$ in Eq. (2.9) and therefore we can *not* just use $-g_{\mu\nu}$ for the polarisation sum. However, it can be shown that

$$S_{\text{unphys.}} \equiv \sum_{\text{unphysical pol.}} |\epsilon_\mu(k_1) \epsilon_\nu(k_2) \mathcal{M}^{\mu\nu}|^2 = \left| i g_s^2 f^{abc} t^c \bar{v}(p_2) \frac{k_1}{(k_1 + k_2)^2} u(p_1) \right|^2. \quad (2.10)$$

Calculating the ghost contribution shown in Fig. 10 however leads to the expression in Eq. (2.10) with opposite sign. This shows that the ghost fields cancel the unphysical polarisations of the gluon fields. Therefore it is also possible to use $-g_{\mu\nu}$ for the polarisation sum if the ghost fields are taken into account when calculating the squared amplitude. Note that closed ghost loops get an additional factor of -1 from the Feynman rules because they obey Fermi statistics.

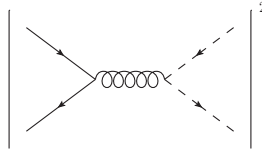
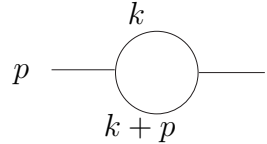


Figure 10: Ghost fields in the polarisation sum.

3 Higher orders in perturbation theory

Tree level results in QCD are mostly not accurate enough to match the current experimental precision and suffer from large scale uncertainties. When calculating higher orders, we will encounter singularities: ultraviolet (UV) singularities, and infrared (IR) singularities due to soft or collinear massless particles. Therefore the introduction of a *regulator* is necessary.

Let us first have a look at UV singularities: The expression for the one-loop two-point function shown below naively would be



$$I_2 = \int_{-\infty}^{\infty} \frac{d^4 k}{(2\pi)^4} \frac{1}{[k^2 - m^2 + i\delta][(k+p)^2 - m^2 + i\delta]} . \quad (3.1)$$

If we are only interested in the behaviour of the integral for $|k| \rightarrow \infty$ we can neglect the masses, transform to polar coordinates and obtain

$$I_2 \sim \int d\Omega_3 \int_0^{\infty} d|k| \frac{|k|^3}{|k|^4} . \quad (3.2)$$

This integral is clearly not well-defined. If we introduce an upper cutoff Λ (and a lower limit $|k|_{\min}$ because we neglected the masses and p^2) it is regulated:

$$I_2 \sim \int_{|k|_{\min}}^{\Lambda} d|k| \frac{1}{|k|} \sim \log \Lambda . \quad (3.3)$$

The integral has a logarithmic UV divergence. The problem with the regulator Λ is that it is neither Lorentz invariant nor gauge invariant. A regularisation method which preserves the symmetries is dimensional regularisation.

3.1 Dimensional regularisation

Dimensional regularisation has been introduced in 1972 by ‘t Hooft and Veltman [16] (and by Bollini and Giambiagi [17]) as a method to regularise UV divergences in a gauge invariant way, thus completing the proof of renormalisability.

The idea is to work in $D = 4 - 2\epsilon$ space-time dimensions. This means that the Lorentz algebra objects (momenta, polarisation vectors, metric tensor) live in a D -dimensional space. The γ -algebra also has to be extended to D dimensions. Divergences for $D \rightarrow 4$ will appear as poles in $1/\epsilon$.

An important feature of dimensional regularisation is that it regulates IR singularities, i.e. soft and/or collinear divergences due to massless particles, as well. Ultraviolet divergences occur if the loop momentum $k \rightarrow \infty$, so in general the UV behaviour becomes better for $\epsilon > 0$, while the IR behaviour becomes better for $\epsilon < 0$. Certainly we cannot have $D < 4$ and $D > 4$ at the same time. What is formally done is to first assume the IR divergences are regulated in some other way, e.g. by assuming all external legs are off-shell or by introducing a small mass for all massless particles. In this case all poles in $1/\epsilon$ will be of UV nature and renormalisation can be performed. Then we can analytically continue to the whole complex D -plane, in particular to $\text{Re}(D) > 4$. If we now remove the auxiliary IR regulator, the IR divergences will show up as $1/\epsilon$ poles. (This is however not done in practice, where all poles just show up as $1/\epsilon$ poles, and after UV renormalisation, the remaining ones must be of IR nature.)

The only change to the Feynman rules to be made is to replace the couplings in the Lagrangian $g \rightarrow g\mu^\epsilon$, where μ is an arbitrary mass scale. This ensures that each term in the Lagrangian has the correct mass dimension.

The momentum integration involves $\int \frac{d^D k}{(2\pi)^D}$ for each loop, which can also be considered as an addition to the Feynman rules.

Further, each closed fermion loop and ghost loop needs to be multiplied by a factor of (-1) due to Fermi statistics.

D -dimensional γ -algebra

Extending the Clifford algebra to D dimensions implies

$$\{\gamma^\mu, \gamma^\nu\} = 2g^{\mu\nu} \quad \text{with} \quad g_\mu^\mu = D , \quad (3.4)$$

leading for example to $\gamma_\mu \not\! \gamma^\mu = (2 - D) \not\! \gamma$. However, it is not obvious how to continue the Dirac matrix γ_5 to D dimensions. In 4 dimensions it is defined as

$$\gamma_5 = i\gamma_0\gamma_1\gamma_2\gamma_3 \quad (3.5)$$

which is an intrinsically 4-dimensional definition. In 4 dimensions, γ_5 has the algebraic properties $\gamma_5^2 = 1$, $\{\gamma_\mu, \gamma_5\} = 0$, $\text{Tr}(\gamma_\mu\gamma_\nu\gamma_\rho\gamma_\sigma\gamma_5) = 4i\epsilon_{\mu\nu\rho\sigma}$. However, in D dimensions, the latter two conditions cannot be maintained simultaneously. This can be seen by considering the expression

$$\epsilon^{\mu\nu\rho\sigma} \text{Tr}(\gamma_\tau\gamma_\mu\gamma_\nu\gamma_\rho\gamma_\sigma\gamma^\tau\gamma_5)$$

(remember $\epsilon_{\mu\nu\rho\sigma} = 1$ if $(\mu\nu\rho\sigma)$ is an even permutation of (0123) , -1 if $(\mu\nu\rho\sigma)$ is an odd permutation of (0123) and 0 otherwise). Using the cyclicity of the trace and

$\{\gamma_\mu, \gamma_5\} = 0$ leads to

$$(D - 4) \epsilon^{\mu\nu\rho\sigma} \text{Tr}(\gamma_\mu \gamma_\nu \gamma_\rho \gamma_\sigma \gamma_5) = 0. \quad (3.6)$$

For $D \neq 4$ we therefore conclude that the trace must be zero, and there is no smooth limit $D \rightarrow 4$ which reproduces the non-zero trace at $D = 4$.

The most commonly used prescription [16, 18, 19] for γ_5 is to define

$$\gamma_5 = \frac{i}{4!} \epsilon_{\mu_1 \mu_2 \mu_3 \mu_4} \gamma^{\mu_1} \gamma^{\mu_2} \gamma^{\mu_3} \gamma^{\mu_4}, \quad (3.7)$$

where the Lorentz indices of the “ordinary” γ -matrices will be contracted in D dimensions. Doing so, Ward identities relying on $\{\gamma_5, \gamma_\mu\} = 0$ break down due to an extra $(D - 4)$ -dimensional contribution. These need to be repaired by so-called “finite renormalisation” terms [19]. For practical calculations it can be convenient to split the other Dirac matrices into a 4-dimensional and a $(D - 4)$ -dimensional part, $\gamma_\mu = \bar{\gamma}_\mu + \tilde{\gamma}_\mu$, where $\bar{\gamma}_\mu$ is 4-dimensional and $\tilde{\gamma}_\mu$ is $(D - 4)$ -dimensional. The definition (3.7) implies

$$\{\gamma^\mu, \gamma_5\} = \begin{cases} 0 & \mu \in \{0, 1, 2, 3\} \\ 2\tilde{\gamma}^\mu \gamma_5 & \text{otherwise.} \end{cases}$$

The second line above can also be read as $[\gamma_5, \tilde{\gamma}^\mu] = 0$, which can be interpreted as γ_5 acting trivially in the non-physical dimensions. There are other prescriptions for γ_5 , which maintain $\{\gamma_\mu^{(D)}, \gamma_5\} = 0$, but then have to give up the cyclicity of the trace.

3.2 Regularisation schemes

Related to the γ_5 -problem, it is not uniquely defined how we continue the Dirac-algebra to D dimensions. Four commonly used schemes are:

- **CDR** (“Conventional dimensional regularisation”): Both internal and external gluons (and other vector fields) are all treated as D -dimensional.
- **HV** (“’t Hooft Veltman scheme”): Internal gluons are treated as D -dimensional but external ones are treated as strictly 4-dimensional.
- **DR** (“original dimensional reduction”): Internal and external gluons are all treated as quasi-4-dimensional.
- **FDH** (“four-dimensional helicity scheme”): Internal gluons are treated as quasi-4-dimensional but external ones are treated as strictly 4-dimensional.

What is the difference between quasi-4-dimensional and strictly 4-dimensional? Formally, one should distinguish 3 spaces [20]:

1. The original 4-dimensional space (4S).
2. The formally D -dimensional space for momenta and momentum integrals. This space is actually an infinite-dimensional vector space with certain D -dimensional properties [21, 22], and is sometimes called “quasi- D -dimensional space” (QDS). The space 4S is therefore a subspace of QDS.
3. The formally 4-dimensional space for e.g. gluons in dimensional reduction. This space has to be a superspace of QDS in order for the dimensionally reduced theory to be gauge invariant. Hence it cannot be identified with the original 4S, it can only be constructed as a “quasi-4-dimensional space” (Q4S) [23] with certain 4-dimensional properties. In practice the distinction between Q4S and 4S often does not matter, but it is important in the definition of the different versions of dimensional reduction and to avoid the inconsistency uncovered in Ref. [24].

These three spaces are characterised by their metric tensors, which we denote by $g^{\mu\nu}$ (for Q4S), $\hat{g}^{\mu\nu}$ (for QDS), and $\bar{g}^{\mu\nu}$ (for 4S). The dimensionalities of the spaces are expressed by the following equations:

$$g^{\mu\nu} g_{\mu\nu} = 4, \quad \hat{g}^{\mu\nu} \hat{g}_{\mu\nu} = D = 4 - 2\epsilon, \quad \bar{g}^{\mu\nu} \bar{g}_{\mu\nu} = 4. \quad (3.8)$$

The following projection relations express that 4S is a subspace of QDS and QDS is a subspace of Q4S:

$$g^{\mu\nu} \hat{g}_\nu^\rho = \hat{g}^{\mu\rho}, \quad g^{\mu\nu} \bar{g}_\nu^\rho = \bar{g}^{\mu\rho}, \quad \hat{g}^{\mu\nu} \bar{g}_\nu^\rho = \bar{g}^{\mu\rho}. \quad (3.9)$$

It is useful to introduce the orthogonal complement to QDS. This is a $4 - D = 2\epsilon$ -dimensional space with metric tensor $\tilde{g}^{\mu\nu}$, which satisfies

$$g^{\mu\nu} = \hat{g}^{\mu\nu} + \tilde{g}^{\mu\nu}, \quad \tilde{g}^{\mu\nu} \tilde{g}_{\mu\nu} = 4 - D = 2\epsilon, \quad (3.10)$$

$$g^{\mu\nu} \tilde{g}_\nu^\rho = \tilde{g}^{\mu\rho}, \quad \hat{g}^{\mu\nu} \tilde{g}_\nu^\rho = 0, \quad \bar{g}^{\mu\nu} \tilde{g}_\nu^\rho = 0. \quad (3.11)$$

At one loop, **CDR** and **HV** are equivalent, similarly **DR** and **FDH** are equivalent, as terms of order ϵ in external momenta do not play a role. The transition formulae to relate results obtained in one scheme to another scheme are well known at one loop [20, 25]. The conventions are summarised in Table 1.

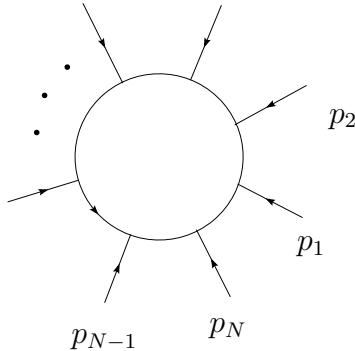
3.3 One-loop integrals

Integration in D dimensions

Consider a generic one-loop diagram with N external legs and N propagators. If k is the loop momentum, the propagators are $q_a = k + r_a$, where $r_a = \sum_{i=1}^a p_i$. If we define all momenta as incoming, momentum conservation implies $\sum_{i=1}^N p_i = 0$ and hence $r_N = 0$.

	CDR	HV	DR	FDH
internal gluon	$\hat{g}^{\mu\nu}$	$\hat{g}^{\mu\nu}$	$g^{\mu\nu}$	$g^{\mu\nu}$
external gluon	$\hat{g}^{\mu\nu}$	$\bar{g}^{\mu\nu}$	$g^{\mu\nu}$	$\bar{g}^{\mu\nu}$

Table 1: Treatment of internal and external gluons in the four different schemes.



If the vertices in the diagram above are non-scalar, this diagram will contain a Lorentz tensor structure in the numerator, leading to tensor integrals of the form

$$I_N^{D, \mu_1 \dots \mu_r}(S) = \int_{-\infty}^{\infty} \frac{d^D k}{i\pi^{\frac{D}{2}}} \frac{k^{\mu_1} \dots k^{\mu_r}}{\prod_{i \in S} (q_i^2 - m_i^2 + i\delta)} , \quad (3.12)$$

but we will first consider the scalar integral only, i.e. the case where the numerator is equal to one. S is the set of propagator labels, which can be used to characterise the integral, in our example $S = \{1, \dots, N\}$.

We use the integration measure $d^D k / i\pi^{\frac{D}{2}} \equiv d\kappa$ to avoid ubiquitous factors of $i\pi^{\frac{D}{2}}$ which will arise upon momentum integration.

Feynman parameters

To combine products of denominators of the type $d_i^{\nu_i} = [(k + r_i)^2 - m_i^2 + i\delta]^{\nu_i}$ into one single denominator, we can use the identity

$$\frac{1}{d_1^{\nu_1} d_2^{\nu_2} \dots d_N^{\nu_N}} = \frac{\Gamma(\sum_{i=1}^N \nu_i)}{\prod_{i=1}^N \Gamma(\nu_i)} \int_0^\infty \prod_{i=1}^N dz_i z_i^{\nu_i-1} \frac{\delta(1 - \sum_{j=1}^N z_j)}{[z_1 d_1 + z_2 d_2 + \dots + z_N d_N]^{\sum_{i=1}^N \nu_i}} \quad (3.13)$$

The integration parameters z_i are called *Feynman parameters*. For generic one-loop diagrams we have $\nu_i = 1 \forall i$. The propagator powers ν_i are also called *indices*.

An alternative to Feynman parametrisation is the so-called “Schwinger parametrisation”, based on

$$\frac{1}{A^\nu} = \frac{1}{\Gamma(\nu)} \int_0^\infty dx x^{\nu-1} \exp(-x A), \quad \text{Re}(A) > 0. \quad (3.14)$$

In this case the Gaussian integration formula

$$\int_{-\infty}^\infty d^D r_E \exp(-\alpha r_E^2) = \left(\frac{\pi}{\alpha}\right)^{\frac{D}{2}}, \quad \alpha > 0 \quad (3.15)$$

is used to integrate over the momenta.

Simple example: one-loop two-point function

For $N = 2$, the corresponding 2-point integral (“bubble”) is given by

$$\begin{aligned} I_2 &= \int_{-\infty}^\infty d\kappa \frac{1}{[k^2 - m^2 + i\delta][(k+p)^2 - m^2 + i\delta]} \\ &= \Gamma(2) \int_0^\infty dz_1 dz_2 \int_{-\infty}^\infty d\kappa \frac{\delta(1 - z_1 - z_2)}{[z_1(k^2 - m^2) + z_2((k+p)^2 - m^2) + i\delta]^2} \\ &= \Gamma(2) \int_0^1 dz_2 \int_{-\infty}^\infty d\kappa \frac{1}{[k^2 + 2k \cdot Q + A + i\delta]^2} \\ Q^\mu &= z_2 p^\mu, \quad A = z_2 p^2 - m^2. \end{aligned} \quad (3.16)$$

How to do the D -dimensional momentum integration will be shown below for a general one-loop integral. The procedure also extends to multi-loop integrals (see later) and is completely straightforward. The tricky bit is usually the integration over the Feynman parameters.

Momentum integration for scalar one-loop N -point integrals

The one-loop N -point integral with rank $r = 0$ (“scalar integral”) defined in Eq. (3.12), after Feynman parametrisation, with all propagator powers $\nu_i = 1$, is of the following form

$$\begin{aligned} I_N^D &= \Gamma(N) \int_0^\infty \prod_{i=1}^N dz_i \delta(1 - \sum_{l=1}^N z_l) \int_{-\infty}^\infty d\kappa \left[k^2 + 2k \cdot Q + \sum_{i=1}^N z_i(r_i^2 - m_i^2) + i\delta \right]^{-N} \\ Q^\mu &= \sum_{i=1}^N z_i r_i^\mu. \end{aligned} \quad (3.17)$$

Now we perform the shift $l = k + Q$ to eliminate the term linear in k in the square bracket to arrive at

$$I_N^D = \Gamma(N) \int_0^\infty \prod_{i=1}^N dz_i \delta(1 - \sum_{l=1}^N z_l) \int_{-\infty}^\infty \frac{d^D l}{i\pi^{\frac{D}{2}}} [l^2 - R^2 + i\delta]^{-N} \quad (3.18)$$

The general form of R^2 is

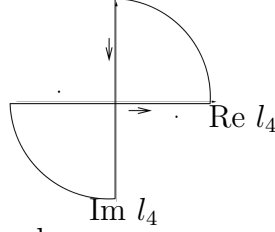
$$\begin{aligned} R^2 &= Q^2 - \sum_{i=1}^N z_i (r_i^2 - m_i^2) \\ &= \sum_{i,j=1}^N z_i z_j r_i \cdot r_j - \frac{1}{2} \sum_{i=1}^N z_i (r_i^2 - m_i^2) \sum_{j=1}^N z_j - \frac{1}{2} \sum_{j=1}^N z_j (r_j^2 - m_j^2) \sum_{i=1}^N z_i \\ &= -\frac{1}{2} \sum_{i,j=1}^N z_i z_j (r_i^2 + r_j^2 - 2 r_i \cdot r_j - m_i^2 - m_j^2) \\ &= -\frac{1}{2} \sum_{i,j=1}^N z_i z_j \mathcal{S}_{ij} \\ \mathcal{S}_{ij} &= (r_i - r_j)^2 - m_i^2 - m_j^2 \end{aligned} \quad (3.19)$$

The matrix \mathcal{S}_{ij} , sometimes also called *Cayley matrix* is an important quantity encoding all the kinematic dependence of the integral. It plays a major role in the algebraic reduction of tensor integrals or integrals with higher N to simpler objects, as well as in the analysis of so-called *Landau singularities*, which are singularities where $\det \mathcal{S}$ or a sub-determinant of \mathcal{S} is vanishing (see below for more details).

Remember that we are in Minkowski space, where $l^2 = l_0^2 - \vec{l}^2$, so temporal and spatial components are not on equal footing. Note that the poles of the denominator in Eq. (3.18) are located at $l_0^2 = R^2 + \vec{l}^2 - i\delta \Rightarrow l_0^\pm \simeq \pm\sqrt{R^2 + \vec{l}^2} \mp i\delta$. Thus the $i\delta$ term shifts the poles away from the real axis in the l_0 -plane.

For the integration over the loop momentum, we better work in Euclidean space where $l_E^2 = \sum_{i=1}^D l_i^2$. Hence we make the transformation $l_0 \rightarrow i l_4$, such that $l^2 \rightarrow -l_E^2 = l_4^2 + \vec{l}^2$, which implies that the integration contour in the complex l_0 -plane is rotated by 90° such that the contour in the complex l_4 -plane looks as shown below. This is called *Wick rotation*. We see that the $i\delta$ prescription is exactly such that the contour does not enclose any poles. Therefore the integral over the closed contour is zero, and we can use the identity

$$\int_{-\infty}^\infty dl_0 f(l_0) = - \int_{i\infty}^{-i\infty} dl_0 f(l_0) = i \int_{-\infty}^\infty dl_4 f(l_4) \quad (3.20)$$



Our integral now reads

$$I_N^D = (-1)^N \Gamma(N) \int_0^\infty \prod_{i=1}^N dz_i \delta(1 - \sum_{l=1}^N z_l) \int_{-\infty}^\infty \frac{d^D l_E}{\pi^{\frac{D}{2}}} [l_E^2 + R^2 - i\delta]^{-N} \quad (3.21)$$

Now we can introduce polar coordinates in D dimensions to evaluate the momentum integral.

$$\int_{-\infty}^\infty d^D l = \int_0^\infty dr r^{D-1} \int d\Omega_{D-1}, \quad r = \sqrt{l_E^2} = \left(\sum_{i=1}^4 l_i^2 \right)^{\frac{1}{2}} \quad (3.22)$$

$$\int d\Omega_{D-1} = V(D) = \frac{2\pi^{\frac{D}{2}}}{\Gamma(\frac{D}{2})} \quad (3.23)$$

where $V(D)$ is the volume of a unit sphere in D dimensions:

$$V(D) = \int_0^{2\pi} d\theta_1 \int_0^\pi d\theta_2 \sin \theta_2 \dots \int_0^\pi d\theta_{D-1} (\sin \theta_{D-1})^{D-2}.$$

Thus we have

$$I_N^D = 2(-1)^N \frac{\Gamma(N)}{\Gamma(\frac{D}{2})} \int_0^\infty \prod_{i=1}^N dz_i \delta(1 - \sum_{l=1}^N z_l) \int_0^\infty dr r^{D-1} \frac{1}{[r^2 + R^2 - i\delta]^N}$$

Substituting $r^2 = x$:

$$\int_0^\infty dr r^{D-1} \frac{1}{[r^2 + R^2 - i\delta]^N} = \frac{1}{2} \int_0^\infty dx x^{D/2-1} \frac{1}{[x + R^2 - i\delta]^N} \quad (3.24)$$

Now the x -integral can be identified as the Euler Beta-function $B(a, b)$, defined as

$$B(a, b) = \int_0^\infty dz \frac{z^{a-1}}{(1+z)^{a+b}} = \int_0^1 dy y^{a-1} (1-y)^{b-1} = \frac{\Gamma(a)\Gamma(b)}{\Gamma(a+b)} \quad (3.25)$$

and after normalising with respect to R^2 we finally arrive at

$$I_N^D = (-1)^N \Gamma(N - \frac{D}{2}) \int_0^\infty \prod_{i=1}^N dz_i \delta(1 - \sum_{l=1}^N z_l) [R^2 - i\delta]^{\frac{D}{2}-N}. \quad (3.26)$$

The integration over the Feynman parameters remains to be done, but for one-loop applications, the integrals we need to know explicitly have maximally $N = 4$ external legs. Integrals with $N > 4$ can be expressed in terms of boxes, triangles, bubbles and tadpoles (in the case of massive propagators). The analytic expressions for these “master integrals” are well-known. The most complicated analytic functions which can appear at one loop are dilogarithms.

The generic form of the derivation above makes clear that we do not have to go through the procedure of Wick rotation explicitly each time. All we need (for scalar integrals) is to use the following general formula for D -dimensional momentum integration (in Minkowski space, and after having performed the shift to have a quadratic form in the denominator):

$$\int \frac{d^D l}{i\pi^{\frac{D}{2}}} \frac{(l^2)^r}{[l^2 - R^2 + i\delta]^N} = (-1)^{N+r} \frac{\Gamma(r + \frac{D}{2})\Gamma(N - r - \frac{D}{2})}{\Gamma(\frac{D}{2})\Gamma(N)} [R^2 - i\delta]^{r-N+\frac{D}{2}} \quad (3.27)$$

Example one-loop two-point function

Applying the above procedure to our two-point function, we obtain

$$I_2 = \Gamma(2) \int_0^1 dz \int_{-\infty}^{\infty} \frac{d^D l}{i\pi^{\frac{D}{2}}} \frac{1}{[l^2 - R^2 + i\delta]^2} \quad (3.28)$$

$$R^2 = Q^2 - A = -p^2 z (1 - z) + m^2 \Rightarrow \\ I_2 = \Gamma(2 - \frac{D}{2}) \int_0^1 dz [-p^2 z (1 - z) + m^2 - i\delta]^{\frac{D}{2}-2}. \quad (3.29)$$

For $m^2 = 0$, the result can be expressed in terms of Γ -functions:

$$I_2 = (-p^2)^{\frac{D}{2}-2} \Gamma(2 - D/2) B(D/2 - 1, D/2 - 1), \quad (3.30)$$

where the $B(a, b)$ is defined in Eq. (3.25). The two-point function has an UV pole which is contained in

$$\Gamma(2 - D/2) = \Gamma(\epsilon) = \frac{1}{\epsilon} - \gamma_E + \mathcal{O}(\epsilon), \quad (3.31)$$

where γ_E is “Euler’s constant”, $\gamma_E = \lim_{n \rightarrow \infty} \left(\sum_{j=1}^n \frac{1}{j} - \ln n \right) = 0.5772156649\dots$

Including the factor $g^2 \mu^{2\epsilon}$ which usually comes with the loop, and multiplying by $\frac{i\pi^{\frac{D}{2}}}{(2\pi)^D}$ for the normalisation conventions, we obtain

$$g^2 \mu^{2\epsilon} I_2 = (4\pi)^\epsilon i \frac{g^2}{(4\pi)^2} \Gamma(\epsilon) (-p^2/\mu^2)^{-\epsilon} B(1 - \epsilon, 1 - \epsilon). \quad (3.32)$$

Useful to know:

- As the combination $\Delta = \frac{1}{\epsilon} - \gamma_E + \ln(4\pi)$ always occurs in combination with a pole, in the so-called $\overline{\text{MS}}$ subtraction scheme (“modified Minimal Subtraction”), the whole combination Δ is subtracted in the renormalisation procedure.
- Scaleless integrals (i.e. integrals containing no dimensionful scale like masses or external momenta) are zero in dimensional regularisation, more precisely:

$$\int_{-\infty}^{\infty} \frac{d^D k}{k^{2\rho}} = i\pi V(D) \delta(\rho - D/2). \quad (3.33)$$

- If we use dimension splitting into $2m$ integer dimensions and the remaining 2ϵ -dimensional space, $k_{(D)}^2 = k_{(2m)}^2 + \tilde{k}_{(-2\epsilon)}^2$, we will encounter additional integrals with powers of $(\tilde{k}^2)^\alpha$ in the numerator. These are related to integrals in higher dimensions by

$$\int \frac{d^D k}{i\pi^{\frac{D}{2}}} (\tilde{k}^2)^\alpha f(k^\mu, k^2) = (-1)^\alpha \frac{\Gamma(\alpha + \frac{D}{2} - 2)}{\Gamma(\frac{D}{2} - 2)} \int \frac{d^{D+2\alpha} k}{i\pi^{\frac{D}{2} + \alpha}} f(k^\mu, k^2). \quad (3.34)$$

Note that $1/\Gamma(\frac{D}{2} - 2)$ is of order ϵ . Therefore the integrals with $\alpha > 0$ only contribute if the k -integral in $4 - 2\epsilon + 2\alpha$ dimensions is divergent. In this case they contribute a part which cannot contain a logarithm or dilogarithm (because it is the coefficient of an UV pole at one loop), so must be a rational function of the invariants involved (masses, kinematic invariants s_{ij}). Such contributions form part of the so-called “rational part” of the full amplitude.

Tensor integrals

If we have loop momenta in the numerator, as in eq. (3.12) for $r > 0$, the integration procedure is essentially the same, except for combinatorics and additional Feynman parameters in the numerator. The substitution $k = l - Q$ introduces terms of the form $(l - Q)^{\mu_1} \dots (l - Q)^{\mu_r}$ into the numerator of eq. (3.18). As the denominator is symmetric under $l \rightarrow -l$, only the terms with even numbers of l^μ in the numerator will give a non-vanishing contribution upon l -integration. Further, we know that integrals where the Lorentz structure is only carried by loop momenta, but not by external momenta, can only be proportional to combinations of metric tensors $g^{\mu\nu}$. Therefore we have, as the tensor-generalisation of eq. (3.27),

$$\int_{-\infty}^{\infty} \frac{d^D l}{i\pi^{\frac{D}{2}}} \frac{l^{\mu_1} \dots l^{\mu_{2m}}}{[l^2 - R^2 + i\delta]^N} = (-1)^N \left[(g^{\cdot\cdot})^{\otimes m} \right]^{\{\mu_1 \dots \mu_{2m}\}} \left(-\frac{1}{2} \right)^m \frac{\Gamma(N - \frac{D+2m}{2})}{\Gamma(N)} (R^2 - i\delta)^{-N+(D+2m)/2}, \quad (3.35)$$

which can be derived for example by taking derivatives of the unintegrated scalar expression with respect to l^μ . $(g^\cdot) \otimes m$ denotes m occurrences of the metric tensor and the sum over all possible distributions of the $2m$ Lorentz indices μ_i to the metric tensors is denoted by $[\dots]^{\{\mu_1 \dots \mu_{2m}\}}$. Thus, for a general tensor integral, working out the numerators containing the combinations of external vectors Q^μ , one finds the following formula:

$$I_N^{D, \mu_1 \dots \mu_r} = \sum_{m=0}^{\lfloor r/2 \rfloor} \left(-\frac{1}{2} \right)^m \sum_{j_1, \dots, j_{r-2m}=1}^{N-1} [(g^\cdot) \otimes m r_{j_1}^\cdot \dots r_{j_{r-2m}}^\cdot]^{\{\mu_1 \dots \mu_r\}} I_N^{D+2m}(j_1, \dots, j_{r-2m}) \quad (3.36)$$

$$I_N^d(j_1, \dots, j_\alpha) = (-1)^N \Gamma(N - \frac{d}{2}) \int \prod_{i=1}^N dz_i \delta(1 - \sum_{l=1}^N z_l) z_{j_1} \dots z_{j_\alpha} (R^2 - i\delta)^{d/2-N} \quad (3.37)$$

$$R^2 = -\frac{1}{2} z \cdot \mathcal{S} \cdot z$$

The distribution of the r Lorentz indices μ_i to the external vectors $r_j^{\mu_i}$ is denoted by $[\dots]^{\{\mu_1 \dots \mu_r\}}$. These are $\binom{r}{2m} \prod_{k=1}^m (2k-1)$ terms. $(g^\cdot) \otimes m$ denotes m occurrences of the metric tensor and $\lfloor r/2 \rfloor$ is the nearest integer less or equal to $r/2$. Integrals with $z_{j_1} \dots z_{j_\alpha}$ in eq. (3.37) are associated with external vectors $r_{j_1} \dots r_{j_\alpha}$, stemming from factors of Q^μ in eq. (3.18).

How the higher dimensional integrals I_N^{D+2m} in eq. (3.36), associated with metric tensors $(g^\cdot) \otimes m$, arise, is left as an exercise.

Form factor representation

A *form factor representation* of a tensor integral (or a tensor in general) is a representation where the Lorentz structure has been extracted, each Lorentz tensor multiplying a scalar quantity, the *form factor*. Distinguishing A, B, C depending on the presence of zero, one or two metric tensors, we can write

$$\begin{aligned} I_N^{D, \mu_1 \dots \mu_r}(S) &= \\ &\sum_{j_1 \dots j_r \in S} r_{j_1}^{\mu_1} \dots r_{j_r}^{\mu_r} A_{j_1 \dots j_r}^{N,r}(S) \\ &+ \sum_{j_1 \dots j_{r-2} \in S} [g^\cdot r_{j_1}^\cdot \dots r_{j_{r-2}}^\cdot]^{\{\mu_1 \dots \mu_r\}} B_{j_1 \dots j_{r-2}}^{N,r}(S) \\ &+ \sum_{j_1 \dots j_{r-4} \in S} [g^\cdot g^\cdot r_{j_1}^\cdot \dots r_{j_{r-4}}^\cdot]^{\{\mu_1 \dots \mu_r\}} C_{j_1 \dots j_{r-4}}^{N,r}(S). \end{aligned} \quad (3.38)$$

Example for the distribution of indices:

$$I_N^{D,\mu_1\mu_2\mu_3}(S) = \sum_{l_1,l_2,l_3 \in S} r_{l_1}^{\mu_1} r_{l_2}^{\mu_2} r_{l_3}^{\mu_3} A_{l_1 l_2 l_3}^{N,3}(S) + \sum_{l \in S} (g^{\mu_1\mu_2} r_l^{\mu_3} + g^{\mu_1\mu_3} r_l^{\mu_2} + g^{\mu_2\mu_3} r_l^{\mu_1}) B_l^{N,3}(S).$$

Note that we never need more than two metric tensors in a gauge where the rank $r \leq N$. Three metric tensors would be needed for rank six, and with the restriction $r \leq N$, rank six could only be needed for six-point integrals or higher. However, we can immediately reduce integrals with $N > 5$ to lower-point ones, because for $N \geq 6$ we have the relation

$$I_N^{D,\mu_1\dots\mu_r}(S) = - \sum_{j \in S} C_j^{\mu_1} I_{N-1}^{D,\mu_2\dots\mu_r}(S \setminus \{j\}) \quad (N \geq 6), \quad (3.39)$$

where $C_l^\mu = \sum_{k \in S} (\mathcal{S}^{-1})_{kl} r_k^\mu$ if \mathcal{S} is invertible (and if not, it can be constructed from the pseudo-inverse [26, 27]). The fact that integrals with $N \geq 6$ can be reduced to lower-point ones so easily (without introducing higher dimensional integrals) is related to the fact that in 4 space-time dimensions, we can have maximally 4 independent external momenta, the additional external momenta must be linearly dependent on the 4 ones picked to span Minkowski space. (Note that for $N = 5$ we can eliminate one external momentum by momentum conservation, to be left with 4 independent ones in 4 dimensions.) In D dimensions there is a subtlety, this is why the case $N = 5$ is special:

$$I_5^D(S) = \sum_{j \in S} b_j \left(I_4^D(S \setminus \{j\}) - (4 - D) I_5^{D+2}(S) \right), \quad (3.40)$$

with $b_j = \sum_{k \in S} (\mathcal{S}^{-1})_{kj}$. As $4 - D = 2\epsilon$ and I_5^{D+2} is always finite, the second term can be dropped for one-loop applications. Similar for pentagon tensor integrals [26].

Historically, tensor integrals occurring in one-loop amplitudes were reduced to scalar integrals using so-called *Passarino-Veltman* reduction [28]. It is based on the fact that at one loop, scalar products of loop momenta with external momenta can always be expressed as combinations of propagators. The problem with Passarino-Veltman reduction is that it introduces powers of inverse Gram determinants $1/(\det G)^r$ for the reduction of a rank r tensor integral. This can lead to numerical instabilities upon phase space integration in kinematic regions where $\det G \rightarrow 0$.

Example for *Passarino-Veltman reduction*:

Consider a rank one three-point integral

$$I_3^{D,\mu}(S) = \int_{-\infty}^{\infty} d\bar{k} \frac{k^\mu}{[k^2 + i\delta][(k + p_1)^2 + i\delta][(k + p_1 + p_2)^2 + i\delta]} = A_1 r_1^\mu + A_2 r_2^\mu$$

$$r_1 = p_1, \quad r_2 = p_1 + p_2.$$

Contracting with r_1 and r_2 and using the identities

$$k \cdot r_i = \frac{1}{2} [(k + r_i)^2 - k^2 - r_i^2], \quad i \in \{1, 2\}$$

we obtain, after cancellation of numerators

$$\begin{pmatrix} 2r_1 \cdot r_1 & 2r_1 \cdot r_2 \\ 2r_2 \cdot r_1 & 2r_2 \cdot r_2 \end{pmatrix} \begin{pmatrix} A_1 \\ A_2 \end{pmatrix} = \begin{pmatrix} R_1 \\ R_2 \end{pmatrix} \quad (3.41)$$

$$R_1 = I_2^D(r_2) - I_2^D(r_2 - r_1) - r_1^2 I_3(r_1, r_2)$$

$$R_2 = I_2^D(r_1) - I_2^D(r_2 - r_1) - r_2^2 I_3(r_1, r_2).$$

We see that the solution involves the inverse of the Gram matrix $G_{ij} = 2r_i \cdot r_j$.

Libraries where the scalar integrals and tensor one-loop form factors can be obtained numerically:

- `LoopTools` [29, 30]
- `OneLoop` [31]
- `golem95` [32–34]
- `Collier` [35]
- `Package-X` [36]

Scalar integrals only: `QCDLoop` [37, 38].

The calculation of one-loop amplitudes with many external legs is most efficiently done using “unitarity-cut-inspired” methods, for a review see Ref. [39]. One of the advantages is that it allows (numerical) reduction at *integrand level* (rather than integral level), which helps to avoid the generation of spurious terms which blow up intermediate expressions before gauge cancellations come into action.

3.4 Renormalisation

We have seen already how UV divergences can arise and how to regularize them. The procedure to absorb the divergences into a re-definition of parameters and fields is called *renormalisation*. How to deal with the finite parts defines the *renormalisation scheme*. Physical observables cannot depend on the chosen renormalisation scheme (but remember that for example the top quark mass is not an observable, so the value for the top quark mass is scheme dependent).

As QCD is renormalisable, the renormalisation procedure does not change the structure of the interactions present at tree level. The renormalised Lagrangian is obtained by rewriting the “bare” Lagrangian in terms of renormalised fields as

$$\mathcal{L}(A_0, q_0, \eta_0, m_0, g_0, \lambda_0) = \mathcal{L}(A, q, \eta, m, g\mu^\epsilon, \lambda) + \mathcal{L}_c(A, q, \eta, m, g\mu^\epsilon, \lambda), \quad (3.42)$$

where \mathcal{L}_c defines the counterterms. The bare and renormalised quantities are related by

$$\begin{aligned} A^\mu &= Z_3^{-\frac{1}{2}} A_0^\mu, \quad \lambda = Z_3^{-1} \lambda_0, \quad q = Z_2^{-\frac{1}{2}} q_0, \quad m = Z_m^{-1} m_0, \quad \eta = \tilde{Z}_3^{-\frac{1}{2}} \eta_0, ; \\ g_0 &= g\mu^\epsilon \frac{Z_1}{Z_3^{\frac{3}{2}}} = g\mu^\epsilon \frac{\tilde{Z}_1}{\tilde{Z}_3 Z_3^{\frac{1}{2}}} = g\mu^\epsilon \frac{Z_1^F}{Z_2} = g\mu^\epsilon \frac{Z_4^{\frac{1}{2}}}{Z_3} = g\mu^\epsilon Z_g . \end{aligned} \quad (3.43)$$

In Eq. (3.43), the renormalisation constants $Z_1, Z_1^F, \tilde{Z}_1, Z_4$ refer to the 3-gluon vertex, quark-gluon-vertex, ghost-gluon vertex and 4-gluon vertex, respectively. The counterterm Lagrangian thus naively is given by

$$\begin{aligned} \mathcal{L}_c = & -\frac{1}{4}(Z_3 - 1)(\partial_\mu A_\nu - \partial_\nu A_\mu)^2 + i(Z_2 - 1)\bar{q} \not{\partial} q \\ & - (Z_2 Z_m - 1)\bar{q} m q + (\tilde{Z}_3 - 1)\partial_\mu \eta^\dagger \partial^\mu \eta \\ & + \frac{g}{2}\mu^\epsilon(Z_1 - 1)f^{abc}(\partial_\mu A_\nu^a - \partial_\nu A_\mu^a)A_b^\mu A_c^\nu + (\tilde{Z}_1 - 1)ig\mu^\epsilon \partial_\mu \eta^\dagger \mathcal{A}^\mu \eta \\ & - (Z_1^F - 1)g\mu^\epsilon \bar{q} \mathcal{A}^\mu q - \frac{g^2}{4}\mu^{2\epsilon}(Z_4 - 1)f^{abc}f^{ade}A_b^\mu A_c^\nu A_d^\mu A_e^\nu . \end{aligned} \quad (3.44)$$

However, not all the constants are independent. Otherwise we would have a problem with the renormalisation of the strong coupling constant in Eq. (3.43), because it would lead to different values for Z_g . Fortunately, we can exploit the Slavnov-Taylor identities

$$\frac{Z_1}{Z_3} = \frac{\tilde{Z}_1}{\tilde{Z}_3} = \frac{Z_1^F}{Z_2} = \frac{Z_4}{Z_1}, \quad (3.45)$$

which are generalisations of the Ward Identity $Z_1^F = Z_2$ for QED.

The β -function in D dimensions

As we saw already, the running of α_s is a consequence of the renormalisation scale independence of physical observables. The bare coupling g_0 knows nothing about our choice of μ . Therefore we must have

$$\frac{dg_0}{d\mu} = 0 . \quad (3.46)$$

Using the definition

$$g_0 = g\mu^\epsilon Z_g \quad (3.47)$$

we obtain

$$\mu^{2\epsilon} \left(\epsilon Z_g \alpha_s + 2\alpha_s \frac{dZ_g}{dt} + Z_g \frac{d\alpha_s}{dt} \right) = 0 , \quad (3.48)$$

where $\frac{d}{dt} = \mu^2 \frac{d}{d\mu^2} = \frac{d}{d\ln \mu^2}$. Z_g depends upon μ only through α_s (at least in the $\overline{\text{MS}}$ scheme). Using $\beta(\alpha_s) = \frac{d\alpha_s}{dt}$ we obtain

$$\beta(\alpha_s) + 2\alpha_s \frac{1}{Z_g} \frac{dZ_g}{d\alpha_s} \beta(\alpha_s) = -\epsilon \alpha_s . \quad (3.49)$$

Now we expand Z_g as

$$Z_g = 1 - \frac{1}{\epsilon} \frac{b_0}{2} \alpha_s + \mathcal{O}(\alpha_s^2) \quad (3.50)$$

and obtain

$$\beta(\alpha_s) = -\epsilon \alpha_s \frac{1}{1 - \frac{b_0 \alpha_s}{\epsilon}} = -b_0 \alpha_s^2 + \mathcal{O}(\alpha_s^3, \epsilon) . \quad (3.51)$$

This means that the β -function can be obtained from the coefficient of the single pole of Z_g . In fact, in the $\overline{\text{MS}}$ scheme, this remains even true beyond one-loop.

Remarks about singularities

- The *overall* UV divergence of an integral can be determined by power counting: if we work in D dimensions at L loops, and consider an integral with P propagators and n_l factors of the loop momentum belonging to loop $l \in \{1, \dots, L\}$ in the numerator, we can define a “superficial” degree of UV divergence by $\omega = D L - 2P + 2 \sum_l \lfloor n_l / 2 \rfloor$, where $\lfloor n_l / 2 \rfloor$ is the nearest integer less or equal to $n_l / 2$. (The actual degree of divergence may be less, for example due to gauge cancellations). We have logarithmic, linear, quadratic, ... divergences for $\omega = 0, 1, 2, \dots$ and no UV divergence for $\omega < 0$. This means for example that in 4 dimensions at one loop, we have UV divergences in all two-point functions, three-point functions with rank ≥ 2 and four-point functions with rank ≥ 4 .

- IR divergences: $1/\epsilon^{2L}$ at worst. Necessary conditions for IR divergences in Feynman parametrised loop integrals are given by the *Landau equations*, which in our notation above read

$$\forall i \ z_i (q_i^2 - m_i^2) = 0 , \sum_{i=1}^N z_i q_i = 0 . \quad (3.52)$$

If eq. (3.52) has a solution $z_i > 0$ for every $i \in \{1, \dots, N\}$, i.e. all particles in the loop are *simultaneously on-shell*, then the integral has a *leading Landau singularity*. If a solution exists where some $z_i = 0$ while the other z_j are positive, the Landau condition corresponds to a sub-leading Landau singularity. Soft and/or collinear singularities appearing as poles in $1/\epsilon$ are always stemming from some $z_i = 0$. At one loop, introducing the matrix Q , which, under the condition $q_i^2 = m_i^2$ (“on-shell”), is equal to \mathcal{S} or a minor of the latter

$$Q_{ij} = 2q_i \cdot q_j = m_i^2 + m_j^2 - (q_i - q_j)^2 = m_i^2 + m_j^2 - (r_i - r_j)^2 , \\ i, j \in \{1, 2, \dots, M\}, (M \leq N), \quad (3.53)$$

the Landau singularities correspond to $\det Q = 0$ for $z_i \neq 0$.

Example: “normal” thresholds contained in triangle diagrams. If all internal masses are equal:

$$\mathcal{S} = \begin{pmatrix} -2m^2 & p_2^2 - 2m^2 & p_1^2 - 2m^2 \\ p_2^2 - 2m^2 & -2m^2 & p_3^2 - 2m^2 \\ p_1^2 - 2m^2 & p_3^2 - 2m^2 & -2m^2 \end{pmatrix} \quad (3.54)$$

Crossing out row and column three corresponds to a two-point diagram stemming from a triangle with propagator 3 omitted (“pinched”). The corresponding submatrix has determinant $\det Q^{(2)} = -p_2^2(p_2^2 - 4m^2)$. So we see that the sub-leading Landau singularity corresponds to the mass threshold of the bubble at $s_2 = p_2^2 = 4m^2$.

3.5 NLO calculations and infrared singularities

3.5.1 Structure of NLO calculations

Next-to-leading order calculations consist of several parts, which can be classified as virtual corrections (containing usually one loop), real corrections (radiation of extra particles relative to leading order) and subtraction terms. In the following we will assume that the virtual corrections already include UV renormalisation, such that the subtraction terms only concern the subtraction of the infrared (IR, soft and collinear)

singularities. We will consider “NLO” as next-to-leading order in an expansion in the strong coupling constant, even though the general structure is very similar for electroweak corrections. The real and virtual contributions to the simple example $\gamma^* \rightarrow q\bar{q}$ are shown in Fig. 11.

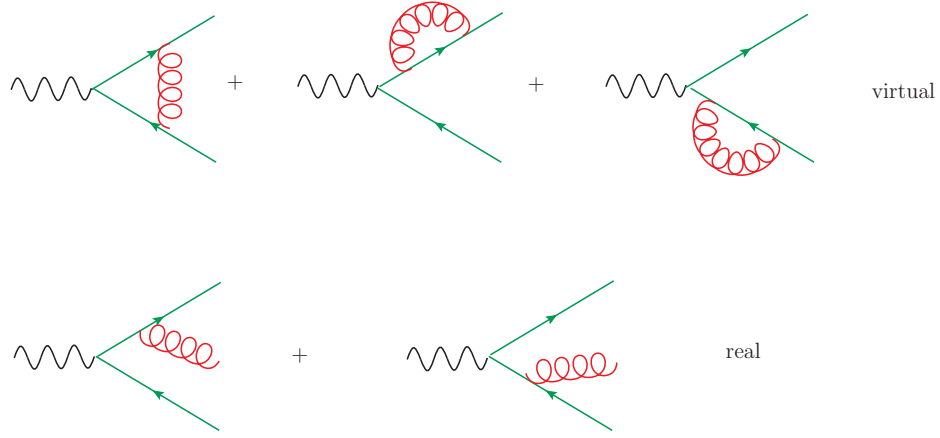


Figure 11: The real and virtual contributions to $\gamma^* \rightarrow q\bar{q}$ at order α_s .

If \mathcal{M}_0 is the leading order amplitude (also called *Born* amplitude) and $\mathcal{M}_{\text{virt}}, \mathcal{M}_{\text{real}}$ are the virtual and real amplitudes as shown in Fig. 11, the corresponding cross section is given by

$$\sigma^{NLO} = \underbrace{\int d\phi_2 |\mathcal{M}_0|^2}_{\sigma^{LO}} + \int_R d\phi_3 |\mathcal{M}_{\text{real}}|^2 + \int_V d\phi_2 2\text{Re}(\mathcal{M}_{\text{virt}} \mathcal{M}_0^*) . \quad (3.55)$$

The sum of the integrals \int_R and \int_V above is finite. However, this is not true for the individual contributions. The real part contains divergences due to soft and collinear radiation of massless particles. While $\mathcal{M}_{\text{real}}$ itself is a tree level amplitude and thus finite, the divergences show up upon integration over the phase space $d\Phi_3$. In \int_V , the phase space is the same as for the *Born* amplitude, but the loop integrals contained in $\mathcal{M}_{\text{virt}}$ contain IR singularities.

Let us anticipate the answer, which we will (partly) calculate later. We find:

$$\begin{aligned} \sigma_R &= \sigma^{\text{Born}} H(\epsilon) C_F \frac{\alpha_s}{2\pi} \left(\frac{2}{\epsilon^2} + \frac{3}{\epsilon} + \frac{19}{2} - \pi^2 \right) , \\ \sigma_V &= \sigma^{\text{Born}} H(\epsilon) C_F \frac{\alpha_s}{2\pi} \left(-\frac{2}{\epsilon^2} - \frac{3}{\epsilon} - 8 + \pi^2 \right) , \end{aligned} \quad (3.56)$$

where $H(\epsilon) = 1 + \mathcal{O}(\epsilon)$, and the exact form is irrelevant here, because the poles in ϵ all cancel! This must be the case according to the KLN (Kinoshita-Lee-Nauenberg)

theorem [40, 41]. It says that *IR singularities must cancel when summing the transition rate over all degenerate (initial and final) states*. In our example, we do not have initial state singularities. However, in the final state we can have massless quarks accompanied by soft and/or collinear gluons (resp. just one extra gluon at order α_s). Such a state cannot be distinguished from just a quark state, and therefore is degenerate. Only when summing over all the final state multiplicities (at each order in α_s), the divergences cancel. Another way of stating this is looking at the squared amplitude at order α_s and considering all cuts, see Fig. 12 (contributions which are zero for massless quarks are not shown). The KLN theorem states that the sum of all cuts leading to physical final states is free of IR poles. We will later calculate the real radiation amplitude and

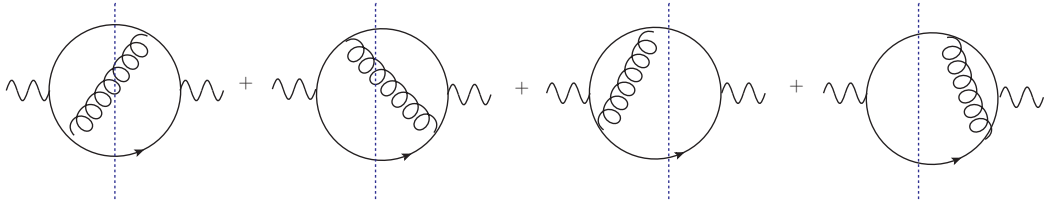


Figure 12: The sum over cuts of the amplitude squared shown above is finite according to the KLN theorem.

see how the singularities come about.

Note that the general formula to obtain a cross section from the amplitude is given by

$$d\sigma = \frac{S}{\text{flux}} \bar{\Sigma} |\mathcal{M}|^2 d\Phi , \quad (3.57)$$

where $S = 1/j!$ is a symmetry factor for j identical particles in the final state and $\bar{\Sigma}$ usually means the average over colours and polarisation states of initial state particles and the sum over colours and polarisations of final state particles. Note that the flux factor for two massless initial state particles (e.g. in $e^+e^- \rightarrow \text{hadrons}$) is just $4 p_1 \cdot p_2 = 2 \hat{s}$.

The cancellations between \int_R and \int_V in Eq. (3.55) are highly non-trivial, because the phase space integrals contain a different number of particles in the final state. If we want to calculate a prediction for a certain observable, we need to multiply the amplitude by a *measurement function* $J(p_1 \dots p_n)$ containing for example a jet definition, acting on the n particles in the final state. Schematically, the structure of the cross section then is the following. Let us consider the case where we have an IR pole if the variable x , denoting for example the energy of an extra gluon in the real

radiation part, goes to zero. If we define

$$\begin{aligned}\mathcal{B}_n &= \int d\phi_n |\mathcal{M}_0|^2 = \int d\phi_n B_n \\ \mathcal{V}_n &= \int d\phi_n 2Re(\mathcal{M}_{\text{virt}}\mathcal{M}_0^*) = \int d\phi_n \frac{V_n}{\epsilon} \\ \mathcal{R}_n &= \int d\phi_{n+1} |\mathcal{M}_{\text{real}}|^2 = \int d\phi_n \int_0^1 dx x^{-1-\epsilon} R_n(x)\end{aligned}\quad (3.58)$$

and a measurement function $J(p_1 \dots p_n, x)$ we have

$$\sigma^{NLO} = \int d\phi_n \left\{ \left(B_n + \frac{V_n}{\epsilon} \right) J(p_1 \dots p_n, 0) + \int_0^1 dx x^{-1-\epsilon} R_n(x) J(p_1 \dots p_n, x) \right\}. \quad (3.59)$$

The cancellation of the pole in $\frac{V_n}{\epsilon}$ by the integral over $R_n(x)$ will only work if

$$\lim_{x \rightarrow 0} J(p_1 \dots p_n, x) = J(p_1 \dots p_n, 0). \quad (3.60)$$

This is a non-trivial condition for the definition of an observable, for example a jet algorithm, and is called *infrared safety*. Note that the measurement function is also important if we define differential cross sections $d\sigma/dX$ (also called distributions), for example the transverse momentum distribution $d\sigma/dp_T$ of one of the final state particles. In this case we have $J(p_1 \dots p_n) = \delta(X - \chi_n(p_i))$, where $\chi_n(p_i)$ is the definition of the observable, based on n partons. Again, infrared safety requires $\chi_{n+1}(p_i) \rightarrow \chi_n$ if one of the p_i becomes soft or two of the momenta become collinear to each other, see below.

3.5.2 Soft gluon emission

Soft gluon emission is very important in QCD, and also simpler in structure than collinear singularities. Soft gluons are insensitive to the spin of the partons. The only feature they are sensitive to is the colour charge.

To see this, consider the amplitude for the second line in Fig. 11, with momentum k and colour index a for the gluon, and momenta, colour indices $p, i (\bar{p}, j)$ for the quark (antiquark). The amplitude for massless quarks is given by (suppressing colour indices on the left-hand side)

$$\mathcal{M}^\mu = t_{ij}^a g_s \bar{u}(p) \not{\epsilon}(k) \frac{\not{p} + k}{(p+k)^2} \Gamma^\mu v(\bar{p}) - t_{ij}^a g_s \bar{u}(p) \Gamma^\mu \frac{\not{p} + k}{(\bar{p}+k)^2} \not{\epsilon}(k) v(\bar{p}), \quad (3.61)$$

where Γ^μ describes the interaction vertex with the photon. Now we take the soft limit, which means that all components of k are much smaller than p and \bar{p} , thus neglecting

factors of \not{k} in the numerator and k^2 in the denominator. Using the Dirac equation leads to

$$\begin{aligned}\mathcal{M}_{soft}^\mu &= t_{ij}^a g_s \mu^\epsilon \left(\bar{u}(p) \frac{2\epsilon(k) \cdot p}{2p \cdot k} \Gamma^\mu v(\bar{p}) - \bar{u}(p) \Gamma^\mu \frac{2\epsilon(k) \cdot \bar{p}}{2\bar{p} \cdot k} v(\bar{p}) \right) \\ &= g_s \mu^\epsilon \mathbf{J}^{a,\nu}(k) \epsilon_\nu(k) \mathcal{M}_{Born}^\mu, \quad \mathcal{M}_{Born}^\mu = \bar{u}(p) \Gamma^\mu v(\bar{p}).\end{aligned}\quad (3.62)$$

We see that the amplitude factorises completely into the product of the Born amplitude and the *soft gluon current*

$$\mathbf{J}^{a,\mu}(k) = \sum_{r=p,\bar{p}} \mathbf{T}^a \frac{r^\mu}{r \cdot k}, \quad (3.63)$$

where in our example $\mathbf{T}^a = t_{ij}^a$ for $r = p$ and $\mathbf{T}^a = -t_{ij}^a$ for $r = \bar{p}$. This type factorisation actually holds for an arbitrary number of soft gluon emissions, and can be obtained using the “soft Feynman rules” shown in Fig. 13.

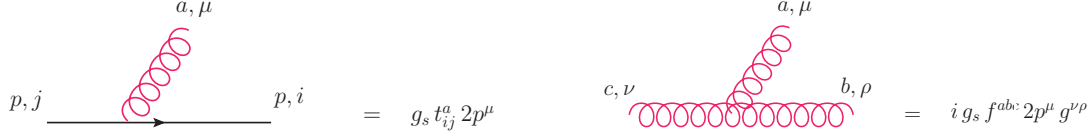


Figure 13: The Feynman rules for gluon emission in the soft limit.

Following the standards set by Refs. [42, 43], the soft gluon current is more conveniently expressed in terms of colour charge operators \mathbf{T}_i , where i now labels the *parton* i emitting a gluon (not its colour index), defined as follows: if the emitted gluon has colour index a , the colour-charge operator is:

$$\mathbf{T}_i \equiv T_i^a |a> \quad (3.64)$$

and its action onto the colour space is defined by

$$\langle a_1, \dots, a_i, \dots a_m, a | \mathbf{T}_i | b_1, \dots, b_i, \dots b_m \rangle = \delta_{a_1 b_1} \dots \delta_{a_m b_m} T_{a_i b_i}^a, \quad (3.65)$$

where $T_{bc}^a \equiv -i f_{abc}$ ($SU(3)$ generator in the adjoint representation) if the emitting particle i is a gluon and $T_{kl}^a \equiv t_{kl}^a$ ($SU(3)$ generator in the fundamental representation) if the emitting particle i is a quark. In the case of an emitting antiquark $T_{kl}^a \equiv \bar{t}_{kl}^a = -t_{lk}^a$.

The dependence of the matrix element on the colour indices c_1, \dots, c_m of the partons is written as

$$\mathcal{M}_{c_1, \dots, c_m}(p_1, \dots, p_m) \equiv \langle c_1, \dots, c_m | \mathcal{M}(p_1, \dots, p_m) \rangle. \quad (3.66)$$

Thus $\{|c_1, \dots, c_m\rangle\}$ is an abstract basis in colour space and the ket $|\mathcal{M}(p_1, \dots, p_m)\rangle$ is a vector in this space. According to this notation, the matrix element squared $|\mathcal{M}|^2$ (summed over the colours and spins of the partons) can be written as

$$|\mathcal{M}(p_1, \dots, p_m)|^2 = \langle \mathcal{M}(p_1, \dots, p_m) | \mathcal{M}(p_1, \dots, p_m) \rangle . \quad (3.67)$$

Note that, by definition, each vector $|\mathcal{M}(p_1, \dots, p_m)\rangle$ is a colour-singlet state. Therefore colour conservation is simply

$$\sum_{i=1}^m \mathbf{T}_i |\mathcal{M}(p_1, \dots, p_m)\rangle = 0 . \quad (3.68)$$

We can write down the universal behaviour of the matrix element $\mathcal{M}(k, p_1, \dots, p_m)$ in the limit where the momentum k of the gluon becomes soft. Denoting by a and $\varepsilon^\mu(k)$ the colour and the polarisation vector of the soft gluon, the matrix element fulfils the following factorisation formula:

$$\langle a | \mathcal{M}(k, p_1, \dots, p_m) \rangle \simeq g_s \mu^\epsilon \varepsilon^\mu(k) J_\mu^a(k) |\mathcal{M}(p_1, \dots, p_m)\rangle , \quad (3.69)$$

where $|\mathcal{M}(p_1, \dots, p_m)\rangle$ is obtained from the original matrix element by simply removing the soft gluon k . The factor $\mathbf{J}_\mu(k)$ is the soft-gluon current

$$\mathbf{J}^\mu(k) = \sum_{i=1}^m \mathbf{T}_i \frac{p_i^\mu}{p_i \cdot k} , \quad (3.70)$$

which depends on the momenta and colour charges of the hard partons in the matrix element on the right-hand side of Eq. (3.69). The symbol ‘ \simeq ’ means that on the right-hand side we have neglected contributions that are less singular than $1/|k|$ in the soft limit $k \rightarrow 0$.

An important property of the soft-gluon current is current conservation. Multiplying Eq. (3.70) by k^μ , we obtain

$$k^\mu \mathbf{J}_\mu(k) = \sum_{i=1}^m \mathbf{T}_i , \quad (3.71)$$

and thus

$$k^\mu \mathbf{J}_\mu(k) |\mathcal{M}(p_1, \dots, p_m)\rangle = \sum_{i=1}^m \mathbf{T}_i |\mathcal{M}(p_1, \dots, p_m)\rangle = 0 , \quad (3.72)$$

where the last equality follows from colour conservation as in Eq. (3.68). Although the factorisation formula (3.69) is most easily derived by working in a physical gauge,

the conservation of the soft-gluon current implies that Eq. (3.69) is actually gauge invariant. Any gauge transformation is equivalent to an addition of a longitudinal component to the polarisation vector of the soft gluon through the replacement $\varepsilon^\mu(k) \rightarrow \varepsilon^\mu(k) + \lambda k^\mu$. The factorisation formula (3.69) is invariant under this replacement, because of Eq. (3.72).

Squaring Eq. (3.69) and summing over the gluon polarisations leads to the universal soft-gluon factorisation formula at $\mathcal{O}(\alpha_s)$ for the squared amplitude [42]

$$|\mathcal{M}(k, p_1, \dots, p_m)|^2 \simeq -g_s^2 \mu^{2\epsilon} 2 \sum_{i,j=1}^m S_{ij}(k) |\mathcal{M}_{(i,j)}(p_1, \dots, p_m)|^2 , \quad (3.73)$$

where the factor

$$S_{ij}(p_s) = \frac{p_i \cdot p_j}{2(p_i \cdot p_s)(p_j \cdot p_s)} = \frac{s_{ij}}{s_{is}s_{js}} \quad (3.74)$$

is called *Eikonal factor*. It can be generalised to the emission of n soft gluons and plays an important role in resummation.

The colour correlations produced by the emission of a soft gluon are taken into account by the square of the colour-correlated amplitude $|\mathcal{M}_{(i,j)}|^2$, given by

$$\begin{aligned} |\mathcal{M}_{(i,j)}(p_1, \dots, p_m)|^2 &\equiv \langle \mathcal{M}(p_1, \dots, p_m) | \mathbf{T}_i \cdot \mathbf{T}_j | \mathcal{M}(p_1, \dots, p_m) \rangle \\ &= [\mathcal{M}_{c_1 \dots b_i \dots b_j \dots c_m}(p_1, \dots, p_m)]^* T_{b_i d_i}^a T_{b_j d_j}^a \mathcal{M}_{c_1 \dots d_i \dots d_j \dots c_m}(p_1, \dots, p_m) . \end{aligned} \quad (3.75)$$

3.5.3 Collinear singularities

Let us come back to the amplitude for the real radiation given in Eq. (3.61). In a frame where $p = E_p(1, \vec{0}^{(D-2)}, 1)$ and $k = k_0(1, \vec{0}^{(D-3)} \sin \theta, \cos \theta)$ the denominator $(p+k)^2$ is given by

$$(p+k)^2 = 2k_0 E_p (1 - \cos \theta) \rightarrow 0 \text{ for } \begin{cases} k_0 \rightarrow 0 & (\text{soft}) \\ \theta \rightarrow 0 & (\text{collinear}) \end{cases} \quad (3.76)$$

Note that if the quark line was massive, $p^2 = m^2$, we would have

$$(p+k)^2 - m^2 = 2k_0 E_p (1 - \beta \cos \theta) , \beta = \sqrt{1 - m^2/E_p^2}$$

and thus the collinear singularity would be absent. This is why it is sometimes also called *mass singularity*, since the propagator only can become collinear divergent if the partons are all massless, while the soft singularity is present irrespective of the quark mass.

The important point to remember is that in the collinear limit, we also have a form of factorisation, shown schematically in Fig. 14.

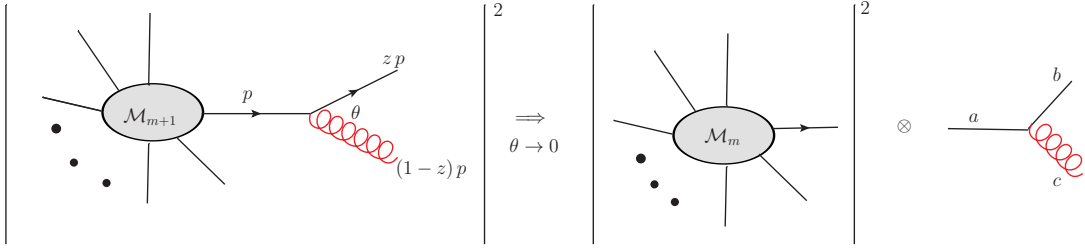


Figure 14: Factorisation in the collinear limit.

The universal factorisation behaviour can be described as

$$|\mathcal{M}_{m+1}|^2 d\Phi_{m+1} \rightarrow |\mathcal{M}_m|^2 d\Phi_m \frac{\alpha_s}{2\pi} \frac{dk_\perp^2}{k_\perp^2} \frac{d\phi}{2\pi} dz P_{a \rightarrow bc}(z) . \quad (3.77)$$

The function $P_{a \rightarrow bc}(z)$ is the so-called Altarelli-Parisi splitting function describing the splitting of parton a into partons b and c , and z is the momentum fraction of the original parton a taken away by parton b after emission of c . For example, consider collinear gluon emission off a quark:

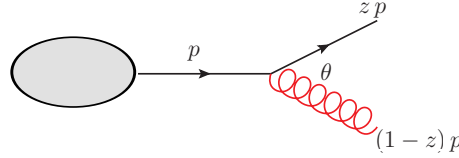


Figure 15: Gluon emission leading to $P_{q \rightarrow qg}(z)$.

The corresponding Altarelli-Parisi splitting function for $z < 1$ is given by

$$P_{q \rightarrow qg}(z) = C_F \frac{1+z^2}{1-z} , \quad (3.78)$$

and is often just denoted as $P_{qg}(z)$. The other possible splitting functions have the following form:

$$P_{q \rightarrow gg}(z) = C_F \frac{1+(1-z)^2}{z} , \quad (3.79)$$

$$P_{g \rightarrow q\bar{q}}(z) = T_R (z^2 + (1-z)^2) , \quad P_{g \rightarrow gg}(z) = C_A \left(z(1-z) + \frac{z}{1-z} + \frac{1-z}{z} \right) .$$

We will come back to them later when we discuss parton distribution functions.

To see how the factorisation formula Eq. (3.77) comes about, a convenient parametrisation of the gluon momentum k is the so-called *Sudakov parametrisation*:

$$k^\mu = (1-z)p^\mu + \beta n^\mu + k_\perp^\mu, \quad k^+ = k \cdot n = (1-z)p \cdot n, \quad k^- = k \cdot p = -\frac{k_\perp^2}{2(1-z)}, \quad (3.80)$$

where n^μ is a light-like vector with $p \cdot n \neq 0$ and $k_\perp \cdot n = 0$, and β can be determined by the requirement that k must be light-like:

$$k^2 = 0 = 2(1-z)\beta p \cdot n + k_\perp^2 \implies \beta = -\frac{k_\perp^2}{2p \cdot n(1-z)}, \quad (3.81)$$

and therefore $(p - k)^2 = k_\perp^2/(1-z)$. The part of the phase space due to the gluon emission then reads (in 4 dimensions, for D dimensions see below)

$$d\Phi_k \equiv \frac{d^4 k}{(2\pi)^3} \delta(k^2) = \frac{1}{8\pi^2} \frac{d\phi}{2\pi} \frac{dk^+}{2k^+} dk_\perp^2 = \frac{1}{16\pi^2} \frac{dz}{(1-z)} dk_\perp^2. \quad (3.82)$$

In this parametrisation, the soft gluon limit is $z \rightarrow 1$, the collinear singularity occurs for $k_\perp^2 \rightarrow 0$.

Now let us see explicitly in the $e^+e^- \rightarrow q\bar{q}$ example how the singularities manifest themselves as $1/\epsilon$ poles when we integrate over the D -dimensional phase space.

3.5.4 Phase space integrals in D dimensions

The general formula for a $1 \rightarrow n$ particle phase space $d\Phi_n$ with $Q \rightarrow p_1 \dots p_n$ is given by

$$d\Phi_{1 \rightarrow n} = (2\pi)^{n-D(n-1)} \left[\prod_{j=1}^n d^D p_j \delta(p_j^2 - m_j^2) \Theta(E_j) \right] \delta(Q - \sum_{j=1}^n p_j). \quad (3.83)$$

In the following we will stick to the massless case $m_j = 0$. We use

$$d^D p_j \delta(p_j^2) \Theta(E_j) = dE_j d^{D-1} \vec{p}_j \delta(E_j^2 - \vec{p}_j^2) \Theta(E_j) = \frac{1}{2E_j} d^{D-1} \vec{p}_j \Big|_{E_j=|\vec{p}_j|} \quad (3.84)$$

for $j = 1, \dots, n-1$ to arrive at

$$d\Phi_{1 \rightarrow n} = (2\pi)^{n-D(n-1)} 2^{1-n} \prod_{j=1}^{n-1} \frac{d^{D-1} \vec{p}_j}{|\vec{p}_j|} \delta((Q - \sum_{j=1}^{n-1} p_j)^2), \quad (3.85)$$

where we have used the last δ -function in Eq. (3.83) to eliminate p_n . We further use

$$\frac{d^{D-1}\vec{p}}{|\vec{p}|} f(|\vec{p}|) = d\Omega_{D-2} d|\vec{p}| |\vec{p}|^{D-3} f(|\vec{p}|), \quad (3.86)$$

$$\int d\Omega_{D-2} = \int d\Omega_{D-3} \int_0^\pi d\theta (\sin \theta)^{D-3} = \int_0^\pi d\theta_1 (\sin \theta_1)^{D-3} \int_0^\pi d\theta_2 (\sin \theta_2)^{D-4} \dots \int_0^{2\pi} d\theta$$

$$\int_{S_{D-2}} d\Omega_{D-2} = V(D-1) = \frac{2\pi^{\frac{D-1}{2}}}{\Gamma(\frac{D-1}{2})},$$

to obtain

$$d\Phi_{1 \rightarrow n} = (2\pi)^{n-D(n-1)} 2^{1-n} d\Omega_{D-2} \prod_{j=1}^{n-1} d|\vec{p}_j| |\vec{p}_j|^{D-3} \delta\left((Q - \sum_{j=1}^{n-1} p_j)^2\right). \quad (3.87)$$

Example 1 → 2:

For $n = 2$ the momenta can be parametrised by

$$Q = (E, \vec{0}^{(D-1)}) , \quad p_1 = E_1 (1, \vec{0}^{(D-2)}, 1) , \quad p_2 = Q - p_1 . \quad (3.88)$$

Integrating out the δ -distribution leads to

$$d\Phi_{1 \rightarrow 2} = (2\pi)^{2-D} 2^{1-D} (Q^2)^{D/2-2} d\Omega_{D-2} . \quad (3.89)$$

Example 1 → 3:

For $n = 3$ one can choose a coordinate frame such that

$$\begin{aligned} Q &= (E, \vec{0}^{(D-1)}) \\ p_1 &= E_1 (1, \vec{0}^{(D-2)}, 1) \\ p_2 &= E_2 (1, \vec{0}^{(D-3)}, \sin \theta, \cos \theta) \\ p_3 &= Q - p_2 - p_1 , \end{aligned} \quad (3.90)$$

leading to

$$\begin{aligned} d\Phi_{1 \rightarrow 3} &= \frac{1}{4} (2\pi)^{3-2D} dE_1 dE_2 d\theta_1 (E_1 E_2 \sin \theta)^{D-3} d\Omega_{D-2} d\Omega_{D-3} \\ &\Theta(E_1) \Theta(E_2) \Theta(E - E_1 - E_2) \delta((Q - p_1 - p_2)^2) . \end{aligned} \quad (3.91)$$

In the following a parametrisation in terms of the Mandelstam variables $s_{ij} = 2 p_i \cdot p_j$ will be useful, therefore we make the transformation $E_1, E_2, \theta \rightarrow s_{12}, s_{23}, s_{13}$. To work

with dimensionless variables we define $y_1 = s_{12}/Q^2$, $y_2 = s_{13}/Q^2$, $y_3 = s_{23}/Q^2$ which leads to (see *Exercise 4*)

$$\begin{aligned} d\Phi_{1 \rightarrow 3} = & (2\pi)^{3-2D} 2^{-1-D} (Q^2)^{D-3} d\Omega_{D-2} d\Omega_{D-3} (y_1 y_2 y_3)^{D/2-2} \\ & dy_1 dy_2 dy_3 \Theta(y_1) \Theta(y_2) \Theta(y_3) \delta(1 - y_1 - y_2 - y_3). \end{aligned} \quad (3.92)$$

Now we are in the position to calculate the full real radiation contribution. The matrix element (for one quark flavour with charge Q_f) in the variables defined above, where p_3 in our case is the gluon, is given by

$$|\mathcal{M}|_{\text{real}}^2 = C_F e^2 Q_f^2 g_s^2 8(1-\epsilon) \left\{ \frac{2}{y_2 y_3} + \frac{-2 + (1-\epsilon)y_3}{y_2} + \frac{-2 + (1-\epsilon)y_2}{y_3} - 2\epsilon \right\}. \quad (3.93)$$

In our variables, soft singularities mean gluon momentum $p_3 \rightarrow 0$ and therefore both y_2 and $y_3 \rightarrow 0$. While $p_3 \parallel p_1$ means $y_2 \rightarrow 0$ and $p_3 \parallel p_2$ means $y_3 \rightarrow 0$. Combined with the factors $(y_2 y_3)^{D/2-2}$ from the phase space it is clear that the first term in the bracket of Eq. (3.93) will lead to a $1/\epsilon^2$ pole, coming from the region in phase space where soft and collinear limits coincide. To eliminate the δ -distribution, we make the substitutions

$$y_1 = 1 - z_1, y_2 = z_1 z_2, y_3 = z_1(1 - z_2), \det J = z_1$$

to arrive at

$$\begin{aligned} \int d\Phi_3 |\mathcal{M}|_{\text{real}}^2 = & \alpha C_F \frac{\alpha_s}{\pi} Q_f^2 \tilde{H}(\epsilon) (Q^2)^{1-2\epsilon} \int_0^1 dz_1 \int_0^1 dz_2 z_1^{-2\epsilon} \left(z_2(1-z_1)(1-z_2) \right)^{-\epsilon} \\ & \left\{ \frac{2}{z_1 z_2 (1-z_2)} + \frac{-2 + (1-\epsilon)z_1(1-z_2)}{z_2} + \frac{-2 + (1-\epsilon)z_1 z_2}{1-z_2} - 2\epsilon z_1 \right\}. \end{aligned} \quad (3.94)$$

The integrals can be expressed in terms of Euler Beta-functions and lead to the result quoted in Eq. (3.56).

3.5.5 Jet cross sections

Jets can be pictured as clusters of particles (usually hadrons) which are close to each other in phase space, resp. in the detector. Fig. 16 illustrates what happens between the partonic interaction and the hadrons seen in the detector.

Historically, one of the first suggestions to define jet cross sections was by Sterman and Weinberg [44]. In their definition, a final state is classified as two-jet-like if all but a fraction ϵ of the total available energy E is contained in two cones of opening angle δ . The two-jet cross section is then obtained by integrating the matrix elements

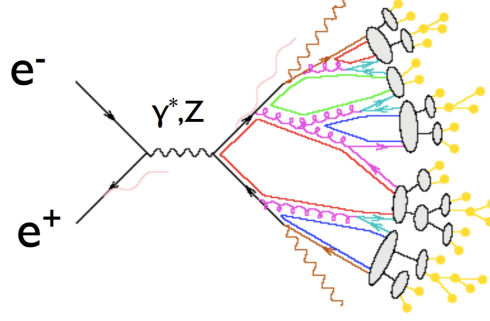


Figure 16: Parton branching and hadronisation in e^+e^- annihilation to hadrons.
Figure by Fabio Maltoni.

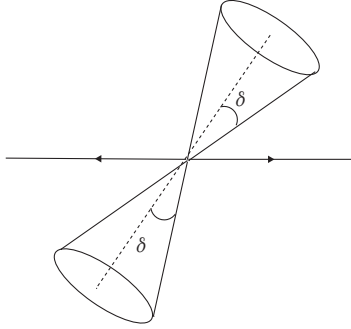


Figure 17: Two jet cones according to the definition of Sterman and Weinberg.

for the various quark and gluon final states over the appropriate region of phase space determined by ε and δ .

Let us have a look at the different contributions to the 2-jet cross section at $\mathcal{O}(\alpha_s)$, see Fig. 18.

- (a) The Born contribution σ_0 . As we have only two partons, this is always a 2-jet configuration, no matter what the values for ε and δ are.
- (b) The virtual contribution

$$\sigma^V = -\sigma_0 C_F \frac{\alpha_s}{2\pi} 4 \int_0^E \frac{dk_0}{k_0} \frac{d\cos\theta}{(1-\cos\theta)(1+\cos\theta)}.$$

- (c) The soft contribution ($k_0 < \varepsilon E$):

$$\sigma^{\text{soft}} = \sigma_0 C_F \frac{\alpha_s}{2\pi} 4 \int_0^{\varepsilon E} \frac{dk_0}{k_0} \frac{d\cos\theta}{(1-\cos\theta)(1+\cos\theta)}.$$

(d) The collinear contribution ($k_0 > \varepsilon E$, $\theta < \delta$):

$$\sigma^{\text{coll}} = \sigma_0 C_F \frac{\alpha_s}{2\pi} 4 \int_{\varepsilon E}^E \frac{dk_0}{k_0} \left(\int_0^\delta + \int_{\pi-\delta}^\pi \right) \frac{d \cos \theta}{(1 - \cos \theta)(1 + \cos \theta)}.$$

Summing up all these contributions leads to

$$\begin{aligned} \sigma^{2\text{jet}} &= \sigma_0 \left(1 - C_F \frac{\alpha_s}{2\pi} 4 \int_{\varepsilon E}^E \frac{dk_0}{k_0} \int_\delta^{\pi-\delta} \frac{d \cos \theta}{(1 - \cos^2 \theta)} \right) \\ &= \sigma_0 \left(1 - 4 C_F \frac{\alpha_s}{2\pi} \ln \varepsilon \ln \delta \right). \end{aligned} \quad (3.95)$$

Of course the two-jet cross section depends on the values for ε and δ . If they are

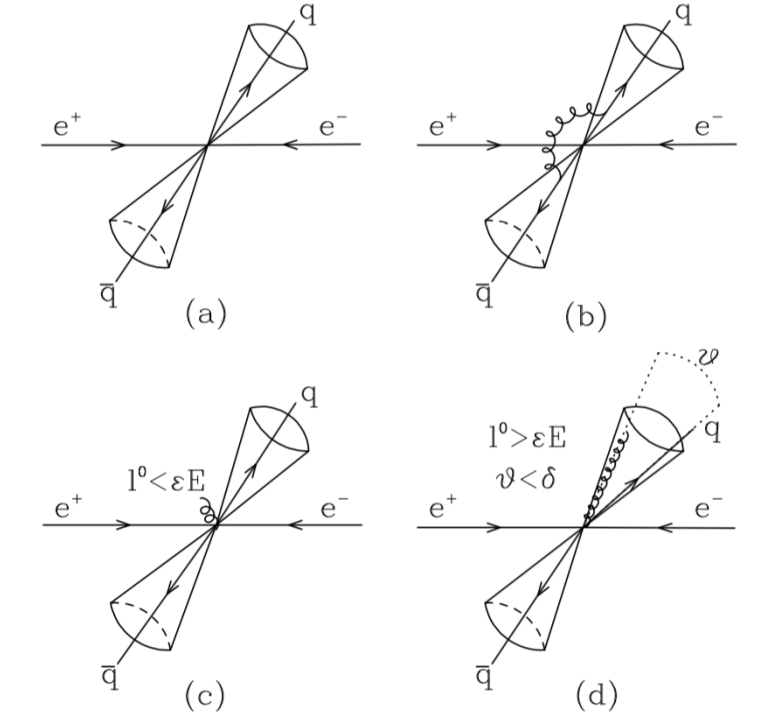


Figure 18: Different configurations contributing to the 2-jet cross section at $\mathcal{O}(\alpha_s)$.

very large, even extra radiation at a relatively large angle $\theta < \delta$ will be “clustered” into the jet cone and almost all events will be classified as 2-jet events. Note that the partonic 3-jet cross section at $\mathcal{O}(\alpha_s)$ is given by $\sigma^{3\text{jet}} = \sigma_{NLO}^{\text{total}} - \sigma^{2\text{jet}}$, because from the theory point of view, we cannot have more than 3 partons at NLO in the process $e^+e^- \rightarrow \text{hadrons}$. In the experiment of course we can have more jets, which come from parton branchings (“parton shower”) before the process of hadronisation. Fig. 19 shows that it is not obvious how many events are identified as 2-jet (or 3-jet, 4-jet, …)

events after parton showering and hadronisation. This depends on the jet algorithm used to identify the jets. It is clear from Fig. 19 that a lot of information is lost when

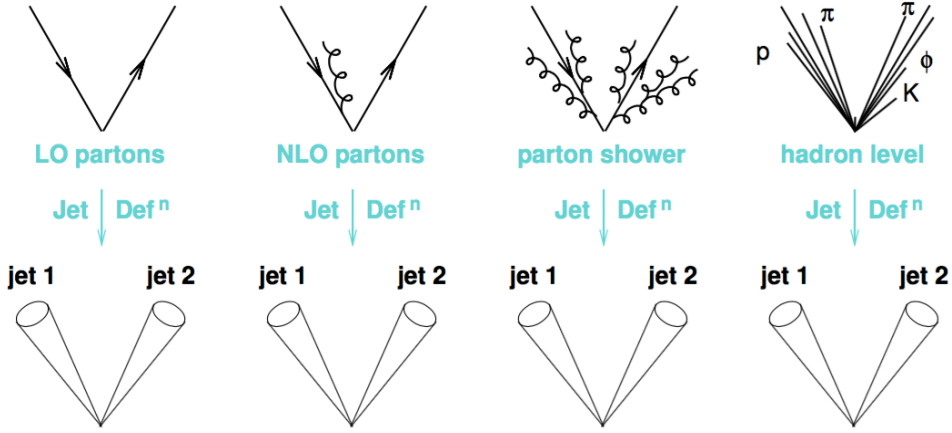


Figure 19: Projections to a 2-jet event at various stages of the theoretical description. Figure by Gavin Salam.

projecting a complex hadronic track structure onto an n -jet event. Modern techniques also identify a *jet substructure*, in particular for highly energetic jets. This can give valuable information on the underlying partonic event (e.g. distinguishing a gluon from a quark, a b -quark from a light quark, etc).

The Sterman-Weinberg jet definition based on cones is not very practical to analyse multijet final states. A better alternative is for example the following:

1. starting from n particles, for all pairs i and j calculate $(p_i + p_j)^2$.
2. If $\min(p_i + p_j)^2 < y_{\text{cut}} Q^2$ then define a new “pseudo-particle” $p_J = p_i + p_j$, which decreases $n \rightarrow n - 1$. Q is the center-of-mass energy, y_{cut} is the jet resolution parameter.
3. if $n = 1$ stop, else repeat the step above.

After this algorithm all partons are clustered into jets. With this definition one finds at $\mathcal{O}(\alpha_s)$:

$$\sigma^{2\text{jet}} = \sigma_0 \left(1 - C_F \frac{\alpha_s}{\pi} \ln^2 y_{\text{cut}} \right) . \quad (3.96)$$

Algorithms which are particularly useful for hadronic initial states are for example the so-called Durham- k_T algorithm [45] or the anti- k_T algorithm [46] (see also [47] for a summary of different jet algorithms).

The Durham- k_T -jet algorithm clusters particles into jets by computing the distance measure

$$y_{ij,D} = \frac{2 \min(E_i^2, E_j^2)(1 - \cos \theta_{ij})}{Q^2} \quad (3.97)$$

for each pair (i, j) of particles. The pair with the lowest $y_{ij,D}$ is replaced by a pseudo-particle whose four-momentum is given by the sum of the four-momenta of particles i and j ('E' recombination scheme). This procedure is repeated as long as pairs with invariant mass below the predefined resolution parameter $y_{ij,D} < y_{\text{cut}}$ are found. Once the clustering is terminated, the remaining (pseudo-)particles are the jets. It is evident that a large value of y_{cut} will ultimately result in the clustering all particles into only two jets, while higher jet multiplicities will become more and more frequent as y_{cut} is lowered. In experimental jet measurements, one therefore studies the jet rates (jet cross sections normalised to the total hadronic cross section) as function of the jet resolution parameter y_{cut} . Fig. 20 (a) shows the jet rates (normalised to the total hadronic cross section) as a function of y_{cut} , compared to ALEPH data. Fig. 20 (b) shows corrections up to NNLO to the 3-jet rate as a function of y_{cut} . Note that for small values of y_{cut} the 2-jet rate diverges $\sim -\log^2(y_{\text{cut}})$ because only three partons are present at LO.

At the LHC, the most commonly used jet algorithm is the *anti- k_T algorithm* [46]. The anti- k_T algorithm is similar to the Durham- k_T algorithm, but introduces a different distance measure:

$$y_{ij,a} = \frac{1}{8} Q^2 \min \left(\frac{1}{E_i^2}, \frac{1}{E_j^2} \right) (1 - \cos \theta_{ij}) \quad (3.98)$$

Since very recently, methods based on *Deep Learning* are applied to identify jets, and seem to be quite successful.

A short word on infrared safe jet algorithms: Fig. 22 shows an example where the divergences between virtual and real radiation parts contributing to an NLO cross section do not fully cancel because the virtual part is classified as an n -jet event while the corresponding divergent real radiation part is classified as an $(n + 1)$ -jet event.

Of course, jets are not the only observables one can define based on hadronic tracks in the detector. Another very useful observable is *thrust*, which describes how “pencil-like” an event looks like. Thrust is an example of so-called *event-shape* observables. Thrust T is defined by

$$T = \max_{\vec{n}} \frac{\sum_{i=1}^m |\vec{p}_i \cdot \vec{n}|}{\sum_{i=1}^m |\vec{p}_i|}, \quad (3.99)$$

where \vec{n} is a three-vector (the direction of the thrust axis) such that T is maximal. The particle three-momenta \vec{p}_i are defined in the e^+e^- centre-of-mass frame. T is an example of a jet function $J(p_1, \dots, p_m)$. It is infrared safe because neither $p_j \rightarrow 0$, nor replacing p_i with $zp_i + (1 - z)p_i$ change T .

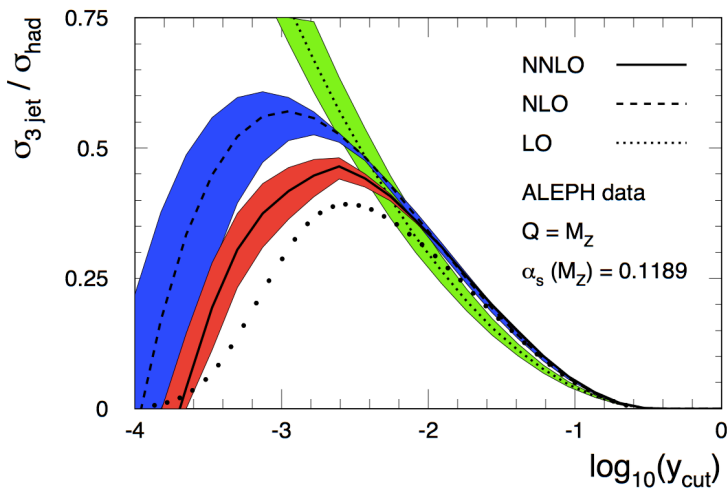
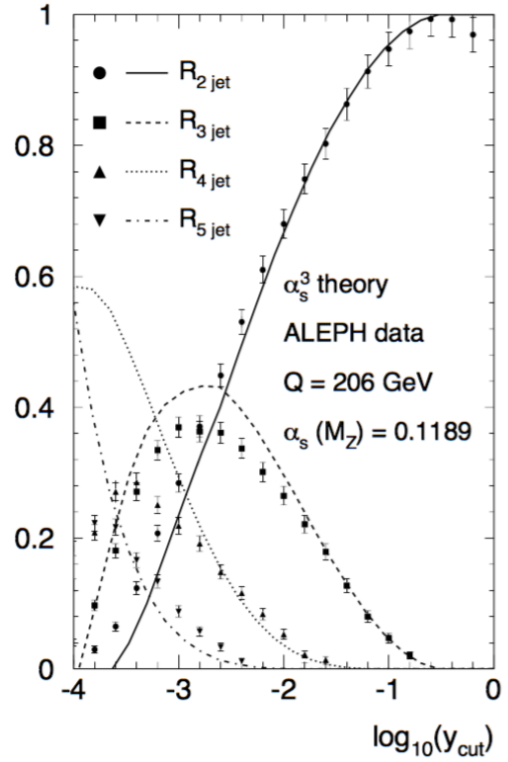


Figure 20: Jet rates as a function of the jet resolution parameter y_{cut} (upper figure) and higher order corrections to the 3-jet rate from Ref. [48] (lower figure).

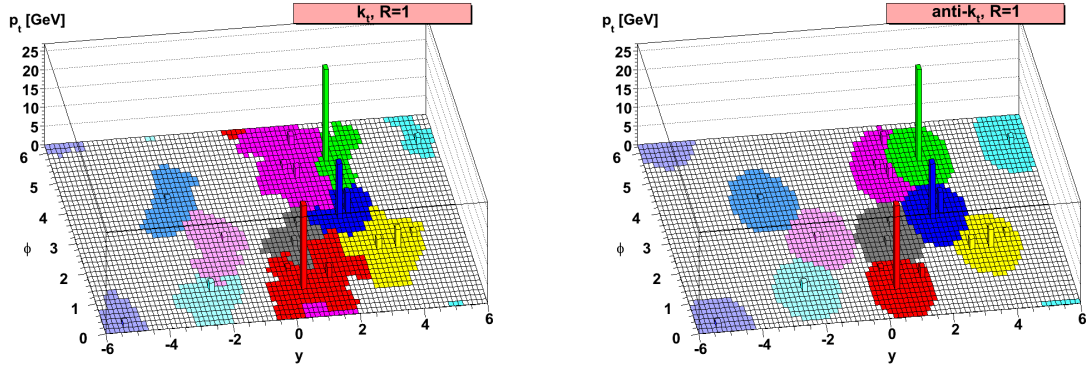


Figure 21: Jet areas as a result of (a) the Durham- k_T algorithm, (b) the anti- k_T algorithm. Figures from Ref. [46].

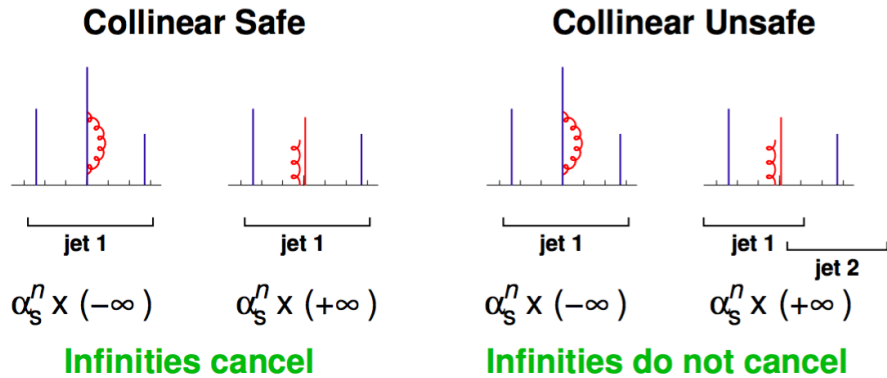


Figure 22: Infrared safety can be spoiled by using jet algorithms like certain cone algorithms. Figure by Gavin Salam.

At leading order it is possible to perform the phase space integrations analytically, to obtain

$$\frac{1}{\sigma} \frac{d\sigma}{dT} = C_F \frac{\alpha_s}{2\pi} \left[\frac{2(3T^2 - 3T + 2)}{T(1-T)} \ln \left(\frac{2T-1}{1-T} \right) - 3(3T-2) \frac{2-T}{1-T} \right]. \quad (3.100)$$

We see that the perturbative prediction for the thrust distribution becomes singular as $T \rightarrow 1$. In addition to the factor of $1-T$ in the denominator, there is also a logarithmic divergence $\sim \ln(1-T)$. The latter is characteristic for events shape distributions. In perturbation theory at n th order logarithms of the form $\alpha_s^n \ln^m(1/(1-T))$ with $m \leq 2n$ appear. These spoil the convergence of the perturbative series and should be

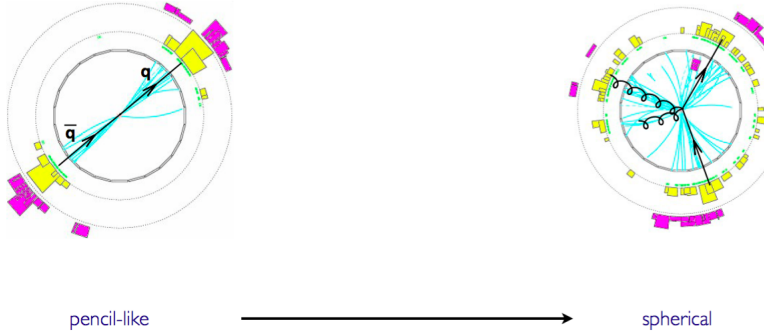


Figure 23: The thrust event shape ranges from “pencil-like” to “spherical”. Figure: Fabio Maltoni.

“resummed” if we want to make reliable prediction near the phase space region where $T \rightarrow 1$.

3.6 Parton distribution functions

3.6.1 Deeply inelastic scattering

So far we have only considered leptons in the initial state (e^+e^- annihilation). Now we consider the case where we have an electron-proton collider, like for example HERA (at DESY Hamburg), which operated until 2007 and offered unique opportunities to study the proton structure. We consider the scattering of leptons off the proton, as depicted in Fig. 24, in a kinematic regime where the squared momentum transfer Q^2 is large compared to the proton mass squared ($M \sim 1$ GeV), so we consider deeply inelastic scattering. The relations between the involved momenta and kinematic variables are

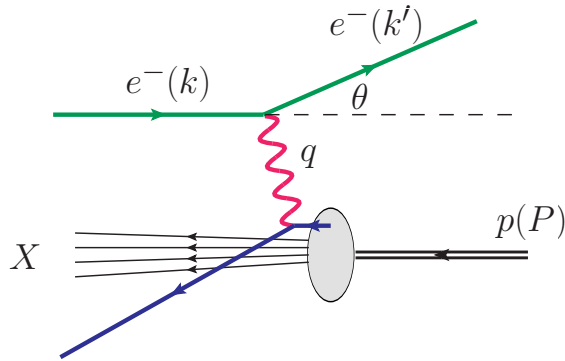


Figure 24: Deeply inelastic scattering, partonic picture. Figure from Ref. [49].

$$\begin{aligned}
s &= (P + k)^2 \text{ [cms energy]}^2 \\
q^\mu &= k^\mu - k'^\mu \text{ [momentum transfer]} \\
Q^2 &= -q^2 = 2MExy \\
x &= \frac{Q^2}{2P \cdot q} \text{ [scaling variable]} \\
\nu &= \frac{P \cdot q}{M} = E - E' \text{ [energy loss]} \\
y &= \frac{P \cdot q}{P \cdot k} = 1 - \frac{E'}{E} \text{ [relative energy loss]} . \tag{3.101}
\end{aligned}$$

The cross section for $e(k) + p(P) \rightarrow e(k') + X$ can be written as

$$d\sigma = \sum_X \frac{1}{4ME} \int d\Phi \frac{1}{4} \sum_{\text{spins}} |\mathcal{M}|^2 . \tag{3.102}$$

We can factorise the phase space and the squared matrix element into a leptonic and a hadronic part:

$$d\Phi = \frac{d^3k'}{(2\pi)^3 2E'} d\Phi_X , \quad \frac{1}{4} \sum_{\text{spins}} |\mathcal{M}|^2 = \frac{e^4}{Q^4} L^{\mu\nu} H_{\mu\nu} . \tag{3.103}$$

Then the hadronic part of the cross section can be described by the dimensionless Lorentz tensor $W_{\mu\nu} = \frac{1}{8\pi} \sum_X \int d\Phi_X H_{\mu\nu}$. As it depends only on two momenta P^μ and q^μ , the most general gauge and Lorentz invariant expression must be of the form

$$W_{\mu\nu}(P, q) = \left(-g_{\mu\nu} + \frac{q_\mu q_\nu}{q^2} \right) W_1(x, Q^2) + \left(P_\mu - q_\mu \frac{P \cdot q}{q^2} \right) \left(P_\nu - q_\nu \frac{P \cdot q}{q^2} \right) \frac{W_2(x, Q^2)}{P \cdot q} , \tag{3.104}$$

where the structure functions $W_i(x, Q^2)$ are dimensionless functions of the scaling variable x and the momentum transfer Q^2 .

For the leptonic part we use the relations $E' = (1 - y)E$, $\cos\theta = 1 - \frac{xyM}{(1-y)E}$ to change variables to the so-called *scaling variable* x and the relative energy loss y

$$\frac{d^3k'}{(2\pi)^3 2E'} = \frac{d\phi}{2\pi} \frac{E'}{8\pi^2} dE' d\cos\theta = \frac{d\phi}{2\pi} \frac{yME}{8\pi^2} dy dx ,$$

and compute the trace $L^{\mu\nu} = \frac{1}{2} Tr[\not{k}\gamma^\mu \not{k}'\gamma^\nu] = k^\mu k'^\nu + k^\nu k'^\mu - g^{\mu\nu} k \cdot k'$. Then the differential cross section in x and y is obtained from Eq. (3.102) as

$$\frac{d^2\sigma}{dx dy} = \frac{4\pi\alpha^2}{y Q^2} \left[y^2 W_1(x, Q^2) + \left(\frac{1-y}{x} - xy \frac{M^2}{Q^2} \right) W_2(x, Q^2) \right] .$$

In the *scaling limit*, defined by $Q^2 \rightarrow \infty$ with x fixed, we use $W_1 \rightarrow -F_1, W_2 \rightarrow F_2$, neglect the term $\sim M^2/Q^2$ and obtain

$$\frac{d^2\sigma}{dx dy} = \frac{4\pi\alpha^2}{y Q^2} \left[(1 + (1-y)^2) F_1 + \frac{1-y}{x} (F_2 - 2xF_1) \right]. \quad (3.105)$$

The functions F_1 and F_2 are called “structure functions”, where the combination $F_L = F_2 - 2xF_1$ is also called the longitudinal structure function because it is related to the absorption of a longitudinally polarised virtual photon. They were first measured by the SLAC-MIT experiment (USA) in 1970, and have been measured very accurately at the HERA collider. The interesting feature is that, in the scaling limit, $2xF_1 \rightarrow F_2$ and F_2 becomes independent of Q^2 , $F_2(x, Q^2) \rightarrow F_2(x)$, a feature which is often called *Bjorken scaling*. How this looks in experiment is shown in Fig. 25. We will see in the following that scaling is violated at higher orders.

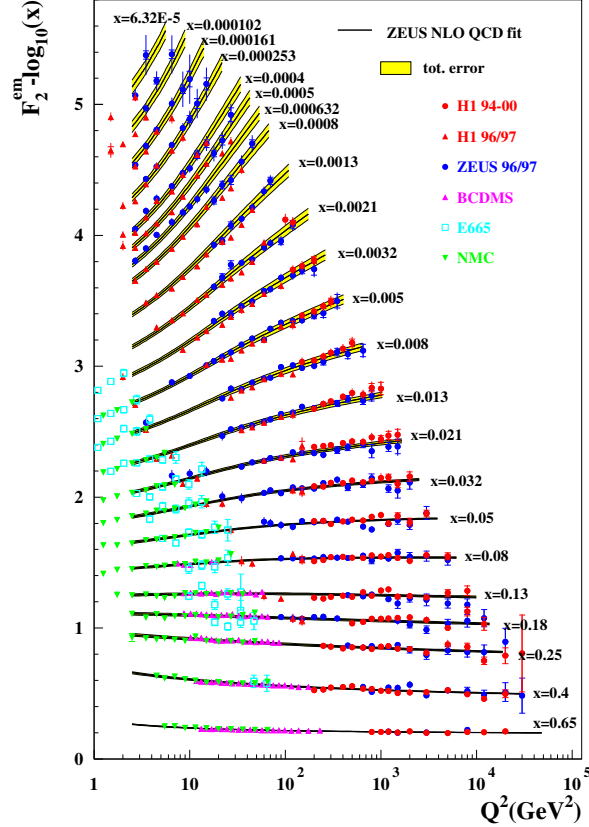


Figure 25: The structure function F_2 for different values of Q^2 . Figure from Ref. [50].

3.6.2 Proton structure in the parton model

Now let us assume the proton consists of free quarks and the lepton exchanges a hard virtual photon with one of those quarks as shown in Fig. 24. The struck quark carries a momentum p^μ , which is a fraction of the proton momentum, $p^\mu = \xi P^\mu$, so we consider the process $e(k) + q(p) \rightarrow e(k') + q(p')$. The corresponding cross section is

$$\hat{\sigma} = \frac{1}{2\hat{s}} \int d\Phi_2 \frac{1}{4} \sum_{\text{spins}} |\mathcal{M}|^2 . \quad (3.106)$$

with $\hat{s} = (p+k)^2$. The “hat” indicates that we consider the partonic cross section. The squared matrix element is proportional to the product of the lepton tensor $L^{\mu\nu}$ and a quark tensor $Q_{\mu\nu} = \frac{1}{2} Tr[p\gamma^\mu \ p'\gamma^\nu] = p^\mu p'^\nu + p^\nu p'^\mu - g^{\mu\nu} p \cdot p'$, leading to $L^{\mu\nu} Q_{\mu\nu} = 2(\hat{s}^2 + \hat{u}^2)$, where $\hat{u} = (p-k')^2 = -2p \cdot k'$. As $y = Q^2/\hat{s}$ we can derive, using $\hat{u}^2 = (1-y)^2 \hat{s}^2$,

$$\frac{1}{4} \sum_{\text{spins}} |\mathcal{M}|^2 = \frac{e_q^2 e^4}{Q^4} L^{\mu\nu} Q_{\mu\nu} = 2e_q^2 e^4 \frac{\hat{s}^2}{Q^4} (1 + (1-y)^2) . \quad (3.107)$$

Using $p'^2 = 2p \cdot q - Q^2 = Q^2(\xi/x - 1)$, the two-particle phase space (in 4 dim.) can be written as (*see Exercise 5*)

$$d\Phi_2 = \frac{d^3 k'}{(2\pi)^3 2E'} \frac{d^4 p'}{(2\pi)^3} \delta(p'^2) (2\pi)^4 \delta^{(4)}(k + p - k' - p') = \frac{d\phi}{(4\pi)^2} dy dx \delta(\xi - x) . \quad (3.108)$$

The differential cross section in x and y for one quark flavour is then given by

$$\frac{d^2 \hat{\sigma}}{dx dy} = \frac{4\pi \alpha^2}{y Q^2} [1 + (1-y)^2] \frac{1}{2} e_q^2 \delta(\xi - x) . \quad (3.109)$$

Comparing Eqs. (3.105) and (3.109), we find the parton model predictions

$$\hat{F}_1(x) \propto e_q^2 \delta(\xi - x) , \quad F_2 - 2xF_1 = 0 . \quad (3.110)$$

The above relations are called *Callan-Gross* relations. Thus the structure functions probe the quark constituents of the proton with $\xi = x$. However, this prediction cannot be the end of the story because experimentally, we observe that F_2 does depend on Q^2 , as can be seen from Fig. 25, even though the dependence is not strong.

To see how the Q^2 dependence comes in, let us define the following:

$f_i(\xi) d\xi$ is the probability that a parton (q, \bar{q}, g) with flavour i carries a momentum fraction of the proton between ξ and $\xi + \delta\xi$.

The function $f_i(\xi)$ is called *parton distribution function (PDF)*.

Using the relations $dy = dQ^2/\hat{s}$ and $\delta(\xi - x) = \frac{1}{\xi}\delta\left(1 - \frac{x}{\xi}\right)$, we can write the full cross section as a combination of the PDF and the differential cross section (3.109),

$$\frac{d^2\sigma}{dx dQ^2} = \int_x^1 \frac{d\xi}{\xi} \sum_i f_i(\xi) \frac{d^2\hat{\sigma}}{dx dQ^2}\left(\frac{x}{\xi}, Q^2\right). \quad (3.111)$$

This means that the cross section is a convolution of a long-distance component, the parton distribution function $f_i(\xi)$ for a parton of type i , and a short-distance component, the partonic hard scattering cross section $\hat{\sigma}$. This form is highly non-trivial, because it means that we can separate *short-distance* effects, which are calculable in perturbation theory, from *long-distance* effects, which belong to the domain of non-perturbative QCD and have to be modelled and fitted from data (or calculated by lattice QCD if possible). This *factorisation*, shown schematically in Fig. 26, can be proven rigorously in DIS using operator product expansion, and less rigorously in hadron-hadron collisions. It also holds once higher orders in α_s are taken into account (in a form which we will discuss below). Factorisation only holds for large Q^2 , it has corrections which are suppressed by powers of order $(\Lambda/Q)^p$ (called “power corrections”).

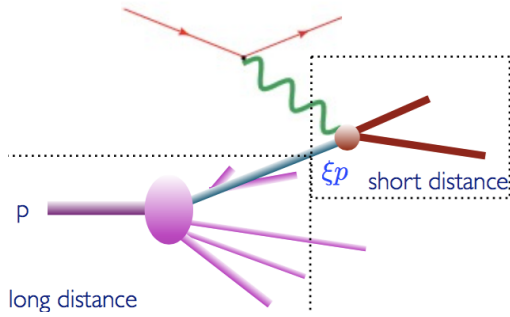


Figure 26: Deeply inelastic scattering, partonic picture of factorisation. Figure by F. Maltoni.

According to eqs. (3.105) and (3.111), we find in the naïve parton model

$$F_2(x) = 2xF_1(x) = \sum_i \int_0^1 d\xi f_i(\xi) x e_{q_i}^2 \delta(x - \xi) = x \sum_i e_{q_i}^2 f_i(x). \quad (3.112)$$

For a proton probed at a scale Q , we expect it consists mostly of uud . Writing $f_i(x) = u(x), d(x)$ etc. for $i = u, d, \dots$ we have in the naïve parton model

$$F_2^{\text{proton}}(x) = x \left[\frac{4}{9} (u(x) + \bar{u}(x)) + \frac{1}{9} (d(x) + \bar{d}(x)) \right]. \quad (3.113)$$

If we define the so-called “valence quarks” $u_v(x)u_v(x)d_v(x)$,

$$u(x) = u_v(x) + \bar{u}(x), \quad d(x) = d_v(x) + \bar{d}(x), \quad s(x) = \bar{s}(x),$$

we expect the “sum rules”

$$\int_0^1 dx u_v(x) = 2, \quad \int_0^1 dx d_v(x) = 1, \quad \int_0^1 dx (s(x) - \bar{s}(x)) = 0. \quad (3.114)$$

In Figs. 27 and 28 it is illustrated that the smaller x and the larger Q^2 , the more the “sea quarks” and gluons in the proton are probed. In fact, it turns out that $\sum_{i=q,\bar{q}} \int_0^1 dx x f_{i/p}(x) \simeq 0.5$, so quarks carry only about half of the momentum of the proton. We know that the other half is carried by gluons, but clearly the naïve parton model is not sufficient to describe the gluon distribution in the proton.

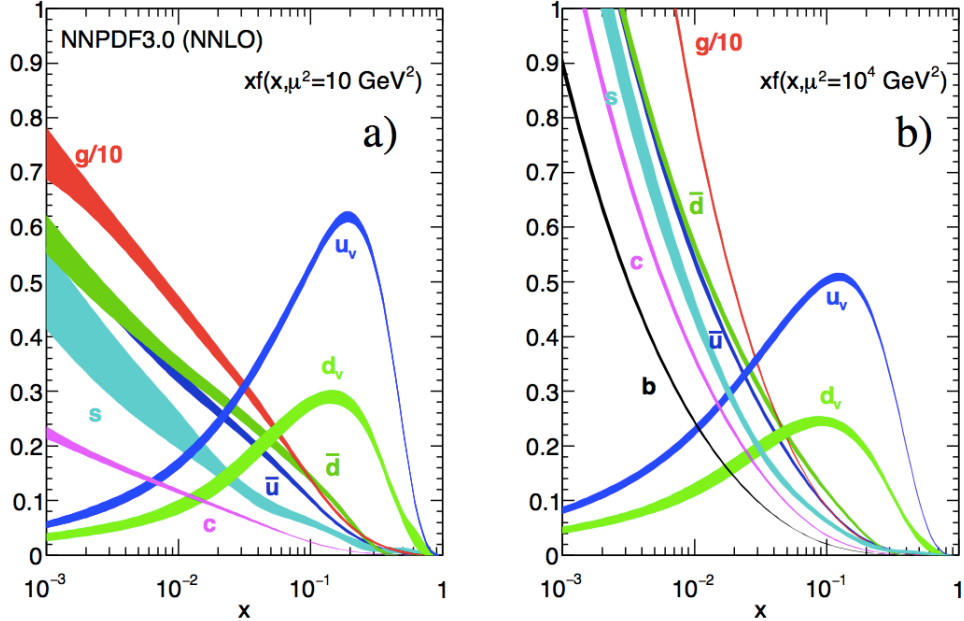


Figure 27: Parton distribution functions in the proton as a function of x . Source: Particle Data Group.

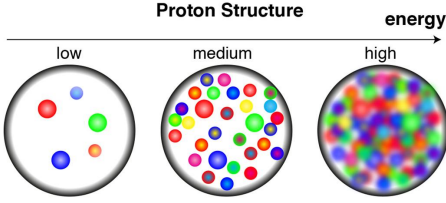


Figure 28: Proton structure depending on how well it can be resolved. Source: Utrecht University.

3.6.3 Proton structure in perturbative QCD

To see what happens in the “QCD-improved” parton model, we will encounter again IR singularities and splitting functions. Let us denote the hard scattering cross section by σ_h . For final state radiation, we found that the IR singularities due to soft and collinear configurations cancel against IR divergences in the virtual correction for infrared safe quantities.

If there is a coloured parton in the *initial* state, the splitting may occur *before* the hard scattering, such that the momentum of the parton that enters the hard process is reduced to xp^μ .

$$\sigma_{h+g}(p) \simeq \sigma_h(xp) 2C_F \frac{\alpha_s}{\pi} \frac{dE}{E} \frac{d\theta}{\theta} \rightarrow \sigma_h(xp) C_F \frac{\alpha_s}{\pi} dx (1-x)^{-1-\epsilon} dk_\perp^2 (k_\perp^2)^{-1-\epsilon}.$$

Integrating over x up to one and over k_\perp we again find a soft and collinear divergence. The corresponding ϵ poles multiply $\sigma_h(xp)$, while in the virtual correction the poles multiply $\sigma_h(p)$, irrespective whether the IR divergence is in the initial or final state:

$$\sigma_{h+V} \simeq -\sigma_h(p) C_F \frac{\alpha_s}{\pi} dx (1-x)^{-1-\epsilon} dk_\perp^2 (k_\perp^2)^{-1-\epsilon}.$$

The sum of the real and virtual corrections contains an uncanceled singularity!

$$\sigma_{h+g} + \sigma_{h+V} \simeq C_F \frac{\alpha_s}{\pi} \int_0^{Q^2} dk_\perp^2 (k_\perp^2)^{-1-\epsilon} dx \underbrace{(1-x)^{-1-\epsilon} [\sigma_h(xp) - \sigma_h(p)]}_{\text{finite}} , \quad (3.115)$$

Note that the soft singularity for $x \rightarrow 1$ vanishes in the sum of real and virtual parts. The uncanceled collinear singularity in the initial state however remains. Fortunately its form is universal, i.e. independent of the details of the hard scattering process, only dependent on the type of parton splittings. Therefore we can also eliminate it in a universal way: It is absorbed into “bare” parton densities, $f_i^{(0)}(x)$, such that the measured parton densities are the “renormalised” ones. This procedure is very similar

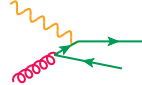
to the renormalisation of UV divergences and introduces a scale μ_f , the *factorisation scale*, into the parton densities. Let us see how this works for the structure function F_2 . We first consider the *partonic* structure functions $\hat{F}_{2,q}, \hat{F}_{2,g}$, where the subscript q indicates that a quark is coming out of the proton, analogous for a gluon g . Note that a gluon coming from the proton does not interact with a photon, therefore the gluonic contribution is zero at leading order, but it will appear at order α_s because the gluon can split into a $q\bar{q}$ pair and then one of the quarks interacts with the photon. Therefore we have

$$\hat{F}_{2,q}(x) = \frac{d^2\hat{\sigma}}{dx dQ^2} \Big|_{F_2} = e_q^2 x \left[\delta(1-x) + \frac{\alpha_s}{4\pi} \left(- \left(\frac{Q^2}{\mu^2} \right)^{-\epsilon} \frac{1}{\epsilon} P_{q \rightarrow qg}(x) + C_2^q(x) \right) \right], \quad (3.116)$$



and

$$\hat{F}_{2,g}(x) = \frac{d^2\hat{\sigma}}{dx dQ^2} \Big|_{F_2} = \sum_q e_q^2 x \left[0 + \frac{\alpha_s}{4\pi} \left(- \left(\frac{Q^2}{\mu^2} \right)^{-\epsilon} \frac{1}{\epsilon} P_{g \rightarrow q\bar{q}}(x) + C_2^g(x) \right) \right], \quad (3.117)$$



where $P_{j \rightarrow ik}(x)$ is the Altarelli-Parisi splitting function (regularised at $x = 1$) which we already encountered when discussing collinear singularities. It denotes the probability that a parton j splits collinearly into partons i and k , with i carrying a momentum fraction x of the original parton j . Note that the type of parton k is fixed by i and j . Therefore i and j are sufficient to label the splitting functions. For the labelling different conventions are in use. They are summarised in Table 2. $C_2(x)$ is the remaining finite term, sometimes called coefficient function. The partonic scattering function \hat{F}_2 is not measurable, only the structure function is physical. Therefore we have to form the convolution of the partonic part with the parton distribution functions.

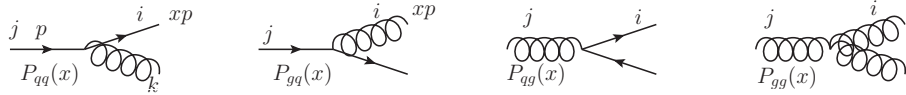


Figure 29: Splitting functions with labelling.

$$F_{2,q}(x, Q^2) = x \sum_i e_{qi}^2 \left[f_i^{(0)}(x) + \frac{\alpha_s}{2\pi} \int_0^1 \frac{d\xi}{\xi} f_i^{(0)}(\xi) \left(- \left(\frac{Q^2}{\mu^2} \right)^{-\epsilon} \frac{1}{\epsilon} P_{q \rightarrow qg} \left(\frac{x}{\xi} \right) + C_2^q \left(\frac{x}{\xi} \right) \right) \right].$$

$P_{ij}(x)$	$P_{j \rightarrow ik}(x)$	$P_{i/j}(x)$
$P_{qq}(x)$	$P_{q \rightarrow qg}(x)$	$P_{q/q}(x)$
$P_{gg}(x)$	$P_{g \rightarrow gg}(x)$	$P_{g/g}(x)$
$P_{qg}(x)$	$P_{g \rightarrow q\bar{q}}(x)$	$P_{q/g}(x)$
$P_{gg}(x)$	$P_{g \rightarrow gg}(x)$	$P_{g/g}(x)$

Table 2: Translation between different conventions for the labelling of the splitting functions, see also Fig. 29.

Now we absorb the singularity into the parton distribution function (PDF) by the definition

$$f_i(x, \mu_f^2) = f_i^{(0)}(x) + \frac{\alpha_s}{2\pi} \int_x^1 \frac{d\xi}{\xi} \left\{ f_i^{(0)}(\xi) \left[-\frac{1}{\epsilon} \left(\frac{\mu_f^2}{\mu^2} \right)^{-\epsilon} P_{q \rightarrow qg} \left(\frac{x}{\xi} \right) + K_{qq} \right] \right\}. \quad (3.118)$$

Then the structure function becomes

$$\begin{aligned} F_{2,q}(x, Q^2) &= x \sum_i e_{qi}^2 \int_x^1 \frac{d\xi}{\xi} f_i(\xi, \mu_f^2) \left\{ \delta(1 - \frac{x}{\xi}) + \frac{\alpha_s(\mu_r)}{2\pi} \left[P_{q \rightarrow qg} \left(\frac{x}{\xi} \right) \ln \frac{Q^2}{\mu_f^2} + (C_2^q - K_{qq}) \right] \right\} \\ &= x \sum_i e_{qi}^2 \int_x^1 \frac{d\xi}{\xi} f_i(\xi, \mu_f^2) \hat{F}_{2,i} \left(\frac{x}{\xi}, Q^2, \mu_r, \mu_f \right). \end{aligned} \quad (3.119)$$

Defining a convolution in x -space by $f \otimes_x g \equiv \int_x^1 \frac{d\xi}{\xi} f(\xi) g \left(\frac{x}{\xi} \right)$, we see that the structure function is factorised in the form of a convolution,

$$F_{2,q}(x, Q^2) = x \sum_i e_{qi}^2 f_i(\mu_f) \otimes_x \hat{F}_{2,i}(\mu_r, t) \quad \text{with } t = \ln \frac{Q^2}{\mu_f^2}. \quad (3.120)$$

The long distance physics is factored into the PDFs which depend on the *factorisation scale* μ_f . The short distance physics is factored into the hard scattering cross section which depends on both the factorisation and the renormalisation scales. Both scales are arbitrary, unphysical scales. The term K_{ij} depends on the *factorisation scheme*. It is not unique, as finite terms can be shifted between the short and long distance parts. It is important that the same scheme is used for the real and virtual corrections (usually $\overline{\text{MS}}$).

3.6.4 Parton evolution and the DGLAP equations

With eq. (3.120) we again have an equation where an unphysical scale appears on the right-hand side, while the left-hand side is a physical quantity and therefore should

not depend on the scale μ_f (when calculated to all orders in perturbation theory). This gives us something like a renormalisation group equation, which means that we can calculate how the PDFs evolve as the scale μ_f is changed. As the convolution in Eq. (3.120) is somewhat inconvenient, we go to Mellin space, where the convolution in the factorisation formula Eq. (3.120) above turns into simple products. The Mellin transform is defined by

$$f(N) \equiv \int_0^1 dx x^{N-1} f(x) .$$

The structure function in Mellin space then becomes

$$F_{2,q}(N, Q^2) = x \sum_i e_{qi}^2 f_i(N, \mu_f^2) \hat{F}_{2,i}(N, \mu_r, t) . \quad (3.121)$$

As a measurable quantity, the structure function must be independent of μ_f , therefore

$$\mu_f \frac{dF_{2,q}(N, Q^2)}{d\mu_f} = 0 . \quad (3.122)$$

Note that if F_2 is calculated to order α_s^n , we have $\mu_f dF_{2,q}(N, Q^2)/d\mu_f = \mathcal{O}(\alpha_s^{n+1})$. For simplicity, let us leave out the sum over i in Eq. (3.121) and consider only one quark flavour q . We obtain from Eq. (3.122)

$$\hat{F}_{2,q}(N, t) \frac{df_q(N, \mu_f^2)}{d\mu_f} + f_q(N, \mu_f^2) \frac{d\hat{F}_{2,q}(N, t)}{d\mu_f} = 0 . \quad (3.123)$$

Dividing by $f_q \hat{F}_{2,q}$ we obtain

$$\mu_f \frac{d \ln f_q(N, \mu_f^2)}{d\mu_f} = -\mu_f \frac{d \ln \hat{F}_{2,q}(N, t)}{d\mu_f} . \quad (3.124)$$

Introducing $t = \ln(Q^2/\mu_f^2)$ this can be written as

$$t \frac{df_q(N, t)}{dt} = \gamma_{qq}(N, \alpha_s(t)) f_q(N, t) , \quad (3.125)$$

where

$$\gamma_{qq}(N) = \int_0^1 dx x^{N-1} P_{qq}(x) = P_{qq}(N) . \quad (3.126)$$

$\gamma_{qq}(N)$ is called the *anomalous dimension* because it measures the deviation of $\hat{F}_{2,q}$ from its naïve scaling dimension. Very importantly, Eq. (3.126) implies that the *scale dependence* of the PDFs can be calculated in perturbation theory. The PDFs themselves are non-perturbative, so they have to be extracted from experiment. However, the

universality of the PDFs (for each flavour) and the calculable scale dependence means that we can measure the PDFs in one process at a certain scale and then use it in another process at a different scale.

A rigorous treatment based on operator product expansion and the renormalisation group equations extends the above result to all orders in perturbation theory, leading to

$$t \frac{\partial}{\partial t} f_{q_i}(x, t) = \int_x^1 \frac{d\xi}{\xi} P_{q_i/q_j} \left(\frac{x}{\xi}, \alpha_s(t) \right) f_{q_j}(\xi, t). \quad (3.127)$$

The splitting functions $P_{ij}(x, \alpha_s)$ are calculated as a power series in α_s :

$$P_{ij}(x, \alpha_s) = \frac{\alpha_s}{2\pi} P_{ij}^{(0)}(x) + \left(\frac{\alpha_s}{2\pi} \right)^2 P_{ij}^{(1)}(x) + \left(\frac{\alpha_s}{2\pi} \right)^3 P_{ij}^{(2)}(x) + \mathcal{O}(\alpha_s^4). \quad (3.128)$$

Eq. (3.127) holds for distributions which are *non-singlets* under the flavour group: either a single flavour or a combination $q_{ns} = f_{q_i} - f_{q_j}$ with q_i, q_j being a quark or antiquark of any flavour. The cutting edge calculations for the non-singlet splitting functions are four loops ($P_{ns}^{(3)}(x)$) in the planar limit [51]. More generally, the DGLAP equation is a $(2n_f + 1)$ -dimensional matrix equation in the space of quarks, antiquarks and gluons,

$$t \frac{\partial}{\partial t} \begin{pmatrix} f_{q_i}(x, t) \\ f_g(x, t) \end{pmatrix} = \sum_{q_j, \bar{q}_j} \int_x^1 \frac{d\xi}{\xi} \begin{pmatrix} P_{q_i/q_j} \left(\frac{x}{\xi}, \alpha_s(t) \right) & P_{q_i/g} \left(\frac{x}{\xi}, \alpha_s(t) \right) \\ P_{g/q_j} \left(\frac{x}{\xi}, \alpha_s(t) \right) & P_{g/g} \left(\frac{x}{\xi}, \alpha_s(t) \right) \end{pmatrix} \begin{pmatrix} f_{q_j}(\xi, t) \\ f_g(\xi, t) \end{pmatrix}. \quad (3.129)$$

Eq. (3.129) and (3.127) are called *DGLAP equations*, named after Dokshitzer [52], Gribov, Lipatov [53] and Altarelli, Parisi [54]. They are among the most important equations in perturbative QCD.

Let us now solve the simplified DGLAP equation, Eq. (3.125), in Mellin space. It is a simple first order differential equation, solved by the ansatz

$$f_{q_i}(N, Q^2) = f_{q_i}(N, Q_0^2) \exp \left[\int_{t_0}^{\tilde{t}} dt \gamma_{qq}(N, \alpha_s) \right].$$

Let us recall the one-loop formula $\alpha_s(Q^2) = 1/(b_0 \tilde{t})$ with $\tilde{t} = \ln \frac{Q^2}{\Lambda^2}$ and introduce the abbreviation $d_{qq}(N) = \gamma_{qq}(N)/(2\pi b_0)$. We obtain

$$\begin{aligned} f_{q_i}(N, Q^2) &= f_{q_i}(N, Q_0^2) \exp \left[d_{qq}(N) \int_{t_0}^{\tilde{t}} \frac{dt}{t} \right] \\ \Rightarrow f_{q_i}(N, Q^2) &= f_{q_i}(N, Q_0^2) \left(\frac{\tilde{t}}{t_0} \right)^{d_{qq}(N)} \simeq f_{q_i}(N, Q_0^2) \left(\frac{\alpha_s(Q_0^2)}{\alpha_s(Q^2)} \right)^{d_{qq}(N)}. \end{aligned} \quad (3.130)$$

Now we see how the *scaling violations* arise, and how they are related to the anomalous dimension $\gamma_{qq}(N)$.

As $d_{qq}(1) = 0$, the valence quark with flavour i in the proton, given by the integral $\int_0^1 dx f_{q_i}(x, Q^2)$, is independent of Q^2 . Further, $d_{qq}(N) < 0$ for $N > 1$ and higher Mellin moments vanish more rapidly, therefore the average x decreases as Q^2 increases. Therefore, as Q^2 increases, f_{q_i}, f_g decrease at large x and increases at small x . Physically this can be attributed to an increase in the phase space for gluon emission by quarks as Q^2 increases, leading to a loss of momentum. This trend can be seen in Fig. 25.

3.6.5 Hadron-hadron collisions

The extension of the above to two hadrons in the initial state (e.g. proton-proton collisions as at the LHC at CERN) is straightforward. In this case we have the convolution of the hard scattering cross section with two PDFs, one for each colliding hadron. Thus, the differential cross section for a process like the production of a Higgs boson, $p_a + p_b \rightarrow H + X$, has the form

$$\begin{aligned} d\sigma_{pp \rightarrow H+X} = & \sum_{i,j} \int_0^1 dx_1 f_{i/p_a}(x_1, \alpha_s, \mu_f) \int_0^1 dx_2 f_{j/p_b}(x_2, \alpha_s, \mu_f) \\ & \times d\hat{\sigma}_{ij \rightarrow H+X}(x_1, x_2, \alpha_s(\mu_r), \mu_r, \mu_f) + \mathcal{O}\left(\frac{\Lambda}{Q}\right)^p. \end{aligned} \quad (3.131)$$

Factorisation holds up the the so-called *power corrections* of order $\left(\frac{\Lambda}{Q}\right)^p$ (the power p is process-dependent, but always positive, Λ is the QCD parameter introduced in Eq. (1.27)). Therefore, the larger the energy scale Q^2 of the hard process, the smaller the power corrections.

3.7 Beyond one loop

At one loop, the last ~ 15 years have seen huge progress in the construction of automated tools to generate amplitudes “on the fly”, reduce it to a small set of building blocks, and evaluate it. Examples for automated tools are FEYNARTS/FORMCALC [55, 56], FEYNCALC [57, 58], GoSAM [59, 60], HELAC-NLO [61], MadGraph5_aMC@NLO [62, 63], OPENLOOPS [64], RECOLA [65]. Some of them are pure loop amplitude generators, so need to be linked to (NLO-capable) Monte Carlo programs for the real radiation parts and the phase space integration. Such programs are e.g. HERWIG7 [66], MADGRAPH5 [63], POWHEG [67–69], SHERPA [70, 71]. A standardised interface has been proposed for this link [72, 73]. There are also libraries of pre-calculated processes like BLACKHAT [74], GRACE [75], MCFM [76], NJET [77], VBFNLO [78]. The automation at one loop is facilitated by the fact that

- (a) all one-loop integrals are *reducible*, which means that integrals with loop momenta in the numerator can always be expressed in terms of integrals with trivial numerator,
- (b) the class of the functions the analytic results belong to is a priori known: the most complicated functions which can occur at one loop are dilogarithms.

Related is the fact that one-loop integrals with any number of external legs (where the external momentum vectors are assumed to be 4-dimensional) can be reduced to a combination of “basis integrals” with maximally four external legs, with coefficients involving the dimension D and the kinematic Lorentz invariants s_{ij}, m_i^2 related to the integrals.

Beyond one loop, (a) and (b) are no longer generally fulfilled. The integrals can have *irreducible numerators*, and the function class the amplitude lives in is not necessarily known. However there are large classes of amplitudes where we know that the function class is multiple polylogarithms [79, 80].

3.7.1 Integral families, reduction to master integrals

Multi-loop amplitudes are usually generated from Feynman diagrams (other approaches, based on unitarity-inspired techniques, also exist, but are as yet at a less automated state). Automated tools like FEYNARTS [55] or QGRAF [81] can be used to generate the amplitudes. The algebraic expressions produced in this way are usually large (so they are conveniently processed using FORM [82, 83]) and contain integrals with loop momenta in the numerator, contracted with external momenta and/or polarisation vectors. These integrals are not linearly independent. They can be related to each other

using algebraic identities, the most important ones being *integration-by-parts (IBP) identities* [84].

Integration-by-parts identities are based on the fact that the integral of a total derivative is zero:

$$\int d^D k \frac{\partial}{\partial k^\mu} v^\mu f(k, p_i) = 0 , \quad (3.132)$$

where v can either be a loop momentum or an external momentum. Working out the derivative for a certain number of numerators yields systems of relations among scalar integrals which can be solved systematically. The endpoints of the reduction are called *master integrals*.

An integral with L loops in D dimensions, with N propagators P_j , raised to the power ν_j , can be written as

$$G(\nu_1 \dots \nu_N) = \int \prod_{l=1}^L \frac{d^D k_l}{i\pi^{\frac{D}{2}}} \prod_{j=1}^N \frac{1}{P_j^{\nu_j}(\{k\}, \{p\}, m_j^2)} . \quad (3.133)$$

The propagators $P_j(\{k\}, \{p\}, m_j^2)$ depend on the loop momenta k_l , the external momenta $\{p_1, \dots, p_E\}$ and the (not necessarily nonzero) masses m_j . The propagator powers ν_j need not all be positive. A scalar integral with no loop-momentum dependence in the numerator would correspond to $\nu_j \geq 0$ for all j .

The set of integrals $G(\nu_1 \dots \nu_N)$ is called an *integral family*. It contains all graphs with a certain propagator configuration such that any scalar product of a loop momentum with another loop momentum or with an external momentum can be expressed as a linear combination of inverse propagators contained in the same family. If some of the propagator powers are zero, this corresponds to subgraphs of the same family. The integrals in a family are in general linearly dependent. Finding a convenient basis, in terms of which all integrals of a given family can be expressed, corresponds to the reduction to *master integrals*.

Note that for a process with N external particles in D dimensions, only $E = \min(N - 1, D)$ of these external momenta will be independent (N is reduced by one due to momentum conservation). In a D -dimensional space (with D assumed to be an integer), any vector can be expressed as a linear combination of D basis vectors. For an N -point process with L loops, the number n of genuinely different scalar products of the type $k_i \cdot k_j$ or $k_i \cdot p_j$ is given by

$$n = L(L + 1)/2 + LE , \quad (3.134)$$

where the first term comes from contracting the loop momenta with themselves, and the second from contraction the loop momenta with the external ones.

As an example for IBP reduction, consider a massive vacuum bubble with an arbitrary propagator power ν :

$$F(\nu) = \int d\bar{k} \frac{1}{(k^2 - m^2 + i\delta)^\nu}, \quad (3.135)$$

where we have used the abbreviation $d\bar{k} = d^D k / (i\pi^{\frac{D}{2}})$. In this simple example we know that there is only one master integral,

$$F(1) = -\Gamma(1 - D/2) (m^2)^{\frac{D}{2}-1}. \quad (3.136)$$

Using the integration-by-parts identity

$$\int d\bar{k} \frac{\partial}{\partial k^\mu} \left\{ \frac{k_\mu}{(k^2 - m^2 + i\delta)^\nu} \right\} = 0$$

leads to

$$\begin{aligned} 0 &= \int d\bar{k} \left\{ \frac{1}{(k^2 - m^2 + i\delta)^\nu} \frac{\partial}{\partial k^\mu} (k_\mu) - \nu k_\mu \frac{2k^\mu}{(k^2 - m^2 + i\delta)^{\nu+1}} \right\} \\ &= D F(\nu) - 2\nu (F(\nu) + m^2 F(\nu + 1)) \\ \Rightarrow F(\nu + 1) &= \frac{D - 2\nu}{2\nu m^2} F(\nu). \end{aligned} \quad (3.137)$$

In less trivial cases, an *order relation* among the integrals has to be introduced to be able to solve the system for a set of master integrals. For example, a topology T_1 is considered to be smaller than a topology T_2 if T_1 can be obtained from T_2 by omitting some of the propagators. Within the same topology, the integrals can be ordered according to the powers of their propagators.

A systematic approach has first been formulated by Laporta [85], therefore it is sometimes also called *Laporta-algorithm*. Completely automated programs for IBP reductions are REDUZE [86, 87], FIRE [88, 89], LITERED [90, 91] and KIRA [92]. Other, more specialised automated reduction programs are FORCER [93] (for two-point integrals up to 4 loops) and AIR [94].

Note: It is not uniquely defined which integrals are master integrals. For complicated multi-loop examples, it is in general not clear before the reduction which integrals will be master integrals. Further, it can sometimes be more convenient to define an integral with a loop momentum in the numerator rather than its scalar counterpart as a master integral, and/or to have master integrals where the power of several propagators is different from one. The main aim is to have an integral basis which is convenient for the subsequent steps to be performed. For example, a *finite basis* [95, 96] is convenient

if the master integrals are to be evaluated numerically. *Finite basis* means that all poles in ϵ are contained in the coefficients of the integrals rather than in the integrals themselves. If the integrals are to be evaluated by *differential equations* [97–102], a basis where the master integrals are of *uniform weight*² is convenient. Ideally, the basis of master integrals has both properties [103].

3.7.2 Multi-loop integrals in Feynman parameter space

Multi-loop integrals can be transformed into integrals over Feynman parameters in a way analogous to the one-loop case, for an arbitrary number of loops. In order to keep the index structure simple, we focus on integrals with no loop momenta in the numerator here. Consider the general integral of Eq. (3.133), where for simplicity of notation we now assume that all propagator powers are positive, $\nu_j > 0$. After Feynman parametrisation, it has the following form:

$$\begin{aligned} G &= \Gamma(N_\nu) \int \prod_{j=1}^N dx_j x_j^{\nu_j-1} \delta(1 - \sum_{i=1}^N x_i) \int d\bar{k}_1 \dots d\bar{k}_L \left[\sum_{j,l=1}^L k_j \cdot k_l M_{jl} - 2 \sum_{j=1}^L k_j \cdot Q_j + J \right]^{-N_\nu} \\ &= (-1)^{N_\nu} \frac{\Gamma(N_\nu - LD/2)}{\prod_{j=1}^N \Gamma(\nu_j)} \int_0^\infty \prod_{j=1}^N dx_j x_j^{\nu_j-1} \delta(1 - \sum_{i=1}^N x_i) \frac{\mathcal{U}^{N_\nu - (L+1)D/2}}{\mathcal{F}^{N_\nu - LD/2}} \quad (3.138) \\ \mathcal{U} &= \det(M) \quad , \quad N_\nu = \sum_{j=1}^N \nu_j \quad , \\ \mathcal{F} &= \det(M) \left[\sum_{i,j=1}^L Q_i M_{ij}^{-1} Q_j - J - i\delta \right] . \end{aligned}$$

The functions \mathcal{U} and \mathcal{F} can be straightforwardly derived from the momentum representation, an example is given below. The functions \mathcal{U} and \mathcal{F} can also be constructed from the topology of the corresponding Feynman graph, as explained in Appendix A.4.

A necessary condition for the presence of infrared divergences is $\mathcal{F} = 0$. The function \mathcal{U} cannot lead to infrared divergences of the graph, since giving a mass to all external legs would not change \mathcal{U} . Apart from the fact that the graph may have an overall UV divergence contained in the overall Γ -function in Eq. (3.138), UV subdivergences may also be present. A necessary condition for these is that \mathcal{U} is vanishing.

Example: planar two-loop box with $p_1^2 = p_2^2 = p_3^2 = 0$, $p_4^2 \neq 0$:

²The definition of *weight* ω (sometimes also called “transcendentality”) for functions with trivial argument is the following: $\omega(r) = 0$ if r is a rational number, $\omega(\pi^k) = \omega(\zeta(k)) = k$, $\omega(x \cdot y) = \omega(x) + \omega(y)$.

Using $k_1 = k$, $k_2 = l$ and propagator number one as $1/(k^2 + i\delta)$, the denominator, after Feynman parametrisation, can be written as

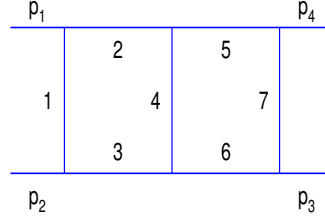


Figure 30: Labelling for the planar two-loop box example.

$$\begin{aligned} \mathcal{D} &= x_1 k^2 + x_2 (k - p_1)^2 + x_3 (k + p_2)^2 + x_4 (k - l)^2 + x_5 (l - p_1)^2 + x_6 (l + p_2)^2 + x_7 (l + p_2 + p_3)^2 \\ &= (k, l) \begin{pmatrix} x_{1234} & -x_4 \\ -x_4 & x_{4567} \end{pmatrix} \begin{pmatrix} k \\ l \end{pmatrix} - 2 (Q_1, Q_2) \begin{pmatrix} k \\ l \end{pmatrix} + x_7 (p_2 + p_3)^2 + i\delta \\ Q &= (Q_1, Q_2) = (x_2 p_1 - x_3 p_2, x_5 p_1 - x_6 p_2 - x_7 (p_2 + p_3)) , \end{aligned}$$

where we have used the short-hand notation $x_{ijk\dots} = x_i + x_j + x_k + \dots$. Therefore

$$\begin{aligned} \mathcal{U} &= x_{123} x_{567} + x_4 x_{123567} \\ \mathcal{F} &= (-s_{12}) (x_2 x_3 x_{4567} + x_5 x_6 x_{1234} + x_2 x_4 x_6 + x_3 x_4 x_5) \\ &\quad + (-s_{23}) x_1 x_4 x_7 + (-p_4^2) x_7 (x_2 x_4 + x_5 x_{1234}) . \end{aligned}$$

A general representation for tensor integrals is straightforward, it can be found e.g. in Ref. [104].

3.7.3 Calculation of master integrals

Broadly speaking, there are two ways to calculate master integrals:

1. Analytically, such that the result can be expressed in terms of analytic functions: in rare cases in closed form, otherwise as an expansion in the regularisation parameter ϵ .
2. Numerically, where the coefficient of each term in the Laurent series in ϵ is just a number.

To have the result in analytic form is usually preferable to the numerical approach, however it may not always be possible.

For the analytic evaluation, various methods exist. Direct integration in Feynman parameter space is the most straightforward option, but for multi-scale integrals this becomes quickly very cumbersome. The choice of a convenient parametrisation and the order of the integrations over Feynman parameters is very important. Another method which was successfully applied to two-loop integrals is to transform the integral to a Mellin-Barnes representation [105–107]. However, the most successful method nowadays to obtain analytic results is via *differential equations* [97–102].

On the numerical side, there are various methods, see e.g. [108] for a review. We will focus here on the method of sector decomposition [109–111]. It is not purely numerical, as it first employs an algebraic method to isolate the $1/\epsilon$ poles from an integral in Feynman parameter representation.

3.7.4 Sector decomposition

Sector decomposition is a method operating in Feynman parameter space which is useful to extract singularities regulated by dimensional regularisation, converting the integral into a Laurent series in ϵ . It is particularly useful if the singularities are overlapping in the sense specified below. The coefficients of the poles in $1/\epsilon$ will be finite integrals over Feynman parameters, which, for most examples beyond one loop, will be too complicated to be integrated analytically, so they have to be integrated numerically.

To introduce the basic concept, let us look at the simple example of a two-dimensional parameter integral of the following form:

$$I = \int_0^1 dx \int_0^1 dy x^{-1-a\epsilon} y^{-b\epsilon} (x+y)^{-1}. \quad (3.139)$$

The integral contains a singular region where x and y vanish *simultaneously*, i.e. the singularities in x and y are *overlapping*. Our aim is to factorise the singularities for $x \rightarrow 0$ and $y \rightarrow 0$. Therefore we divide the integration range into two sectors where x and y are ordered (see Fig. 31)

$$I = \int_0^1 dx \int_0^1 dy x^{-1-a\epsilon} y^{-b\epsilon} (x+y)^{-1} \underbrace{[\Theta(x-y) + \Theta(y-x)]}_{(1)}_{(2)}.$$

Now we substitute $y = x t$ in sector (1) and $x = y t$ in sector (2) to remap the integration range to the unit square and obtain

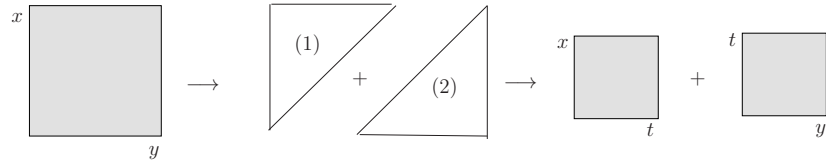


Figure 31: Sector decomposition schematically.

$$I = \int_0^1 dx x^{-1-(a+b)\epsilon} \int_0^1 dt t^{-b\epsilon} (1+t)^{-1} + \int_0^1 dy y^{-1-(a+b)\epsilon} \int_0^1 dt t^{-1-a\epsilon} (1+t)^{-1}. \quad (3.140)$$

We observe that the singularities are now factorised such that they can be read off from the powers of simple monomials in the integration variables, while the polynomial denominator goes to a constant if the integration variables approach zero.

The same concept can be applied to N -dimensional parameter integrals over polynomials raised to some power, as for example the functions \mathcal{F} and \mathcal{U} appearing in loop integrals, where the procedure in general has to be iterated to achieve complete factorisation. It also can be applied to phase space integrals, where (multiple) soft/collinear limits are regulated by dimensional regularisation.

A review on sector decomposition can be found in ref. [104]. Public implementations of the sector decomposition algorithm can be found in [112–120].

A Appendix

A.1 Evidence for colour

Adapted from Ref. [121].

How can it be experimentally verified that the QCD colour quantum numbers exist? This is not straightforward, since colour is confined (hadrons are “white”), so that its existence can only be inferred.

Consider the total cross section for the production of a fermion-antifermion pair $f\bar{f}$ in an electron-positron collision, to lowest order in the electromagnetic coupling. The fermion has electromagnetic charge eQ_f and mass m , and we approximate the electron to be massless. The answer is in fact quite simple

$$\sigma_f(s) = \frac{4\pi\alpha^2 Q_f^2}{3s} \beta \left(1 + \frac{2m_f^2}{s}\right) \theta(s - 4m_f^2), \quad (\text{A.1})$$

where s is the center-of-mass energy squared. Note that we have attached a label f to the mass the type of fermion f . The factor involving the electric charges also depends on the fermion “flavour”. Thus, for an electron, muon and tau $Q_f = -1$, for up, charm, and top quarks $Q_f = 2/3$, while for down, strange and bottom quarks $Q_f = -1/3$. The factor $\beta = \sqrt{1 - 4m_f^2/s}$ is a phase space volume factor: when s is just a little bit larger than $4m_f^2$, β is close to zero, i.e. near threshold the cross section is small. Far above threshold $\beta \sim 1$. The theta function ensures that the cross section is only non-zero if the center of mass energy is large enough to produce the fermion pair.

We can use this result to infer the number of colour charges because quarks of each colour make their contribution to the total cross section. If the produced fermions are charged leptons (electrons, muons or taus), we can directly confront the result with data, and agreement is in fact very good. However, if the produced fermions are quarks, we have to sum over the additional flavours and colours in Eq. (A.1). The inclusive hadronic cross section (based in the production of quark-antiquark pairs) reads

$$\sigma_{had}(s) = \sum_{f=u,d,s,c,\dots} \frac{4\pi\alpha^2 Q_f^2}{3s} \beta \left(1 + \frac{2m_f^2}{s}\right) \theta(s - 4m_f^2) N_c \quad (\text{A.2})$$

The extra factor N_c at the end accounts for the fact that quarks come in $N_c = 3$ colours. We may interpret this as a prediction for the inclusive hadronic cross section because the quarks in the final state must, before they reach any detector, make a transition to a hadronic final state, see the illustration in Fig. 32. In Fig. 33 we see the confrontation of this result with data, and that the agreement is very good, except that we did not anticipate the huge peak near $\sqrt{s} \simeq 90\text{GeV}$. That is because we did

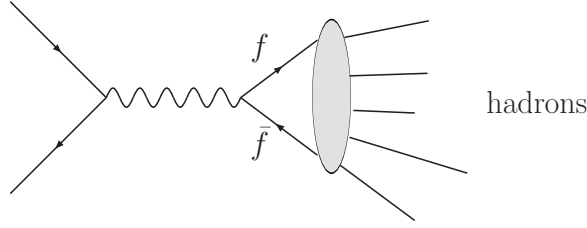


Figure 32: $e^+e^- \rightarrow$ hadrons; the blob represents the “hadronization” process, where the quarks get confined into hadrons.

not include in our calculation of $\sigma_f(s)$ in eq. (A.1) a second diagram in which not a photon (as in Fig. 32) but a Z -boson of mass $M_Z \simeq 91\text{GeV}$ is exchanged between the e^+e^- and the $f\bar{f}$ pair. Had we done so, we would have more terms in the final answer for $\sigma(s)$ in Eq. (A.1), with the factor $1/s$ replaced by $1/(s - M_Z^2 + \Gamma_Z^2)$, where Γ_Z is the Z -boson decay width (about 2.5 GeV). The good agreement also implies that the effect of higher order corrections to $\sigma(s)$ should be small, and indeed they turn out to be so, after calculation. We can now define an observable traditionally called the R -ratio:

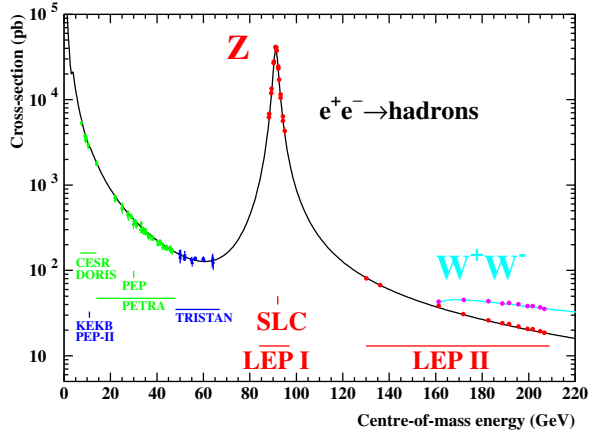


Figure 33: Total cross section for e^+e^- to hadrons.

$$R(s) = \frac{\sigma(e^+e^- \rightarrow \text{hadrons})}{\sigma(e^+e^- \rightarrow \mu^+\mu^-)} . \quad (\text{A.3})$$

The benefit of defining such a ratio is that many common factors cancel in the theoretical prediction, and that many experimental uncertainties cancel in the experimental measurement. We have

$$R(s) = \frac{\sum_{f=u,d,s,c,\dots} \sigma(e^+e^- \rightarrow f\bar{f})}{\sigma(e^+e^- \rightarrow \mu^+\mu^-)} . \quad (\text{A.4})$$

For large center-of-mass energy \sqrt{s} we can derive from (A.2) that

$$R(s) \xrightarrow{s \rightarrow \infty} N_c \sum_{f=u,d,s,c,\dots} Q_f^2 \theta(s - 4m_f^2) \quad (\text{A.5})$$

In Fig. 34 we confront this result with experiment. We can draw the conclusions that

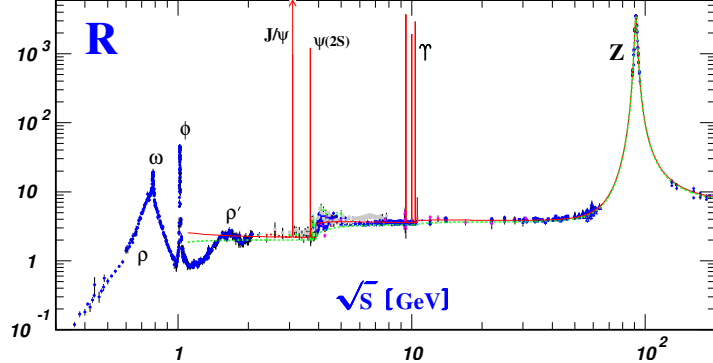


Figure 34: R-ratio vs. center of mass energy

- (i) there is again fairly good agreement between prediction and measurement; (ii) we see the effects of new quark flavour f being “turned on” as the energy increases beyond the production threshold $2m_f$ ($m_c \simeq 1.5$ GeV, $m_b \simeq 4.5$ GeV); (iii) the larger step at charm than at bottom (proportional to $Q_c^2 = 4/9$ and $Q_b^2 = 1/9$, respectively) is well-predicted; (iv) the value of $R(s)$ beyond the bottom quark threshold

$$R(s) = N_c \sum_{f=u,d,s,c,b} Q_f^2 \theta(s - 4m_f^2) = 3 \left(\frac{4}{9} + \frac{1}{9} + \frac{1}{9} + \frac{4}{9} + \frac{1}{9} \right) = \frac{11}{3} \quad (\text{A.6})$$

agrees with experiment, and indicates that quarks come indeed in 3 colours.

A.2 The strong CP problem

In addition to the Yang-Mills Lagrangian, one can construct an additional gauge invariant dimension-four operator, the Θ -term:

$$\mathcal{L}_\Theta = \frac{\Theta g_s}{32\pi^2} \sum_a F_{\mu\nu}^a \tilde{F}^{a,\mu\nu}, \quad \text{with} \quad \tilde{F}^{a,\mu\nu} = \frac{1}{2} \epsilon^{\mu\nu\alpha\beta} F_{\alpha\beta}^a.$$

As it would give a (CP-violating) contribution to the electric dipole moment of the neutron, we know that Θ must be very small, $\Theta < 10^{-10}$. Why this term is so small (or probably zero) is not known. This is called the “strong CP problem”. A possible solution has been suggested by Peccei and Quinn (1977), where the Θ -term belongs to

an additional $U(1)$ symmetry, associated with a complex scalar field, called the *axion*. This symmetry is spontaneously broken by the vacuum expectation value obtained by this scalar field; the axion is the (almost) massless Goldstone boson of this broken symmetry. Searches for the axion are ongoing in several experiments.

A.3 Form factors for tensor two-point functions

We provide the form factors for one- and two-point functions in this appendix. We give the kinematical arguments in terms of kinematic invariants, as \mathcal{S} is trivial in these cases. In order to have a shift invariant formulation, we define differences of external momenta

$$\Delta_{ia}^\mu = r_i^\mu - r_a^\mu .$$

Usually one chooses $a = N$ and $r_N = 0$.

$$I_1^D(m_1^2) = -r_\Gamma \Gamma\left(1 - \frac{D}{2}\right) (m^2 - i\delta)^{\frac{D}{2}-1}, \quad r_\Gamma = \frac{\Gamma(1+\epsilon)\Gamma^2(1-\epsilon)}{\Gamma(1-2\epsilon)} . \quad (\text{A.7})$$

Note that 1-point functions can be written as degenerate 2-point functions:

$$I_1^D(m_1^2) = m_1^2 I_2^D(0, 0, m_1^2) . \quad (\text{A.8})$$

The kinematical matrix for general 2-point functions is

$$\mathcal{S} = - \begin{pmatrix} 2m_1^2 & -s + m_1^2 + m_2^2 \\ -s + m_1^2 + m_2^2 & 2m_2^2 \end{pmatrix} \quad (\text{A.9})$$

The Lorentz tensor decomposition for the tensor 2-point functions with maximal rank 2, defined by

$$I_2^{D,\mu_1\mu_2}(a_1, a_2; s, m_1^2, m_2^2) = \int \frac{d^D k}{i\pi^{D/2}} \frac{q_{a_1}^{\mu_1} q_{a_2}^{\mu_2}}{\prod_{i \in S} (q_i^2 - m_i^2 + i\varepsilon)} \quad (\text{A.10})$$

is

$$I_2^{D,\mu_1}(a_1; s, m_1^2, m_2^2) = \sum_{l_1 \in S} \Delta_{l_1 a_1}^{\mu_1} A_{l_1}^{2,1}(S) \quad (\text{A.11})$$

$$I_2^{D,\mu_1\mu_2}(a_1, a_2; s, m_1^2, m_2^2) = g^{\mu_1\mu_2} B^{2,2}(S) + \sum_{l_1, l_2 \in S} \Delta_{l_1 a_1}^{\mu_1} \Delta_{l_2 a_2}^{\mu_2} A_{l_1 l_2}^{2,2}(S) . \quad (\text{A.12})$$

The form factors are given by

$$\begin{aligned}
A_1^{2,1}(s, m_1^2, m_2^2) &= -\frac{1}{2} I_2^D(s, m_1^2, m_2^2) \\
&\quad + \frac{m_1^2 - m_2^2}{2s} [I_2^D(s, m_1^2, m_2^2) - I_2^D(0, m_1^2, m_2^2)] \\
B^{2,2}(s, m_1^2, m_2^2) &= \frac{1}{2(D-1)} \left[2m_2^2 I_2^D(s, m_1^2, m_2^2) + m_1^2 I_2^D(0, 0, m_1^2) \right. \\
&\quad + \frac{-s + m_1^2 - m_2^2}{2} \left(I_2^D(s, m_1^2, m_2^2) \right. \\
&\quad \left. \left. - \frac{m_1^2 - m_2^2}{s} [I_2^D(s, m_1^2, m_2^2) - I_2^D(0, m_1^2, m_2^2)] \right) \right] \\
A_{11}^{2,2}(s, m_1^2, m_2^2) &= \frac{1}{2(D-1)s} \left[\frac{D(s - m_1^2 + m_2^2)}{2} \left(I_2^D(s, m_1^2, m_2^2) \right. \right. \\
&\quad \left. \left. - \frac{m_1^2 - m_2^2}{s} [I_2^D(s, m_1^2, m_2^2) - I_2^D(0, m_1^2, m_2^2)] \right) \right. \\
&\quad \left. - 2m_2^2 I_2^D(s, m_1^2, m_2^2) + (D-2)m_1^2 I_2^D(0, 0, m_1^2) \right] \quad (\text{A.13})
\end{aligned}$$

The other tensor coefficients are obtained by the following relations

$$\begin{aligned}
A_1^{2,1} + A_2^{2,1} &= -I_2^D \\
A_{11}^{2,2} + A_{12}^{2,2} &= -A_1^{2,1} \\
A_{21}^{2,2} + A_{22}^{2,2} &= -A_2^{2,1} \\
A_{11}^{2,2} + A_{12}^{2,2} + A_{21}^{2,2} + A_{22}^{2,2} &= I_2^D \quad (\text{A.14})
\end{aligned}$$

which follow directly from the fact that in one-loop parameter integrals, the sum of all Feynman parameters is equal to one. The general 2-point scalar integral is well known [38]. We give here the integral representation for completeness.

$$I_2^D(s, m_1, m_2) = \Gamma(\epsilon) - \int_0^1 dx \log(-sx(1-x) + xm_1^2 + (1-x)m_2^2 - i\delta) + \mathcal{O}(\epsilon)$$

If the external vector is light-like the formulae degenerate to

$$\begin{aligned}
A_1^{2,1}(0, m_1^2, m_2^2) &= + \frac{(4m_1^2 - Dm_1^2 + Dm_2^2)m_1^2}{2D(m_2^2 - m_1^2)^2} I_2^D(0, 0, m_1^2) \\
&\quad + \frac{(-4m_2^2 - Dm_1^2 + Dm_2^2)m_2^2}{2D(m_2^2 - m_1^2)^2} I_2^D(0, 0, m_2^2) \\
&\quad - \frac{1}{2(m_1^2 - m_2^2)} (m_1^2 I_2^D(0, 0, m_1^2) - m_2^2 I_2^D(0, 0, m_2^2)) \\
B^{2,2}(0, m_1^2, m_2^2) &= - \frac{m_1^4}{D(m_2^2 - m_1^2)} I_2^D(0, 0, m_1^2) + \frac{m_2^4}{D(m_2^2 - m_1^2)} I_2^D(0, 0, m_2^2) \\
A_{11}^{2,2}(0, m_1^2, m_2^2) &= \frac{1}{(D+2)D(m_1^2 - m_2^2)^3} \left([(m_1^2 - m_2^2)^2 D(D+2) \right. \\
&\quad \left. - 4m_1^2(D(m_1^2 - m_2^2) - 2m_2^2)] m_1^2 I_2^D(0, 0, m_1^2) \right. \\
&\quad \left. - 8m_2^6 I_2^D(0, 0, m_2^2) \right)
\end{aligned} \tag{A.15}$$

where

$$\begin{aligned}
I_2^D(0, m_1^2, m_2^2) &= \frac{m_2^2 I_2^D(0, 0, m_2^2) - m_1^2 I_2^D(0, 0, m_1^2)}{m_2^2 - m_1^2} \\
I_2^D(0, 0, m_1^2) &= \frac{I_1^D(m_1^2)}{m_1^2} = \frac{2}{D-2} I_2^D(0, m_1^2, m_1^2) = -\Gamma(1-D/2) (m_1^2)^{D/2-2}
\end{aligned} \tag{A.16}$$

In the case $m_1 = m_2$ one finds

$$\begin{aligned}
A_1^{2,1}(0, m_1^2, m_1^2) &= -\frac{(D-2)}{4} I_2^D(0, 0, m_1^2) \\
B^{2,2}(0, m_1^2, m_1^2) &= \frac{m_1^2}{2} I_2^D(0, 0, m_1^2) \\
A_{11}^{2,2}(0, m_1^2, m_1^2) &= \frac{n-2}{6} I_2^D(0, 0, m_1^2).
\end{aligned} \tag{A.17}$$

A.4 Construction of the functions \mathcal{F} and \mathcal{U} from topological rules

Cutting L lines of a given connected L -loop graph such that it becomes a connected tree graph T defines a chord $\mathcal{C}(T)$ as being the set of lines not belonging to this tree. The Feynman parameters associated with each chord define a monomial of degree L . The set of all such trees (or 1-trees) is denoted by \mathcal{T}_1 . The 1-trees $T \in \mathcal{T}_1$ define \mathcal{U} as being the sum over all monomials corresponding to a chord $\mathcal{C}(T \in \mathcal{T}_1)$. Cutting one more line of a 1-tree leads to two disconnected trees, or a 2-tree \hat{T} . \mathcal{T}_2 is the set of all such 2-trees. The corresponding chords define monomials of degree $L+1$. Each 2-tree of a graph corresponds to a cut defined by cutting the lines which connected the 2 now

disconnected trees in the original graph. The momentum flow through the lines of such a cut defines a Lorentz invariant $s_{\hat{T}} = (\sum_{j \in \text{Cut}(\hat{T})} p_j)^2$. The function \mathcal{F}_0 is the sum over all such monomials times minus the corresponding invariant:

$$\begin{aligned}\mathcal{U}(\vec{x}) &= \sum_{T \in \mathcal{T}_1} \left[\prod_{j \in \mathcal{C}(T)} x_j \right] , \\ \mathcal{F}_0(\vec{x}) &= \sum_{\hat{T} \in \mathcal{T}_2} \left[\prod_{j \in \mathcal{C}(\hat{T})} x_j \right] (-s_{\hat{T}}) , \\ \mathcal{F}(\vec{x}) &= \mathcal{F}_0(\vec{x}) + \mathcal{U}(\vec{x}) \sum_{j=1}^N x_j m_j^2 .\end{aligned}\tag{A.18}$$

References

- [1] M. Gell-Mann, *A Schematic Model of Baryons and Mesons*, *Phys. Lett.* **8** (1964) 214–215.
- [2] G. Zweig, *An SU_3 model for strong interaction symmetry and its breaking; Version 1*, Tech. Rep. CERN-TH-401, CERN, Geneva, Jan, 1964.
- [3] H. Fritzsch, M. Gell-Mann and H. Leutwyler, *Advantages of the Color Octet Gluon Picture*, *Phys. Lett.* **47B** (1973) 365–368.
- [4] D. J. Gross, *Twenty five years of asymptotic freedom*, *Nucl. Phys. Proc. Suppl.* **74** (1999) 426–446, [[hep-th/9809060](#)].
- [5] P. A. Baikov, K. G. Chetyrkin, J. H. Kühn and J. Rittinger, *Complete $\mathcal{O}(\alpha_s^4)$ QCD Corrections to Hadronic Z-Decays*, *Phys. Rev. Lett.* **108** (2012) 222003, [[1201.5804](#)].
- [6] F. Herzog, B. Ruijl, T. Ueda, J. A. M. Vermaseren and A. Vogt, *On Higgs decays to hadrons and the R-ratio at N^4LO* , *JHEP* **08** (2017) 113, [[1707.01044](#)].
- [7] T. van Ritbergen, J. A. M. Vermaseren and S. A. Larin, *The Four loop beta function in quantum chromodynamics*, *Phys. Lett.* **B400** (1997) 379–384, [[hep-ph/9701390](#)].
- [8] P. A. Baikov, K. G. Chetyrkin and J. H. Kühn, *Five-Loop Running of the QCD coupling constant*, *Phys. Rev. Lett.* **118** (2017) 082002, [[1606.08659](#)].
- [9] F. Herzog, B. Ruijl, T. Ueda, J. A. M. Vermaseren and A. Vogt, *The five-loop beta function of Yang-Mills theory with fermions*, *JHEP* **02** (2017) 090, [[1701.01404](#)].
- [10] T. Luthe, A. Maier, P. Marquard and Y. Schröder, *The five-loop Beta function for a general gauge group and anomalous dimensions beyond Feynman gauge*, *JHEP* **10** (2017) 166, [[1709.07718](#)].

- [11] K. G. Chetyrkin, G. Falcioni, F. Herzog and J. A. M. Verma, *Five-loop renormalisation of QCD in covariant gauges*, *JHEP* **10** (2017) 179, [[1709.08541](#)].
- [12] D. J. Gross and F. Wilczek, *Ultraviolet Behavior of Nonabelian Gauge Theories*, *Phys. Rev. Lett.* **30** (1973) 1343–1346.
- [13] H. D. Politzer, *Reliable Perturbative Results for Strong Interactions?*, *Phys. Rev. Lett.* **30** (1973) 1346–1349.
- [14] P. A. Baikov, K. G. Chetyrkin and J. H. Kühn, *Quark Mass and Field Anomalous Dimensions to $\mathcal{O}(\alpha_s^5)$* , *JHEP* **10** (2014) 076, [[1402.6611](#)].
- [15] P. A. Baikov, K. G. Chetyrkin and J. H. Kühn, *Five-loop fermion anomalous dimension for a general gauge group from four-loop massless propagators*, *JHEP* **04** (2017) 119, [[1702.01458](#)].
- [16] G. 't Hooft and M. J. G. Veltman, *Regularization and Renormalization of Gauge Fields*, *Nucl. Phys.* **B44** (1972) 189–213.
- [17] C. G. Bollini and J. J. Giambiagi, *Dimensional Renormalization: The Number of Dimensions as a Regularizing Parameter*, *Nuovo Cim.* **B12** (1972) 20–26.
- [18] P. Breitenlohner and D. Maison, *Dimensional Renormalization and the Action Principle*, *Commun. Math. Phys.* **52** (1977) 11–38.
- [19] S. A. Larin, *The Renormalization of the axial anomaly in dimensional regularization*, *Phys. Lett.* **B303** (1993) 113–118, [[hep-ph/9302240](#)].
- [20] A. Signer and D. Stöckinger, *Using Dimensional Reduction for Hadronic Collisions*, *Nucl. Phys.* **B808** (2009) 88–120, [[0807.4424](#)].
- [21] K. G. Wilson, *Quantum field theory models in less than four-dimensions*, *Phys. Rev.* **D7** (1973) 2911–2926.
- [22] J. C. Collins, *Renormalization*, vol. 26 of *Cambridge Monographs on Mathematical Physics*. Cambridge University Press, Cambridge, 1986.
- [23] D. Stöckinger, *Regularization by dimensional reduction: consistency, quantum action principle, and supersymmetry*, *JHEP* **03** (2005) 076, [[hep-ph/0503129](#)].
- [24] W. Siegel, *Inconsistency of Supersymmetric Dimensional Regularization*, *Phys. Lett.* **94B** (1980) 37–40.
- [25] S. Catani, M. H. Seymour and Z. Trocsanyi, *Regularization scheme independence and unitarity in QCD cross-sections*, *Phys. Rev.* **D55** (1997) 6819–6829, [[hep-ph/9610553](#)].
- [26] T. Binoth, J. P. Guillet, G. Heinrich, E. Pilon and C. Schubert, *An Algebraic/numerical formalism for one-loop multi-leg amplitudes*, *JHEP* **10** (2005) 015, [[hep-ph/0504267](#)].

- [27] T. Binoth, J. P. Guillet and G. Heinrich, *Reduction formalism for dimensionally regulated one loop N point integrals*, *Nucl. Phys.* **B572** (2000) 361–386, [[hep-ph/9911342](#)].
- [28] G. Passarino and M. J. G. Veltman, *One Loop Corrections for e+ e- Annihilation Into mu+ mu- in the Weinberg Model*, *Nucl. Phys.* **B160** (1979) 151–207.
- [29] T. Hahn, *Feynman Diagram Calculations with FeynArts, FormCalc, and LoopTools*, *PoS ACAT2010* (2010) 078, [[1006.2231](#)].
- [30] T. Hahn and M. Perez-Victoria, *Automatized one loop calculations in four-dimensions and D-dimensions*, *Comput. Phys. Commun.* **118** (1999) 153–165, [[hep-ph/9807565](#)].
- [31] A. van Hameren, *OneLoop: For the evaluation of one-loop scalar functions*, *Comput. Phys. Commun.* **182** (2011) 2427–2438, [[1007.4716](#)].
- [32] J. P. Guillet, G. Heinrich and J. F. von Soden-Fraunhofen, *Tools for NLO automation: extension of the golem95C integral library*, *Comput. Phys. Commun.* **185** (2014) 1828–1834, [[1312.3887](#)].
- [33] G. Cullen, J. P. Guillet, G. Heinrich, T. Kleinschmidt, E. Pilon, T. Reiter et al., *Golem95C: A library for one-loop integrals with complex masses*, *Comput. Phys. Commun.* **182** (2011) 2276–2284, [[1101.5595](#)].
- [34] T. Binoth, J. P. Guillet, G. Heinrich, E. Pilon and T. Reiter, *Golem95: A Numerical program to calculate one-loop tensor integrals with up to six external legs*, *Comput. Phys. Commun.* **180** (2009) 2317–2330, [[0810.0992](#)].
- [35] A. Denner, S. Dittmaier and L. Hofer, *Collier: a fortran-based Complex One-Loop Library in Extended Regularizations*, *Comput. Phys. Commun.* **212** (2017) 220–238, [[1604.06792](#)].
- [36] H. H. Patel, *Package-X: A Mathematica package for the analytic calculation of one-loop integrals*, *Comput. Phys. Commun.* **197** (2015) 276–290, [[1503.01469](#)].
- [37] S. Carrazza, R. K. Ellis and G. Zanderighi, *QCDLoop: a comprehensive framework for one-loop scalar integrals*, *Comput. Phys. Commun.* **209** (2016) 134–143, [[1605.03181](#)].
- [38] R. K. Ellis and G. Zanderighi, *Scalar one-loop integrals for QCD*, *JHEP* **02** (2008) 002, [[0712.1851](#)].
- [39] R. K. Ellis, Z. Kunszt, K. Melnikov and G. Zanderighi, *One-loop calculations in quantum field theory: from Feynman diagrams to unitarity cuts*, *Phys. Rept.* **518** (2012) 141–250, [[1105.4319](#)].
- [40] T. Kinoshita, *Mass singularities of Feynman amplitudes*, *J. Math. Phys.* **3** (1962) 650–677.

- [41] T. D. Lee and M. Nauenberg, *Degenerate Systems and Mass Singularities*, *Phys. Rev.* **133** (1964) B1549–B1562.
- [42] S. Catani and M. H. Seymour, *A General algorithm for calculating jet cross-sections in NLO QCD*, *Nucl. Phys.* **B485** (1997) 291–419, [[hep-ph/9605323](#)].
- [43] S. Catani and M. Grazzini, *The soft gluon current at one loop order*, *Nucl. Phys.* **B591** (2000) 435–454, [[hep-ph/0007142](#)].
- [44] G. F. Sterman and S. Weinberg, *Jets from Quantum Chromodynamics*, *Phys. Rev. Lett.* **39** (1977) 1436.
- [45] S. Bethke, Z. Kunszt, D. E. Soper and W. J. Stirling, *New jet cluster algorithms: Next-to-leading order QCD and hadronization corrections*, *Nucl. Phys.* **B370** (1992) 310–334.
- [46] M. Cacciari, G. P. Salam and G. Soyez, *The Anti- $k(t)$ jet clustering algorithm*, *JHEP* **04** (2008) 063, [[0802.1189](#)].
- [47] S. Weinzierl, *Jet algorithms in electron-positron annihilation: Perturbative higher order predictions*, *Eur. Phys. J.* **C71** (2011) 1565, [[1011.6247](#)].
- [48] A. Gehrmann-De Ridder, T. Gehrmann, E. W. N. Glover and G. Heinrich, *Jet rates in electron-positron annihilation at O(alpha(s)**3) in QCD*, *Phys. Rev. Lett.* **100** (2008) 172001, [[0802.0813](#)].
- [49] Z. Trocsanyi, *QCD for collider experiments*, in *Proceedings, 2013 European School of High-Energy Physics (ESHEP 2013): Paradfurdo, Hungary, June 5-18, 2013*, pp. 65–116, 2015. [1608.02381](#). DOI.
- [50] K. Long, *QCD at high-energy (experiments)*, [hep-ex/0212008](#).
- [51] S. Moch, B. Ruijl, T. Ueda, J. A. M. Vermaseren and A. Vogt, *Four-Loop Non-Singlet Splitting Functions in the Planar Limit and Beyond*, *JHEP* **10** (2017) 041, [[1707.08315](#)].
- [52] Y. L. Dokshitzer, *Calculation of the Structure Functions for Deep Inelastic Scattering and e+ e- Annihilation by Perturbation Theory in Quantum Chromodynamics.*, *Sov. Phys. JETP* **46** (1977) 641–653.
- [53] V. N. Gribov and L. N. Lipatov, *Deep inelastic e p scattering in perturbation theory*, *Sov. J. Nucl. Phys.* **15** (1972) 438–450.
- [54] G. Altarelli and G. Parisi, *Asymptotic Freedom in Parton Language*, *Nucl. Phys.* **B126** (1977) 298–318.
- [55] T. Hahn, *Generating Feynman diagrams and amplitudes with FeynArts 3*, *Comput. Phys. Commun.* **140** (2001) 418–431, [[hep-ph/0012260](#)].

- [56] T. Hahn, S. Paßehr and C. Schappacher, *FormCalc 9 and Extensions*, *PoS LL2016* (2016) 068, [[1604.04611](#)].
- [57] V. Shtabovenko, R. Mertig and F. Orellana, *New Developments in FeynCalc 9.0*, *Comput. Phys. Commun.* **207** (2016) 432–444, [[1601.01167](#)].
- [58] V. Shtabovenko, *FeynHelpers: Connecting FeynCalc to FIRE and Package-X*, *Comput. Phys. Commun.* **218** (2017) 48–65, [[1611.06793](#)].
- [59] G. Cullen, N. Greiner, G. Heinrich, G. Luisoni, P. Mastrolia et al., *Automated One-Loop Calculations with GoSam*, *Eur.Phys.J. C72* (2012) 1889, [[1111.2034](#)].
- [60] G. Cullen et al., *GoSam-2.0: a tool for automated one-loop calculations within the Standard Model and beyond*, *Eur. Phys. J. C74* (2014) 3001, [[1404.7096](#)].
- [61] G. Bevilacqua, M. Czakon, M. V. Garzelli, A. van Hameren, A. Kardos, C. G. Papadopoulos et al., *HELAC-NLO*, *Comput. Phys. Commun.* **184** (2013) 986–997, [[1110.1499](#)].
- [62] V. Hirschi, R. Frederix, S. Frixione, M. V. Garzelli, F. Maltoni and R. Pittau, *Automation of one-loop QCD corrections*, *JHEP 05* (2011) 044, [[1103.0621](#)].
- [63] J. Alwall, R. Frederix, S. Frixione, V. Hirschi, F. Maltoni, O. Mattelaer et al., *The automated computation of tree-level and next-to-leading order differential cross sections, and their matching to parton shower simulations*, *JHEP 07* (2014) 079, [[1405.0301](#)].
- [64] F. Cascioli, P. Maierhofer and S. Pozzorini, *Scattering Amplitudes with Open Loops*, *Phys. Rev. Lett.* **108** (2012) 111601, [[1111.5206](#)].
- [65] S. Actis, A. Denner, L. Hofer, J.-N. Lang, A. Scharf and S. Uccirati, *RECOLA: REcursive Computation of One-Loop Amplitudes*, *Comput. Phys. Commun.* **214** (2017) 140–173, [[1605.01090](#)].
- [66] J. Bellm et al., *Herwig 7.0/Herwig++ 3.0 release note*, *Eur. Phys. J. C76* (2016) 196, [[1512.01178](#)].
- [67] P. Nason, *A New method for combining NLO QCD with shower Monte Carlo algorithms*, *JHEP 11* (2004) 040, [[hep-ph/0409146](#)].
- [68] S. Frixione, P. Nason and C. Oleari, *Matching NLO QCD computations with Parton Shower simulations: the POWHEG method*, *JHEP 11* (2007) 070, [[0709.2092](#)].
- [69] S. Alioli, P. Nason, C. Oleari and E. Re, *A general framework for implementing NLO calculations in shower Monte Carlo programs: the POWHEG BOX*, *JHEP 06* (2010) 043, [[1002.2581](#)].
- [70] T. Gleisberg, S. Höche, F. Krauss, M. Schönher, S. Schumann, F. Siegert et al., *Event generation with SHERPA 1.1*, *JHEP 02* (2009) 007, [[0811.4622](#)].

- [71] S. Höche, F. Krauss, M. Schönher and F. Siegert, *QCD matrix elements + parton showers: The NLO case*, *JHEP* **04** (2013) 027, [[1207.5030](#)].
- [72] T. Binoth et al., *A Proposal for a standard interface between Monte Carlo tools and one-loop programs*, *Comput. Phys. Commun.* **181** (2010) 1612–1622, [[1001.1307](#)].
- [73] S. Alioli et al., *Update of the Binoth Les Houches Accord for a standard interface between Monte Carlo tools and one-loop programs*, *Comput. Phys. Commun.* **185** (2014) 560–571, [[1308.3462](#)].
- [74] C. F. Berger, Z. Bern, L. J. Dixon, F. Febres Cordero, D. Forde, H. Ita et al., *An Automated Implementation of On-Shell Methods for One-Loop Amplitudes*, *Phys. Rev.* **D78** (2008) 036003, [[0803.4180](#)].
- [75] G. Belanger, F. Boudjema, J. Fujimoto, T. Ishikawa, T. Kaneko, K. Kato et al., *Automatic calculations in high energy physics and Grace at one-loop*, *Phys. Rept.* **430** (2006) 117–209, [[hep-ph/0308080](#)].
- [76] J. M. Campbell, R. K. Ellis and W. T. Giele, *A Multi-Threaded Version of MCFM*, *Eur. Phys. J.* **C75** (2015) 246, [[1503.06182](#)].
- [77] S. Badger, B. Biedermann, P. Uwer and V. Yundin, *Numerical evaluation of virtual corrections to multi-jet production in massless QCD*, *Comput. Phys. Commun.* **184** (2013) 1981–1998, [[1209.0100](#)].
- [78] J. Baglio et al., *VBFNLO: A Parton Level Monte Carlo for Processes with Electroweak Bosons – Manual for Version 2.7.0*, [1107.4038](#).
- [79] C. Duhr, *Mathematical aspects of scattering amplitudes*, in *Proceedings, Theoretical Advanced Study Institute in Elementary Particle Physics: Journeys Through the Precision Frontier: Amplitudes for Colliders (TASI 2014): Boulder, Colorado, June 2-27, 2014*, pp. 419–476, 2015. [1411.7538](#). DOI.
- [80] A. B. Goncharov, *Multiple polylogarithms, cyclotomy and modular complexes*, *Math. Res. Lett.* **5** (1998) 497–516, [[1105.2076](#)].
- [81] P. Nogueira, *Automatic Feynman graph generation*, *J.Comput.Phys.* **105** (1993) 279–289.
- [82] J. Vermaseren, *New features of FORM*, [math-ph/0010025](#).
- [83] J. Kuipers, T. Ueda, J. Vermaseren and J. Vollinga, *FORM version 4.0*, *Comput.Phys.Commun.* **184** (2013) 1453–1467, [[1203.6543](#)].
- [84] K. G. Chetyrkin and F. V. Tkachov, *Integration by Parts: The Algorithm to Calculate beta Functions in 4 Loops*, *Nucl. Phys.* **B192** (1981) 159–204.
- [85] S. Laporta, *High precision calculation of multiloop Feynman integrals by difference equations*, *Int. J. Mod. Phys.* **A15** (2000) 5087–5159, [[hep-ph/0102033](#)].

- [86] C. Studerus, *Reduze-Feynman Integral Reduction in C++*, *Comput. Phys. Commun.* **181** (2010) 1293–1300, [[0912.2546](#)].
- [87] A. von Manteuffel and C. Studerus, *Reduze 2 - Distributed Feynman Integral Reduction*, [1201.4330](#).
- [88] A. V. Smirnov, *Algorithm FIRE – Feynman Integral REduction*, *JHEP* **10** (2008) 107, [[0807.3243](#)].
- [89] A. V. Smirnov, *FIRE5: a C++ implementation of Feynman Integral REDuction*, *Comput. Phys. Commun.* **189** (2014) 182–191, [[1408.2372](#)].
- [90] R. N. Lee, *Presenting LiteRed: a tool for the Loop InTEgrals REDuction*, [1212.2685](#).
- [91] R. N. Lee, *LiteRed 1.4: a powerful tool for reduction of multiloop integrals*, *J. Phys. Conf. Ser.* **523** (2014) 012059, [[1310.1145](#)].
- [92] P. Maierhöfer, J. Usovitsch and P. Uwer, *KiraA Feynman integral reduction program*, *Comput. Phys. Commun.* **230** (2018) 99–112, [[1705.05610](#)].
- [93] B. Ruijl, T. Ueda and J. A. M. Vermaasen, *Forcer, a FORM program for the parametric reduction of four-loop massless propagator diagrams*, [1704.06650](#).
- [94] C. Anastasiou and A. Lazopoulos, *Automatic integral reduction for higher order perturbative calculations*, *JHEP* **07** (2004) 046, [[hep-ph/0404258](#)].
- [95] E. Panzer, *On hyperlogarithms and Feynman integrals with divergences and many scales*, *JHEP* **03** (2014) 071, [[1401.4361](#)].
- [96] A. von Manteuffel, E. Panzer and R. M. Schabinger, *A quasi-finite basis for multi-loop Feynman integrals*, *JHEP* **02** (2015) 120, [[1411.7392](#)].
- [97] A. V. Kotikov, *Differential equations method: New technique for massive Feynman diagrams calculation*, *Phys. Lett. B* **254** (1991) 158–164.
- [98] E. Remiddi, *Differential equations for Feynman graph amplitudes*, *Nuovo Cim.* **A110** (1997) 1435–1452, [[hep-th/9711188](#)].
- [99] T. Gehrmann and E. Remiddi, *Differential equations for two loop four point functions*, *Nucl. Phys. B* **580** (2000) 485–518, [[hep-ph/9912329](#)].
- [100] J. M. Henn, *Multiloop integrals in dimensional regularization made simple*, *Phys. Rev. Lett.* **110** (2013) 251601, [[1304.1806](#)].
- [101] M. Argeri and P. Mastrolia, *Feynman Diagrams and Differential Equations*, *Int. J. Mod. Phys. A* **22** (2007) 4375–4436, [[0707.4037](#)].
- [102] J. M. Henn, *Lectures on differential equations for Feynman integrals*, *J. Phys. A* **48** (2015) 153001, [[1412.2296](#)].
- [103] R. M. Schabinger, *Constructing multi-loop scattering amplitudes with manifest singularity structure*, [1806.05682](#).

- [104] G. Heinrich, *Sector Decomposition*, *Int. J. Mod. Phys. A* **23** (2008) 1457–1486, [[0803.4177](#)].
- [105] V. A. Smirnov, *Analytical result for dimensionally regularized massless on shell double box*, *Phys. Lett. B* **460** (1999) 397–404, [[hep-ph/9905323](#)].
- [106] J. B. Tausk, *Nonplanar massless two loop Feynman diagrams with four on-shell legs*, *Phys. Lett. B* **469** (1999) 225–234, [[hep-ph/9909506](#)].
- [107] I. Dubovyk, J. Gluza, T. Jelinski, T. Riemann and J. Usovitsch, *New prospects for the numerical calculation of Mellin-Barnes integrals in Minkowskian kinematics*, *Acta Phys. Polon. B* **48** (2017) 995, [[1704.02288](#)].
- [108] A. Freitas, *Numerical multi-loop integrals and applications*, *Prog. Part. Nucl. Phys.* **90** (2016) 201–240, [[1604.00406](#)].
- [109] K. Hepp, *Proof of the Bogolyubov-Parasiuk theorem on renormalization*, *Commun. Math. Phys.* **2** (1966) 301–326.
- [110] M. Roth and A. Denner, *High-energy approximation of one loop Feynman integrals*, *Nucl. Phys. B* **479** (1996) 495–514, [[hep-ph/9605420](#)].
- [111] T. Binoth and G. Heinrich, *An automatized algorithm to compute infrared divergent multiloop integrals*, *Nucl. Phys. B* **585** (2000) 741–759, [[hep-ph/0004013](#)].
- [112] C. Bogner and S. Weinzierl, *Resolution of singularities for multi-loop integrals*, *Comput. Phys. Commun.* **178** (2008) 596–610, [[0709.4092](#)].
- [113] A. V. Smirnov and M. N. Tentyukov, *Feynman Integral Evaluation by a Sector decompositiOn Approach (FIERA)*, *Comput. Phys. Commun.* **180** (2009) 735–746, [[0807.4129](#)].
- [114] A. V. Smirnov, V. A. Smirnov and M. Tentyukov, *FIERA 2: Parallelizable multiloop numerical calculations*, *Comput. Phys. Commun.* **182** (2011) 790–803, [[0912.0158](#)].
- [115] A. V. Smirnov, *FIERA 3: cluster-parallelizable multiloop numerical calculations in physical regions*, *Comput. Phys. Commun.* **185** (2014) 2090–2100, [[1312.3186](#)].
- [116] A. V. Smirnov, *FIERA4: Optimized Feynman integral calculations with GPU support*, *Comput. Phys. Commun.* **204** (2016) 189–199, [[1511.03614](#)].
- [117] J. Carter and G. Heinrich, *SecDec: A general program for sector decomposition*, *Comput. Phys. Commun.* **182** (2011) 1566–1581, [[1011.5493](#)].
- [118] S. Borowka, J. Carter and G. Heinrich, *Numerical Evaluation of Multi-Loop Integrals for Arbitrary Kinematics with SecDec 2.0*, *Comput. Phys. Commun.* **184** (2013) 396–408, [[1204.4152](#)].
- [119] S. Borowka, G. Heinrich, S. P. Jones, M. Kerner, J. Schlenk and T. Zirke, *SecDec-3.0*:

- numerical evaluation of multi-scale integrals beyond one loop*, *Comput. Phys. Commun.* **196** (2015) 470–491, [[1502.06595](#)].
- [120] S. Borowka, G. Heinrich, S. Jahn, S. P. Jones, M. Kerner, J. Schlenk et al., *pySecDec: a toolbox for the numerical evaluation of multi-scale integrals*, *Comput. Phys. Commun.* **222** (2018) 313–326, [[1703.09692](#)].
- [121] E. Laenen, *QCD*, in *Proceedings, 2014 European School of High-Energy Physics (ESHEP 2014): Garderen, The Netherlands, June 18 - July 01 2014*, pp. 1–58, 2016. [1708.00770](#).